PREDICTING ANGIOGENIC RECEPTOR TRAFFICKING AND SIGNALING VIA COMPUTATIONAL SYSTEMS BIOLOGY

BY

JARED COLIN WEDDELL

DISSERTATION

Submitted in partial fulfillment of the requirements
for the degree of Doctor of Philosophy in Bioengineering
in the Graduate College of the
University of Illinois at Urbana-Champaign, 2016

Urbana, Illinois

Doctoral Committee:

Assistant Professor Princess Imoukhuede, Chair
Professor Michael Insana
Associate Professor Kaustubh Bhalerao
Assistant Professor Wawrzyniec Dobrucki
Assistant Professor Dipanjan Pan

ABSTRACT

Angiogenesis is defined as the growth of new blood vessels from preexisting vessels. Systematic regulation of angiogenesis could lead to new treatments of vascular diseases and cancer. As such, vascular endothelial growth factor (VEGF), a potent angiogenic growth factor, offers a promising therapeutic target. Despite this promise, VEGF targeted therapies are not clinically effective for many pathologies, such as breast cancer. Thus, a better understanding of the VEGF network for regulating angiogenesis, along with identifying key nodes controlling angiogenesis within this network, are necessary to provide effective VEGF therapeutics. Systems biology, defined as applying experiment and computational modeling to understand a biological system, can readily define this VEGF-angiogenesis network. In this dissertation, I provide an overview of how computational systems biology has been used to provide basic biological insights into angiogenesis, explore anti-angiogenic therapeutic options for cancer, and pro-angiogenic therapeutic options for vascular disease.

Using systems biology, I have previously predicted that VEGFR1 acts as a predictive biomarker of anti-VEGF efficacy in breast cancer. Particularly, tumor endothelial cell subpopulations exhibiting high VEGFR1 levels result in ineffective anti-VEGF treatment. These high VEGFR1 subpopulations are characterized by a high amount of VEGF-VEGFR1 complex formation, and subsequently high VEGF-VEGFR1 internalization. The high VEGF-VEGFR1 complex formation implies a possible VEGFR1 signaling role beyond its classically defined decoy status. In this dissertation, I introduce a computational approach that accurately predicts the cell response elicited via VEGFR1 signaling. I show that VEGFR1 promotes cell migration through PLC_{γ} and PI3K pathways, and promotes cell proliferation through a PLC_{γ} pathway.

These results provide new biological insight into VEGFR1 signaling and angiogenesis while offering a system for directing angiogenesis.

Cell subpopulations expressing high VEGFR1 levels are characterized by a large amount of VEGF-VEGFR1 internalization. Thus, endocytosis may regulate VEGFR1 signaling; indeed, intracellular-based receptor signaling has recently emerged as a key component in mediating cell responses for receptor tyrosine kinases (RTKs). However, how endocytosis fundamentally mediates signaling for any RTK remains poorly defined. Understanding how endocytosis fundamentally directs intracellular receptor signaling requires receptor-specific endocytosis mechanisms to be delineated. This delineation requires identifying the signaling mechanisms common to all receptor types. To this end, I conduct a computational meta-analysis predicting endocytic compartment signaling across eight RTKs, and identify their common signaling mechanisms. I find that endocytic vesicles are the primary cell signaling compartment; over 43% total receptor phosphorylation occurs within the endocytic vesicle compartment for all eight RTKs. Conversely, all RTKs exhibit low membrane-based receptor signaling, exhibiting < 1% total receptor phosphorylation. Mechanistically, this high RTK phosphorylation within endocytic vesicles may be attributed to their low volume, which facilitates an enriched ligand concentration. The late endosome and nucleus are also important contributors to receptor signaling, where 26% and 18% average receptor phosphorylation occurs, respectively. Furthermore, nuclear translocation requires late endosomal transport; blocking receptor trafficking from late endosomes to the nucleus reduces nuclear signaling 96%. These findings can be applied to understand specific RTK signaling functions in terms of cell response, and optimize RTK therapeutics targeting endocytic pathways.

Overall, I reveal the role of VEGFR1 and its signaling mechanisms, which is essential information to the field of angiogenesis. This information advances angiogenesis therapeutics by identifying the VEGF-VEGFR1 signaling axis as an essential target. I identify the primary adapters that can be targeted to critically regulate VEGF-VEGFR1 signaling, and endocytic compartmentalization that can be targeted for tuning receptor signaling. Furthermore, the computational techniques I develop advance the field of systems biology by delineating the signal-to-response of receptor signaling, improving receptor investigation by allowing adapter phosphorylation and cell responses to be quantified simultaneously, in addition to compartmentalized receptor signaling. These computational techniques improve disease treatment by allowing optimal receptor signaling targets to be identified quickly. Additionally, unknown receptor signaling can be mapped from adapter phosphorylation to cell response. These computational techniques can be integrated into multiscale computational models to provide clinically relevant, patient-specific platforms for directing disease treatment.

ACKNOWLEDGEMENTS

During my graduate studies, I have received support and encouragement from many individuals. First I would like to thank God, without whom none of this would have been possible. I must also thank my wife, whose love and support has sustained me. I similarly thank my family and friends for being a constant source of encouragement.

I would like to thank Dr. P. Imoukhuede for being a great mentor. I am truly honored to have watched her lab grow and develop from the near beginning. I would like to thank my dissertation committee of Michael Insana, Kaustubh Bhalerao, Wawrzyniec Dobrucki, and Dipanjan Pan for their advice to lead my research to a complete story.

I also thank the colleagues in my lab, specifically Ali Ansari, Stacie Chen, and Spencer Mamer, with whom I spent countless hours discussing my research. Without their feedback and collaboration my research would not have developed to where it is now.

TABLE OF CONTENTS

CHAPTER 1

INTRODUCTION

Angiogenesis is the physiological process where new microvessels form from preexisting microvessels [1], [2]. Similarly, arteriogenesis is where new collateral arteries form from preexisting arteries [3], [4]. As angiogenesis and arteriogenesis are similar processes [4], albeit at different scales, I use either term interchangeably for the purpose of this chapter. Angiogenesis occurs in two different forms: sprouting or intussusceptive angiogenesis [1], [2]. Sprouting angiogenesis involves preexisting blood vessels to sprout and form new blood vessels. Sprouting angiogenesis is initiated by extracellular growth factor binding to endothelial cell surface receptors [5]. This ligand-receptor binding has dual action: 1) it initiates enzyme secretion from endothelial cells, which break down the basement membrane, and 2) it promotes directed endothelial cell migration and proliferation [5]. The migrating endothelial cells result in tube formation and fusion, which are stabilized by pericyte recruitment in microvessels, or smooth muscle cell recruitment in arteries, to result in new, functional blood vessels [1], [6]. The majority of current angiogenesis research focuses on sprouting angiogenesis, due to its prevalence in wound healing [7] and cancer progression [8].

Intussusceptive angiogenesis is the splitting of an existing blood vessel into two blood vessels [2], [9], [10]. Intussusceptive angiogenesis occurs by blood vessel walls continuously extending into the lumen, forming an intravascular pillar, which eventually splits a single tube into two tubes. Unlike sprouting angiogenesis, intussusceptive angiogenesis is ineffective at vascularizing regions lacking blood vessels, instead primarily adding additional vessels to regions already containing blood vessels [2], [9], [10]. Additionally, intussusceptive angiogenesis does not require endothelial cell migration or proliferation [10]. While

intussusceptive angiogenesis can be initiated by growth factor stimulation, it also results from mechanical stress produced by blood flow [11]. Intravascular pillars seem to specifically form at vessel bifurcations when hemodynamics are altered to cause high flow velocity, but low shear stress [12], [13]. As such, intussusceptive angiogenesis is difficult to regulate, as hemodynamics cannot be easily altered and requires invasive procedures [13]. Further research investigating chemical cues, including any mechanotransduction pathways activated through shear stress, is necessary to develop efficient, noninvasive methods for regulating intussusceptive angiogenesis.

Sprouting and intussusceptive angiogenesis are both critical to normal physiological processes, such as wound healing and embryonic development. Moreover, over 70 diseases, including cancer and occlusive vascular disease, are angiogenesis dependent [14], [15]. In 1971, Judah Folkman hypothesized that tumor growth depends on angiogenesis initiated by a tumor-angiogenesis factor [16]. This hypothesis was derived from studies showing that tumors only grow to a dormant state, at 2-3 mm in diameter, in the absence of neovascularization [17]–[19], tumor implantation induces endothelial cell proliferation [16], [20] and formation of new capillaries [21]–[23], and tumor growth is limited by the rate of endothelial cell proliferation [24], [25]. Since this hypothesis, many studies have been conducted to arrive at the current understanding of tumor angiogenesis: tumor cells promote sprouting angiogenesis to provide the necessary nutrients for further tumor growth and metastasis, reviewed in [15], [26], [27]. Inhibiting sprouting angiogenesis is therefore a promising approach to prevent transition of tumors from a benign to malignant stage [28], [29].

In 2005, Rakesh Jain put forth an alternative hypothesis on tumor angiogenesis: rather than destroying tumor vasculature to deprive the tumor of oxygen and nutrients, anti-angiogenic therapies are most effective by normalizing the abnormal tumor vasculature to allow more

efficient drug delivery [30]. This hypothesis was derived from studies showing that tumor vasculature is structurally and functionally abnormal [31]–[33], that this structural abnormality impairs blood flow and compromises the ability for drug delivery to tumors [34]–[36], and that normalizing tumor vasculature allows drug delivery deeper into tumors to cause tumor regression [37]–[39]. Studies have continued to provide support for this hypothesis, reviewed in [40], [41]; a recent clinical trial shows that vascular normalization, measured by pericyte coverage, is associated with improved pathological response to the anti-angiogenic drug bevacizumab [42]. Understanding the mechanisms through which anti-angiogenic drugs normalize tumor vasculature, and optimizing treatment regimens to best regulate sprouting angiogenesis, is a primary challenge for preventing tumor angiogenesis and tumor progression [43], [44].

Occlusive vascular diseases stem from a lack of blood flow, resulting in tissue ischemia, loss of limb function, and death [45]. For occlusive vascular diseases, promoting either sprouting or intussusceptive angiogenesis to reestablish proper blood flow is therefore a promising approach to prevent tissue ischemia [46], [47]. Overall, the ability to control angiogenesis would allow for the prevention and treatment of pathologies: preventing cancer mortality by inhibiting tumor angiogenesis, and treating vascular diseases by promoting angiogenesis.

CHAPTER 2

LITERATURE REVIEW

2.1 The VEGF Family

The vascular endothelial growth factor-A (VEGF-A) is a key growth factor that promotes angiogenesis. The existence of VEGF-A was first hypothesized as an unknown factor by Judah Folkman in 1971, who characterized VEGF-A as an unknown tumor-angiogenesis factor [16]. Senger et al identified this unknown factor as vascular permeability factor (VPF) in 1983 [48], and Leung et al characterized this factor, and termed it VEGF, in 1989 [49]. Keck et al showed in 1989 that VPF and VEGF are the same molecule [50], demonstrating that this single factor has multiple functions. In 1993, Napoleone Ferrara's laboratory demonstrated for the first time that inhibiting VEGF suppresses tumor growth [51]. Since these studies, VEGF has been studied as a promising therapeutic target for cancer and vascular disease, reviewed in [15], [52]. Anti-angiogenic therapeutic approaches that have been applied to inhibit tumor angiogenesis are reviewed in [53]. An overview of the VEGF-directed angiogenesis timeline is given in Figure 2.1.

VEGF-A is now known as one of five related growth factors expressed in humans that make up the VEGF family: VEGF-A, VEGF-B, VEGF-C, VEGF-D, and placental growth factor (PlGF) [54]. There are two additional VEGF ligands: viral VEGF (VEGF-E) [55] and snake venom VEGF (VEGF-F) [56]; these ligands are not expressed in humans, and as such, shall not be discussed in detail here. The VEGF growth factors bind with high affinity to three tyrosine kinase receptors, VEGFR1, VEGFR2, and VEGFR3. Many VEGF ligands also contain a heparin-binding domain, in addition to binding neuropilins, co-receptors to the VEGFRs. VEGF-

A, often referred to simply as VEGF, promotes angiogenesis through interaction with VEGFR1 and VEGFR2. Conversely, all other VEGF growth factors and VEGFR3 exhibit weak angiogenic potential. VEGF-B and PlGF specifically bind VEGFR1, and have been identified as key promotors in neurogenesis and embryogenesis. VEGF-C and VEGF-D promote lymphangiogenesis through VEGFR3 (Table 2.1).

The VEGF ligands and receptors are also expressed in isoform variants, each having specific interactions and functions. VEGF-A has seven currently known splice variants, in addition to full-length VEGF-A, which are distinguished by amino acid length: VEGF-A_{121}, VEGF-A_{145}, VEGF-A_{148}, VEGF-A_{165}, VEGF-A_{183}, VEGF-A_{189}, and VEGF-A_{206}. A VEGF-A_{110} isoform is also created through proteolytic cleavage of longer VEGF isoforms by plasmin [57]. VEGF-regulated angiogenesis research typically focuses on VEGF-A_{165}, the predominant VEGF-A isoform [58]. For this reason, VEGF-A_{165} is often referred to simply as VEGF, a notation I adopt henceforth.

The aforementioned splice variants have recently been typified as the VEGF-A_{xxxa} isoforms, as secondary VEGF-A_{xxxb} isoforms containing the same number of amino acids, but different sequences and function, have emerged. Currently, four VEGF-A_{xxxb} isoforms have been identified: VEGF-A_{121b}, VEGF-A_{145b}, VEGF-A_{165b}, and VEGF-A_{189b}, fully reviewed in [59], [60]. Key points to know about these isoforms include: VEGF-A_{165b} is the best studied VEGF-A_{xxxb} isoform; VEGF-A_{165b} binds to VEGFR2 with the same kinetics as VEGF-A_{165}, but does not activate VEGFR2 nor the signaling pathways that VEGF-A_{165} activates [61]. Subsequently, the VEGF-A_{xxxa} isoforms are characterized as pro-angiogenic, whereas the VEGF-A_{xxxb} isoforms are anti-angiogenic.

Likewise, multiple isoforms of VEGF-B have also been discovered [62], [63]. VEGF-B is considered to primarily be a neuroprotective factor [64]; VEGF-B has also been identified to act as a myocardium-specific angiogenic factor [65], [66] and a regulator of energy metabolism by modulating fatty acid uptake [67], reviewed in [68], [69]. The two discovered VEGF-B isoforms are VEGF-B_{167} and VEGF-B_{186}, differentiated by amino acid length [62], [63]. VEGF-B_{167} has been identified as the predominant isoform, with over 80% total VEGF-B being expressed as VEGF-B_{167} [70]. However, the functional differences between VEGF-B_{167} and VEGF-B_{186}, outside that VEGF-B_{167} contains a heparin-binding domain and VEGF-B_{186} does not [68], are currently unknown.

Conversely, VEGF-C does not exist in multiple isoforms. VEGF-C is considered to primarily promote lymphangiogenesis through interaction with VEGFR3, reviewed in [71]. VEGF-C also interacts with VEGFR2, although VEGF-C/VEGFR2 interactions do not appear sufficient to promote lymphangiogenesis [72]. VEGFR2 might have an indirect modulatory role in VEGF-C lymphangiogenesis: VEGF-C induces VEGFR2/VEGFR3 heterodimerization, unlike VEGF-A, which differentiates VEGF-C signaling from VEGFR3 homodimers [73], [74].

Similarly, VEGF-D does not exist in multiple isoforms, and is considered to primarily promote lymphangiogenesis through VEGFR3, as reviewed in [75]. VEGF-D also binds VEGFR2 [76], implying that VEGFR2/VEGFR3 heterodimerization might be important for VEGF-D signaling. However, unlike with VEGF-C, lymphatic development does not appear to be affected by VEGF-D deletion [77]. As such, VEGF-D signaling and function remains questionable, and additional research is necessary to make any additional assertions about VEGF-D signaling.

PlGF contains four known isoforms, termed PlGF1-4 [78]–[80]. Similar to VEGF, PlGF isoforms result from alternative splicing, each containing a different number of amino acids: 131, 152, 203, and 224. Like the VEGF-B isoforms, PlGF-2 and PlGF-4 contain heparin binding domains, while PlGF-1 and PlGF-3 do not [81]. Also like the VEGF-B isoforms, the functional difference between PlGF isoforms is not currently known.

Similar to the VEGF ligands, the VEGFRs are also expressed in variant isoforms. Soluble isoforms, truncated full-length receptors without the transmembrane or intracellular domains, were identified for all three VEGFRs [82]–[84]. These soluble isoforms are considered to contain no signaling properties, acting to sequester free VEGF [83], [85]. The soluble VEGFR isoforms can dimerize with full-length membrane VEGFRs, which may additionally direct VEGFR signaling [86]. Intracellular VEGFR isoforms also exist; intracellular VEGFR1 isoforms containing either the full or partial intracellular domain of full-length VEGFR1 were identified [87], [88]. It stands to reason that other VEGFR isoforms may yet be undiscovered. Identifying all VEGFR isoforms and functions may be necessary to achieve complete control of angiogenesis.

Dimerization, the binding of two receptor monomers to form a receptor dimer, is a critical step to VEGFR phosphorylation and signal transduction. VEGFR1, VEGFR2, and VEGFR3 all form homodimers: two VEGFR1 monomers bind to form a VEGFR1-VEGFR1 homodimer, etc. Heterodimerization, where two different VEGFR monomers bind, also occurs. VEGFR2 forms heterodimers with both VEGFR1 and VEGFR3, whereas VEGFR1 and VEGFR3 are not able to heterodimerize. These homodimer and heterodimer pairs can activate different intracellular signaling pathways, leading to differential cell responses.

Overall, this VEGF family overview showcases the large VEGF signaling network. The multiple ligand types, receptor types, isoforms, and dimers complicate the ability to understand and predict how angiogenesis occurs. Furthermore, VEGF signaling cooperates with signaling from other receptors to direct angiogenesis: VEGF-VEGFR and Delta-Notch signaling interact to direct tip/stalk cell selection in sprouting angiogenesis, reviewed in [89]. Thus, the ability to effectively regulate angiogenesis for cancer and vascular disease therapeutics has relied on methods that delineate this complex VEGF signaling axis to identify key signaling features and targets.

Here, I discuss how systems biology has been used to provide this delineation of VEGF signaling, to identify key VEGF signaling features and targets, in angiogenesis. Systems biology is an iterative approach between mathematical or computational modeling with quantitative experimentation to understand the entire biological system [90]. Systems biology is also advantageous by being quantitative and predictive in nature, allowing features such as model-directed experiments to quicken discovery of key angiogenesis nodes. Systems biology also has the power to isolate and examine subsystems within angiogenesis, such as receptor signaling pathways to identify critical signaling nodes in angiogenesis. As such, systems biology can examine a system at various scales: angiogenesis can be examined macroscopically, such as sprout formation, or microscopically, such as VEGFR signal propagation.

In this chapter, I provide an overview of systems biology techniques that have been employed to mathematically or computationally explore angiogenesis (Table 2.2). I review studies employing these systems biology techniques to examine the VEGF family in angiogenesis to provide new biological insights, and to design pro-angiogenic or anti-angiogenic therapies. Lastly, I provide a brief overview on the current challenges in manipulating VEGF

signaling and angiogenesis and future research directions to achieve complete angiogenic control.

2.2 Systems Biology Approaches

2.2.1 Deterministic kinetic modeling.

Chemical reactions describing the kinetic reaction network are modeled using the law of mass-action: the rate of a reaction is directly proportional to reactant concentration (1.1):

$$[\mathbf{A}]+[\mathbf{B}]\underset{k_r}{\overset{k_f}{\rightleftharpoons}}[\mathbf{C}] \tag{1.1}$$

Here A, B, and C are species concentrations, A and B interact to form C with forward rate k_f, and C dissociates to form A and B with reverse rate k_r. For systems biology applications, reactions describe interactions between reactants, modeled as biological species such as proteins or genes. For deterministic kinetic models, species are assumed to be contained in a continuous molecular concentration. One typical deterministic kinetic modeling application is to quantify temporal species concentrations using ordinary differential equations (1.2):

$$\frac{d[A]}{dt} = k_r[C] - k_f[A][B] \tag{1. 2}$$

The equation in (1.2) indicates the temporal concentration of species A ([A]) defined by the chemical reaction in (1.1). Kinetic models are also often employed as compartmental models, where species reactions are bounded within a physical space (compartment), but may transport between other compartments that are physically separated (Fig 2.2). In systems biology, a microscale compartmental example is modeling the extracellular and intracellular space, which are physically separated by the cell membrane. A macroscale example is modeling compartments

as different tissues, such as bloodstream and skeletal muscle tissue, which are physically separated by the blood vessel walls. A thorough review on kinetic modeling of signaling networks at micro- and macro-scales can be found by Janes and Lauffenburger in [91].

A second typical deterministic kinetic modeling application is to quantify spatial or spatiotemporal species concentrations are using the advection-diffusion-reaction equation modeled with partial differential equations (1.3):

$$\frac{\partial[A]}{\partial t} = D\nabla^2[A] - \vec{v}\cdot\nabla[A] \pm \mathrm{R} \tag{1.3}$$

where [A] is the concentration of a species A, D is the diffusion coefficient of species A, ∇ is the spatial gradient, $\vec{v}$ is the convective velocity field, and R is any reactions involving species A. In purely kinetic models, modeling species diffusion and convection typically involves compartmental modeling, where species transport between compartments is defined by either constant D and $\vec{v}$ terms, or D and $\vec{v}$ terms that are altered algorithmically (Fig 1.1).

2.2.2 Stochastic modeling

Deterministic kinetic modeling always gives the same results given the same reactions, concentrations, and kinetics. However, biological processes have elements of randomness; deterministic modeling particularly fails at low species concentrations, where the assumption that species are contained in a continuous molecular concentration does not hold, and reactions occur stochastically [92], [93]. Stochastic kinetic models incorporate this random element into deterministic kinetic models to predict biological randomness and noise [94]. Systems biology typically applies stochastic modeling through the Gillespie algorithm or Monte Carlo simulations. Briefly, the Gillespie algorithm simulates time-dependent trajectories of the species

in a chemical reaction network [94]. Monte Carlo simulates stochastic reactions by introducing probability distributions for the occurrence of each reaction [95].

2.2.3 Agent-based modeling

Agent-based models represent each individual species (i.e. cell or protein) as a discrete agent that follows a certain set of rules. Similar to kinetic modeling, agent-based models in systems biology are typically used to quantify spatiotemporal species information [96]. Unlike kinetic modeling, agent-based models do not require kinetic or concentration information; rather, rules define species interactions and transport, which may or may not include kinetic or concentration information [90]. Cellular automaton is one primary example of agent-based modeling: creating a two- or three-dimensional spatial grid, where each lattice on the grid contains an agent of interest, and simulating the spatiotemporal agent movements and interactions across the grid.

Agent-based models are advantageous as they incorporate stochasticity, and provide spatiotemporal information on individual agents, without requiring complex mathematical equations (such as 1.2-1.3) to be defined and solved. Furthermore, agent-based models do not require knowledge of the system mechanisms; agent behavior is governed by rules that can be readily derived from physical laws or empirical observations. One primary limitation of agent-based models is that simulating many agents is highly expensive computationally [97]. Thus, agent-based models are useful for testing multiple system mechanisms to uncover the true system behavior [96].

2.2.4 Molecular modeling

Molecular modeling simulates the three-dimensional structural interactions between atoms and molecules [98]. Here, I focus on molecular modeling in the context of computational drug screening to identifying potential VEGF inhibitors [99]. Computational drug screening is an approach to identify novel therapeutics for targeting signaling proteins. Potential drugs targeting the signal protein of interest are predicted by screening through different molecules, and quantifying their binding strength to the signal protein. Binding strength is typically determined through docking analysis, predicting the ability of a molecule to bind the signal protein through preferred orientation, size, flexibility, predicted interaction kinetics, and atomic structure. The therapeutic efficacy of these drugs is then examined in vitro or in vivo [99].

2.2.5 Finite element modeling

Finite element modeling is based on similar principles of cellular automaton: a spatial domain is bounded and discretized to calculate the quantity of interest within each lattice on the grid temporally [100]. Finite element modeling differs from agent-based modeling in two primary ways: (1) finite element models quantify materials in continuum, such as fluid velocities or temperature fields, and (2) finite element models are defined from conservation laws. A typical finite element application is to quantify hemodynamic forces, velocity, pressure, and shear stresses, through the Navier-Stokes equations [101]:

$$\rho \boldsymbol{u}_{,t} + \rho \boldsymbol{u} \cdot \nabla \boldsymbol{u} - \nabla \cdot \boldsymbol{\sigma}_{\boldsymbol{u}}(\boldsymbol{u}) + \nabla p = \boldsymbol{f} \tag{1.4}$$

$$\nabla \cdot \boldsymbol{u} = \boldsymbol{0} \tag{1.5}$$

where ρ is the fluid density, $\boldsymbol{u}$ is the velocity field, $\boldsymbol{u}_{,t}$ is the time derivative of the velocity field, $\boldsymbol{\sigma}_{\boldsymbol{u}}$ is the viscous stress, p is the pressure, and $\boldsymbol{f}$ is the external forces. The equations in

(1.4) and (1.5) are defined by conservation of momentum and mass respectively. Finite element models could be used to calculate physiologically relevant velocity fields for advection-diffusion-reaction simulations (1.3), allowing multi-scale VEGF modeling. For angiogenesis applications, finite element modeling is typically used to examine how blood flow stress directs vessel growth or intravenous angiogenic drug delivery.

2.2.6 Multivariate models

The above computational techniques require no experimental data training for model development – granted such models are typically trained to ensure physiological accuracy. However, these models require high parameterization when the number of reactions and species becomes large, and not all species or variables related to the system are typically incorporated into these models. To overcome these challenges, multivariate models seek to provide signal-to-response statistical models derived directly from experimental datasets, which do not require explicit definition of system mechanisms. A commonly used multivariate model in systems biology is partial least squares regression (PLSR). PLSR is a regression technique that correlates independent variables to dependent variables within the system [102]. An example is building a PLSR model to correlate ligand stimuli (independent variable) to cell response (dependent variable) using experimental observations, and then applying the PLSR model to predict what cell responses will occur from untested ligand stimuli [102].

Statistical modeling is another commonly used multivariate approach in systems biology, where the probability of observing some response from a system of interest is calculated given a probability model [103]. Bayesian statistics is one such commonly used statistical model; Bayesian statistics infers posterior probabilities of model parameters by model training with empirical data [104]. An example Bayesian model application is predicting receptor signaling

cross-talk involved in drug resistance, using empirical gene expression profiles from drug-resistance and drug-nonresistant patients [105]. Machine learning is a similar statistical modeling approach, which describes a system from empirically derived sample inputs through processing algorithms [106]. Machine learning differs from Bayesian statistics in that machine learning does not describe biological mechanisms of a system, rather providing an optimized fit of input data to response. An example machine learning application is mapping tissue gene expressions to disease groups, to allow predictive disease classification from future tissue gene expression screenings [107].

While multivariate models are powerful at predicting signal-to-responses, they are empirical-based models that are not capable of describing mechanisms of a biological system. Since this literature review focuses on computational systems biology for understanding angiogenesis mechanisms, I do not review multivariate approaches for angiogenesis in detail.

In the following section, I provide an overview of computational systems biology studies that explore angiogenesis mechanisms and methods for regulating angiogenesis.

2.3 Systems Biology for Studying Angiogenesis

2.3.1 Sprouting angiogenesis

Computational modeling, as a tool to understand angiogenesis, has been applied hand-in-hand with experimental investigation since the field of angiogenesis first emerged in the early 1970s, when Judah Folkman discovered the tumor angiogenic factor [16]. The earliest angiogenesis computational models examined vessel sprouting and network formation by diffusion modeling [108], [109]. As VEGF and VEGFRs were not characterized until the late-1980s to early 1990s (Fig 2.1), these initial angiogenesis models examined vessel sprouting in

response to the uncharacterized molecule tumor angiogenic factor [16]. Despite not modeling sprouting directly by VEGF, these early computational models offered many important insights into growth factor directed angiogenesis. Such computational models determined that the presence of an angiogenic factor is necessary to develop high density tumor vascularization, a concept that was contentious for its time [108], [110]. Later sprouting models highlighted the importance of an angiogenic factor, finding that directed vessel growth [111] and vessel loop formation [112] require a growth factor gradient. Cellular automaton and random walk approaches were applied to track individual cells throughout sprouting [113], which captured the proliferative phenotype of cells behind the sprouting tip [114].

As the roles of VEGF and other factors became defined in angiogenesis, computational models began to examine sprouting as a system comprising multiple driving factors or cell types. Some such recent sprouting models have predicted that basic fibroblast growth factor (bFGF) enhances VEGF-directed angiogenesis by upregulating VEGFR2 [115], and that VEGF and angiopoietins coordinate angiogenesis through endothelial cell (EC) migration and vessel maturation by pericytes [116]. Finite element modeling has also been used to identify that traction forces employed by cell growth controls matrix deformation and additional angiogenic growth and remodeling [117]. Additional computational systems biology models that have been specifically studied sprouting angiogenesis are reviewed in [118]. Overall, such sprouting models have advanced the understanding of how single or multiple growth factor gradients direct angiogenesis. Sprouting models also offer a powerful, macroscopic framework to examine specific subsystems within angiogenesis; as such, sprouting models have been extended to understand how VEGF-mediated tip/stalk cell selection directs angiogenesis.

2.3.2 Tip/stalk cell selection and vessel sprouting

Gerhardt *et al* defined vessel patterning for the first time in 2003, characterized by tip cells responding to VEGF with guided migration, and stalk cells responding with proliferation [119]. Vessel patterning has since been well characterized in VEGF-directed sprouting angiogenesis, identified as an important feature for VEGF signaling and lumen formation to create functional blood vessels, reviewed in [120]. As VEGF/VEGFR and Delta/Notch signaling cross-talk was characterized as a key feature in tip/stalk cell selection and vessel patterning [121], [122], agent-based computational models worked hand-in-hand with experimental investigations to explore this relationship. Insights gained from such agent-based models include identifying that Dll4 and VEGFR2 expression oscillate to direct sprouting [123], and the validated prediction that tip/stalk cell selection is driven through tip cell filopodia extension [124]. Perhaps the most important insight into tip/stalk cell selection given by computational models is that this process is reversible; Bentley *et. al.* first reported that DII4/Notch lateral inhibition between ECs during loop formation causes cell fates to flip [124], a process now validated through further model-directed [125] and exploratory [126] experiments. Recent agent-based modeling, integrated with in vivo experiments, identified that the rate of tip cell selection defines a trade-off between sprout extension and vessel branching, dictating vessel network density [127]. Model-derived experiments also found that reversible tip/stalk cell selection is present in embryonic neural crest cells, accurately predicting gene expression patterns that different tip and stalk cells [128], [129]. Some examples of inferences recent tip/stalk cell sprouting models have made include: tip cells migrate back and forth to dynamically alter the leading cell based on VEGFR2 expression [130], stalk cell proliferation is dependent on traction forces applied by tip cell migration [131], and that tip cell polarization and directed movement is mediated by the VEGF-VEGFR binding distribution on the cell surface [132].

2.3.3 VEGF-VEGFR kinetic models

VEGF-VEGFR kinetic models at the single cell scale seek to understand how the kinetics of the ligand-receptor interactions dynamically alter protein and complex concentrations. Typically, these concentrations are taken as the functional output of VEGF-VEGFR interaction models, providing inference to angiogenic potential (i.e. higher phospho-VEGFR2 concentrations imply more angiogenesis will occur). VEGF-VEGFR interaction models are powerful as they quantify protein and complex concentrations that are difficult to probe or differentiate experimentally, and allow perturbations (such as ligand or receptor concertation effects) to be easily examined. While ligand-receptor kinetic models were first introduced in the early-1970s [133], VEGF-VEGFR interactions would not be explored until Mac Gabhann and Popel developed the first VEGF-VEGFR kinetic model in 2004 [134]. This model predicted that the experimental hypothesis that PlGF displaces VEGF from VEGFR1, enhancing VEGF signaling through VEGFR2, was incorrect, and suggested a functional VEGFR1 signaling role [134]. Later experimental evidence backed up this model result, showing that PlGF upregulates pro-angiogenic factors and induces metastasis [135], [136]. This initial model showcases the predictive power of VEGF-VEGFR interaction models. VEGF-VEGFR interaction models have been continuously developed throughout the years to explore VEGFR signaling dynamics. I provide an overview of VEGF-VEGFR kinetic models based on the subsystems they explore.

2.3.4 VEGF expression in hypoxia

Hypoxia inducible factor-1α (HIF-1α) is one of the primary molecules that directs vascularization in response to hypoxic environments by promoting VEGF expression [137], [138], leading to increased tumor cell invasiveness [139]. Systems biology has thus investigated HIF-1α activation in response to oxygen concentration, and subsequent VEGF expression for

promoting angiogenesis. An initial hypoxia kinetic model developed by Qutub and Popel identified that HIF-1α activation from hypoxia either directs steep, switch-like or gradual cell responses; this dual cell response may be an important consideration for HIF-1α targeting therapeutics [140]. Another kinetic model examined how VEGF expression is mediated through HIF-1α degradation by two enzymes, prolyl hydroxylase and asparaginyl hydroxylase [141]. This model identified that prolyl hydroxylase alone is sufficient at abolishing HIF-1α activity, and that regulating prolyl hydroxylase activity may be an effective method for controlling the angiogenesis response to hypoxia [141]. A recent kinetic model examined the role of miRNAs in hypoxia-induced HIF-1α activity and VEGF expression, identifying that argonaute 1 overexpression decreases VEGF production [142]. These potential therapeutic targets identified by hypoxia-induced VEGF expression models offer potential options for controlling angiogenesis, and require further investigation.

2.3.5 VEGFR dimerization models

VEGF signaling can lead to differential signaling outcomes based on whether it signals through VEGFR homodimers or heterodimers [143]. VEGFR dimerization formation is difficult to examine experimentally, making the effects of dimerization parameters, such as dimerization rates or ratio of dimer formation, difficult to elucidate. VEGF computational models have provided VEGFR dimerization to be probed, with such findings as that dimerization does not affect complex formation at membrane patches dominated by stochastic VEGF-VEGFR binding [144]. Modeling competition of VEGF-VEGFR complex formation between VEGFR homodimers and VEGFR1/VEGFR2 heterodimers revealed that 10% - 50% complexes exist as heterodimers [145]. Furthermore, when VEGFR2 concentrations are high, heterodimer formation increases by decreasing VEGFR1 homodimer formation [145], a prediction validated

experimentally [146]. While these computational models elucidated how VEGFR dimers form, understanding functional differences in VEGF signaling through VEGFR1 homodimers, VEGFR2 homodimers, and VEGFR1/VEGFR2 heterodimers remains a challenge that systems biology may yet answer.

2.3.6 VEGF isoform-VEGFR kinetic modeling

Similar to VEGF signaling being directed by VEGFR dimer formation, VEGFR signaling is directed by the type of ligand that binds (Table 2.1). While computational models have examined VEGF isoforms primarily in the context of pathology (described below), I highlight three studies that have examined VEGF isoforms in normal physiology. An early model examining $VEGF_{165}$- and $VEGF_{121}$-VEGFR binding distributions in skeletal muscle tissue found that NRP potentiates $VEGF_{165}$-VEGFR2 binding, and removing NRP causes equal $VEGF_{165}$- and $VEGF_{121}$-VEGFR2 binding [147]. A two compartment blood-tissue model examined $VEGF_{121}$ and $VEGF_{165}$ binding distributions with luminal and abluminal receptors, finding that abluminal VEGF predominantly binds VEGFR1, whereas luminal VEGF predominately binds VEGFR2 [148]. Another study elucidated that VEGF isoform patterning observed in vivo [149], [150] is directed by isoform specific sequestration and degradation through heparan sulfate proteoglycan binding [151]. Furthermore, matrix metalloproteinases increase soluble VEGF by cleaving heparan sulfate proteoglycans and preventing VEGF degradation [151], [152]. Note that these computational models examined $VEGF_{121}$, $VEGF_{165}$, and $VEGF_{189}$ binding distributions with VEGFRs; no other $VEGF_{xxxa}$ isoforms have been modeled, and no $VEGF_{xxxb}$ isoform models exist to the best of my knowledge.

2.3.7 Kinetic modeling of VEGFR internalization and intracellular signaling

These extracellular models provide a template for identifying key extracellular nodes and processes mediating VEGF-VEGFR interactions, but do not characterize how intracellular nodes mediate angiogenesis. To overcome this limitation, VEGF computational models were extended to examine how extracellular factors and VEGF-VEGFR binding couple with intracellular processes, receptor internalization and intracellular signaling, to direct angiogenesis. These VEGFR signaling models have focused on VEGFR2, whose intracellular signaling role in angiogenesis has been well characterized experimentally, relative to VEGFR1 [153], [154]. The earliest VEGFR intracellular signaling model I identified, developed in 2007 by Alarcon and Page, provides the mathematical basis for modeling VEGF binding a generalized VEGFR, VEGFR internalization, and coupling of a generalized src-homology 2 (SH2) containing kinase to the VEGFR [155]. Such mathematical techniques have been applied to examine specific signaling molecules: Mi et al use model-directed experimentation to show that VEGFR2-PLC_{δ} directs intercellular Ca^{2+} signaling, mediating cell-cell communication in wound closure [156]. Napione et al show through model and experimentation that PLC_{γ} and Akt phosphorylation depend on VEGFR2 expression, mediated by cell density [157]. Tan et al predict that VEGFR2 activates multiple different pathways, mediated by Gab1 and Gab2, to control Akt phosphorylation dynamics [158]. Computational analyses have also identified an important role for receptor internalization in intracellular signaling; matrix-bound VEGF is predicted to be internalized slowly by VEGFR2, facilitating higher and sustained ERK phosphorylation, relative to soluble VEGF [159]. Similarly, Anderson et al experimentally show that heparin-bound VEGF increases VEGFR2 phosphorylation, and through computational modeling identify that heparin-bound VEGF slows receptor internalization [160]. Another model predicts that receptor phosphorylation is more dependent on internalization and trafficking rates than phosphorylation

rates, indicating that phosphorylation of specific receptor sites may depend on intracellular compartmentalization [161]. Together, these VEGF-VEGFR interaction models provide systemic information on the VEGF signaling axis: mapping entire extracellular and intracellular processes that mediate VEGF signaling and subsequent angiogenesis.

2.3.8 Multiscale VEGF kinetic models

VEGF interaction models have been expanded from the cell surface to macroscale. These systemic VEGF computational studies model the same VEGF-VEGFR interactions as at the cell scale, but expand the model scope to and interactions to examine VEGF distribution and binding at tissue or whole-body scales. At the tissue scale, $VEGF_{165}$ and $VEGF_{121}$ binding distributions to VEGFRs and NRP1 were modeled in skeletal muscle tissue, providing tissue scale findings such as that $VEGF_{165}$ concentrations in interstitial space does not affect steady-state VEGF binding distributions [147]. VEGF interactions are also modeled at the whole-body scale, using compartmental modeling to simultaneously quantify VEGF interactions and transport between biological compartments. Whole-body VEGF models first emerged by examining VEGF in tissue and blood compartments [162], providing the notable insights that unbound VEGF primarily localizes to tissue compartments [163], and but that soluble VEGFR1, which sequesters unbound VEGF, does not decrease VEGF signaling potential in those tissue compartments [164]. These macroscopic VEGF-VEGFR interaction models are also regularly used to explore angiogenesis in pathology: understanding both how VEGF signaling is important to pathology, and testing VEGF therapeutics. In the following section, I review modeling approaches to explore and optimize VEGF therapeutics, specifically pro-angiogenic therapeutics for vascular disease, and anti-angiogenic therapeutics for cancer.

2.3.9 Systems biology for pro-angiogenic therapies

Pro-angiogenic treatments have exhibited continuous success at vascularizing ischemic tissue in animal models, but such treatments have not translated to clinical benefits [165]. Computational models for pro-angiogenic therapies seek to optimize VEGF signaling to vascularize ischemic tissue and provide clinically effective options for treating vascular diseases [166]. Pro-angiogenic computational models first examined VEGF gradients in rest and exercise [167], [168], as exercise is the most effective preventer of vascular disease [169]. Some key findings from these computational studies include (1) that skeletal muscle VEGF gradients result in heterogeneous VEGFR activation, which may define the mechanism for stochastic sprout locations [168], (2) exercise increases VEGF signaling by upregulating VEGFRs and NRP1 [167], and (3) VEGF signaling and subsequent tissue vascularization is most effective within the first week of starting exercise regimes [167]. Unfortunately, patients with progressed vascular disease are unable to exercise; thus, computational models also examined other pro-angiogenic therapies in severe artery diseases [142], [170], [171]. One model suggested that injecting myoblasts overexpressing VEGF may effectively promote angiogenesis [171], and although further study identified this treatment to be less effective than exercise [170], it may be a promising therapeutic for patients unable to exercise. A recent model suggests that targeting miRNA, specifically inhibiting miR-15a, may effectively increasing VEGF synthesis and function in peripheral artery disease [142]. Further exploration into miR-15a in peripheral artery disease, along with additional computationally derived therapeutic options for vascular diseases, may overcome the barrier currently preventing clinical efficacy of pro-angiogenic therapies.

2.3.10 Systems biology for anti-angiogenic therapies

Whole-body pharmacokinetic/pharmacodynamics VEGF interaction models have been developed to systemically quantify VEGF-targeting therapeutic efficacies to inhibit tumor

angiogenesis. These tumor angiogenesis models extend compartmental models of VEGF interactions with VEGFRs and extracellular proteins [148], [164], [172] to account for drug administration to the blood stream, absorption into healthy and diseased tissue, and drug-target interactions. Compartmental models examined VEGF dynamics following anti-VEGF injection [173]–[175], identifying that $VEGF_{121}$ inhibition is more effective at reducing tumor angiogenic potential than $VEGF_{165}$ inhibition [176] and predicted that anti-VEGF efficacy is sensitive to VEGFR levels on tumor cells [177]. Further investigation into physiological VEGFR heterogeneity identified that high VEGFR1 levels result in ineffective anti-VEGF therapy [178], implicating VEGFR heterogeneity as a drug resistance mechanism. Pharmacokinetic modeling has also identified potential drug interaction mechanisms: the anti-VEGF drug aflibercept may bind NRP-bound VEGF, in addition to free VEGF [179]. Overall, these systemic VEGF models offer a powerful platform for testing anti-tumor angiogenesis therapies, which can be applied to study patient-specific therapeutic efficacy, in addition to elucidating mechanisms of drug interactions and resistance.

2.3.11 Computational drug screening for VEGF-therapeutics

Computational drug screening has recently been applied to identify possible molecular compounds that selectively inhibit VEGFR2. These screening approaches typically iterate through compounds available in molecular databases, and identify potential novel VEGFR2-inhibitors through a computational structural comparison to an established VEGFR2 inhibitor [180]. The compounds exhibiting the greatest therapeutic potential are then tested experimentally. Such structural screening studies have identified a compound, termed HP-14, that exhibits a four-fold higher reduction in HUVEC proliferation than the established VEGFR inhibitor Vatalanib [181], [182]. Other screening studies have identified compounds that

significantly inhibit VEGFR1 and VEGFR2 phosphorylation to prevent HUVEC tube formation in vitro [183], inhibit VEGFR2 kinase activity and HUVEC wound closure without affecting HUVEC proliferation [184], and inhibit vessel sprouting ex vivo [185]. Further review of anti-angiogenic VEGFR2-targeting therapies identified through computational screening can be found in [186]. This computational screening approach, linked with experimental validation, offers rapid identification of promising VEGF inhibitors that may allow optimizing patient-specific therapeutics.

2.4 Current Challenges in Angiogenesis Research

2.4.1 Overcoming resistance of VEGF-targeting therapeutics.

Overall, computational studies and systems biology have driven angiogenic research fundamentally and to direct angiogenic therapeutics. Many challenges remain to be overcome to obtain complete control of angiogenesis. Overcoming anti-VEGF drug resistances is a large challenge in providing effective cancer treatment by inhibiting angiogenesis [187]–[189]. Such therapeutic resistance was connected with heterogeneity in endothelial cell protein profiles [190], leading to systems biology studies that provided mechanistic insight into anti-VEGF resistance: high VEGFR1 cell subpopulations result in ineffective anti-VEGF treatment [178], a result observed clinically [191]–[193]. Despite such advances, anti-VEGF and other VEGF targeting therapeutics are still met with resistance in many patients [194]. A complete, systematic and quantitative understanding of VEGF signaling is necessary to overcome VEGF-targeted drug resistance and deliver personalized treatment regimes.

2.4.2 Quantifying VEGFR signaling throughout endocytosis.

One primary challenge in achieving complete angiogenic control is to understand the relationship between endocytosis and VEGFR signaling. Recently, intracellular-based receptors have emerged as key signal transducers [195], [196], yet signaling from intracellular VEGFRs remains undefined. While recent computational models have examined intracellular-based VEGFR2 phosphorylation [161] and kinase phosphorylation [158], [159], only the VEGFR recycling pathway was modeled; no known computational models account for VEGFR nuclear translocation or modulation of gene expression via intracellular VEGFRs. Furthermore, the high intracellular expression of VEGFR1 and VEGFR2 [197] indicates that intracellular VEGFRs endocytosis may have a crucial role in mediating VEGFR signaling.

2.4.3 Mapping the VEGF isoform functions.

Another primary challenge in controlling angiogenesis is elucidating the function of all VEGF proteins. Specific functions for most VEGF isoforms remain undefined. While systems biology has identified differential $VEGF_{165}$ and $VEGF_{121}$-VEGFR binding and function, few of the other VEGF isoforms have been studied computationally or experimentally. $VEGF_{xxxb}$ functions in particular remain undefined, but may be important for angiogenesis; a recent study identifying that $VEGF_{165b}$ alters Dll4 expression [198], together with evidence that targeting Delta-Notch signaling may be effective anti-cancer therapeutic [199], implies an important $VEGF_{xxxb}$ role for tumor angiogenesis. Additionally, $VEGF_{xxxb}$ may have higher expression than $VEGF_{xxxa}$ in certain diseases [200], further highlighting the necessity to understand $VEGF_{xxxb}$ functions. Unlocking the mechanisms that mediate VEGF isoform expression, binding, and signaling may be the key to overcoming VEGF therapeutic resistance.

2.4.4 Uncovering the VEGFR1 signaling role.

Similarly, the VEGFR1 signaling function remains poorly defined, and there are currently no known intracellular signaling molecules that have examined VEGFR1 signaling specifically. Computational studies have generally ignored VEGFR1-based signaling due to the its classically defined decoy status in angiogenesis; VEGFR1 is thought to exhibit no intracellular signaling, serving to bind VEGF with high affinity to module VEGF binding and signaling through VEGFR2. However, emerging evidence implies an active VEGFR1 signaling role in angiogenesis: membrane VEGFR1 is upregulated during vascular reperfusion stages in ischemic tissue [201], hypoxic tumor cells, and tumor endothelial cells [202], and VEGFR1 tyrosine kinase-deficient mice exhibit reduced angiogenesis [203]. Furthermore, PlGF stimulates endothelial cell growth and migration [204], [205], and inhibiting PlGF prevents tumor growth and metastasis [206]. Computational models identifying receptor post-translational modifications are able to determine receptor signaling pathways and function [207], [208]; therefore, computational models exploring VEGFR1 post-translational modifications can identify first whether VEGFR1 actively signals, and if so, map the VEGFR1 signaling pathways and VEGFR1-induced cell responses.

2.4.5 VEGF signaling models for clinical applications.

Towards using systems biology to guide angiogenic therapeutics, developing clinically relevant models that allow patient-specific investigation are essential [209], [210]. Developing such personalized models is a nontrivial task [211], necessitating multiscale modeling approaches to capture all clinical features relevant to angiogenesis, such as VEGF interactions at the microscale and hemodynamics at the macroscale [212], [213]. Integrating macroscale blood flow stress with microscale VEGFR signaling may be an important clinical consideration; shear stress induces VEGFR signaling [214], directs vessel patterning [215], and vessel sprouting may

be dependent on fluid flow-directed VEGF gradients [216]. Choosing which modeling approach to use also must be balanced between computational complexity and physiological accuracy; take hemodynamic modeling as an example: while modeling blood properties as Newtonian is less mathematically complex than modeling the shear thinning properties of blood, Newtonian models do not provide physiologically relevant hemodynamics [101]. Comprehensive angiogenesis computational models that guide therapeutic development for clinicians in an accessible, clinically relevant way is a large challenge in systems biology today, but would provide a platform for effective personalized medicine that no other approach can.

2.5 Dissertation Research Overview

To address the challenge of overcoming drug resistance in anti-angiogenic cancer therapeutics, I developed a whole-body model quantifying how VEGFR heterogeneity directs bevacizumab (anti-VEGF) efficacy [178]. I also developed a benchmark platform for quantifying hemodynamics [101], as a first step to overcoming the challenge of modeling microscale VEGF kinetics with macroscale hemodynamics for physiologically and clinically relevant models. VEGFR heterogeneity was experimentally measured and converted to quantitative parameters for computational modeling using an approach I helped develop with my lab collaborators [217]. From this VEGFR heterogeneity study, I identified that high VEGFR1 levels, present on tumor associated endothelial cell subpopulations, result in ineffective anti-VEGF treatment [178], a result also found in clinical trials [191]–[193]. This effect did not occur from physiological VEGFR2 levels. From this model, I identified the anti-VEGF resistance mechanism in patients with high VEGFR1: VEGFR1 acts as a pool to protect VEGF from anti-VEGF.

Particularly, this resistance mechanism can be broken into three stages: (i) before anti-VEGF administration, (ii) short-term effects of anti-VEGF treatment, and (iii) long-term effects

of anti-VEGF treatment (Fig 2.3). (i) Before anti-VEGF is administered, high VEGFR1 subpopulations reach an equilibrium state exhibited by a high VEGF concentration bound at the cell membrane and low free VEGF concentration extracellularly. Conversely, low VEGFR1 subpopulations exhibit a low VEGF concentration bound at the cell membrane and high extracellular VEGF concentration at equilibrium. (ii) At short time points after anti-VEGF treatment, both high and low VEGFR1 subpopulations exhibit nearly complete sequestration of free VEGF, which is then rapidly cleared from the body. This results in a concentration gradient of high VEGF at the cell membrane and low extracellular VEGF, causing VEGF to unbind from the cell surface and diffuse into the extracellular space. (iii) Due to this VEGF diffusion away from the cell surface, high VEGFR1 subpopulations result in an increased free VEGF concentration following anti-VEGF treatment; low VEGFR1 subpopulations conversely result in a decreased free VEGF concentration (Fig 2.3).

The anti-VEGF resistance exhibited by high VEGFR1 subpopulations is characterized by two additional physiological phenomena: high VEGF-VEGFR1 binding and high VEGF-VEGFR1 internalization (Fig 2.3). This first physiological phenomena, high VEGF-VEGFR1 binding, implies these subpopulations purposefully express high VEGFR1 levels to produce high VEGFR1 signaling. However, the VEGFR1 signaling role and pathways has not been previously defined. Chapter 3 discusses my research to understand the VEGFR1 signaling role, showing that VEGFR1 actively signals to promote cell migration and proliferation through PLC_{γ} and PI3K pathways. This second physiological phenomena, high VEGF-VEGFR1 internalization, implies that endocytosis is an important VEGFR1 signaling regulator. However, how endocytosis quantitatively regulates receptor signaling is not defined. Chapter 4 discusses my research to quantify the relationship between endocytosis and receptor signaling, showing that

receptor signaling primarily occurs intracellularly from endocytic vesicles, late endosomes, and the nucleus. Within these chapters, I also discuss the implications of my results to the larger fields of angiogenesis, systems biology, and therapeutics.

2.6 Figures and Tables

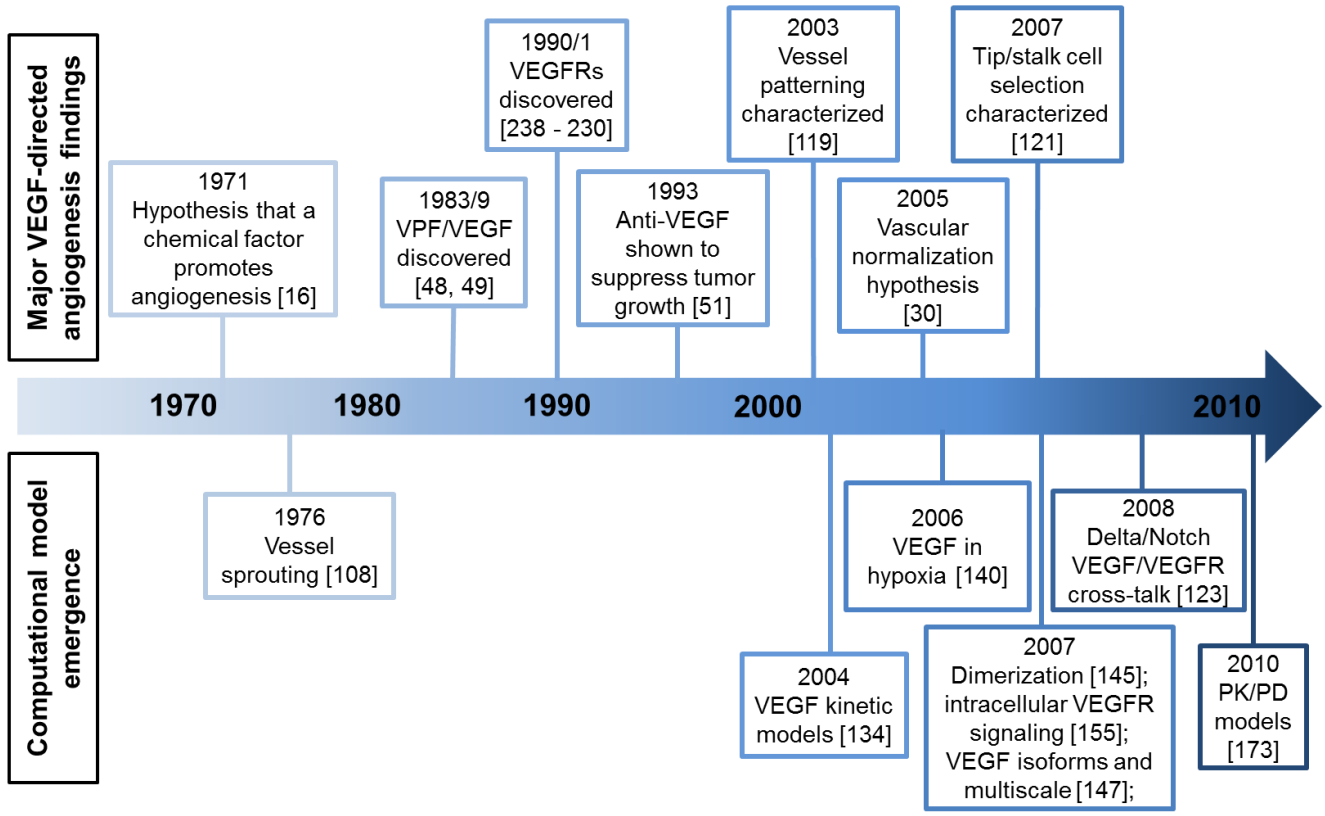

Figure 2.1: Timeline of VEGF-directed angiogenesis research.

Timeline highlighting the major discoveries and emergence of computational models in VEGF-directed angiogenesis. References refer to the discovery or the first known study to develop a computational model for that specific research area.

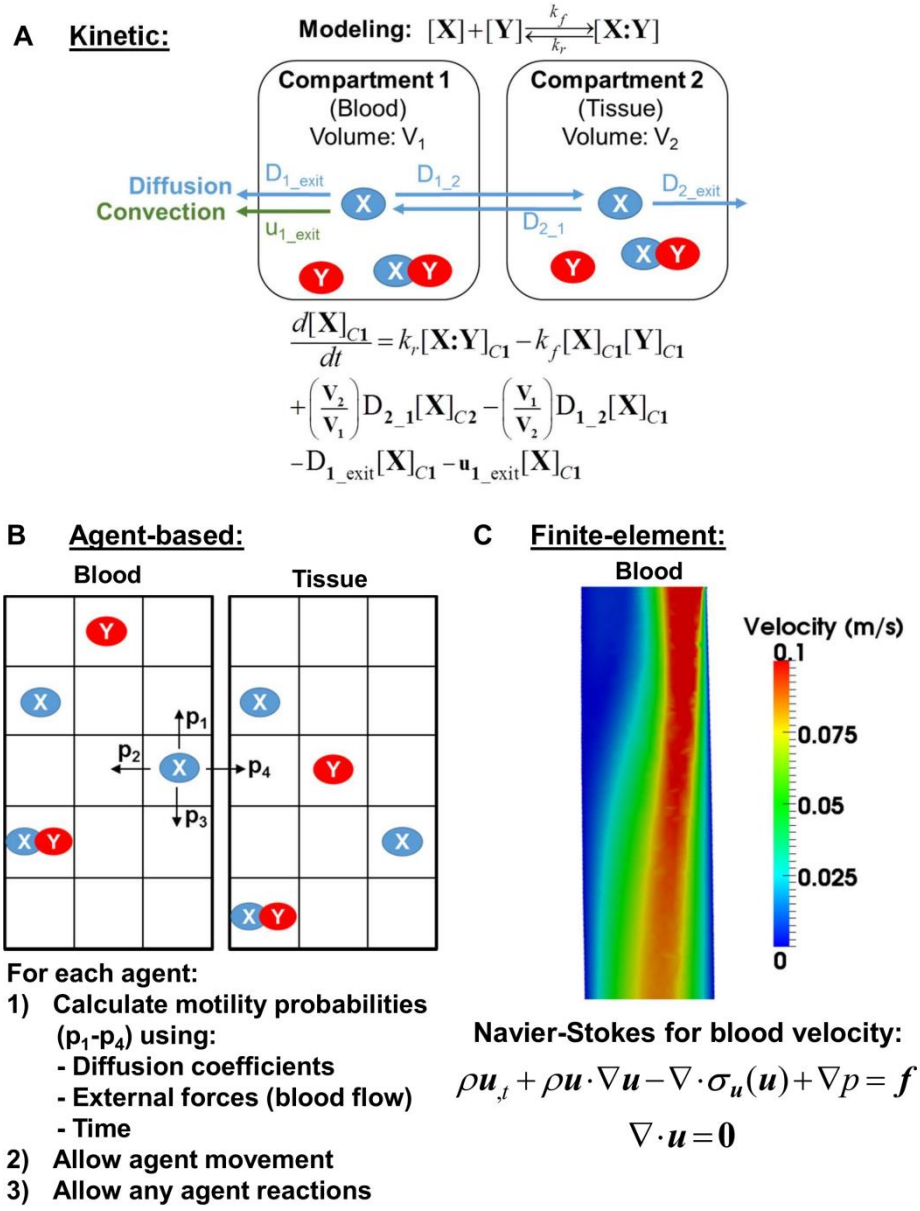

Figure 2.2: Example systems biology techniques to model protein transport and interactions.

(A) A deterministic kinetic compartmental model containing a single chemical reaction involving two molecules [X] and [Y] binding to form [X:Y], all with units of M. The reaction is defined by the forward rate k_f ($M^{-1}s^{-1}$) and reverse rate k_r (s^{-1}). In this example, X is a free molecule able to move across compartments, while Y is anchored within the compartment. Compartment 1 is blood that is spatially close enough to interact with tissue defined by Compartment 2, both with units of L. Blue arrows indicate diffusion, while the green arrow indicates convention from blood flow. For this kinetic model, diffusion and convection terms are assumed to have units of s^{-1}. An example ordinary differential equation governing [X] in Compartment 1 is shown. (B) An agent-based model using a grid for spatial discretization. Pseudo-rules are given for directing agent motility and interactions. (C) Example of finite element modeling to determine blood flow velocities, taken from simulations performed in [101]. The blood velocity field can be integrated with kinetic or agent-based models to provide more physiologically relevant convection rates or movement probabilities, respectively. Conversely, the tissue could also be modeled with finite elements, and advection-diffusion-reaction could be solved.

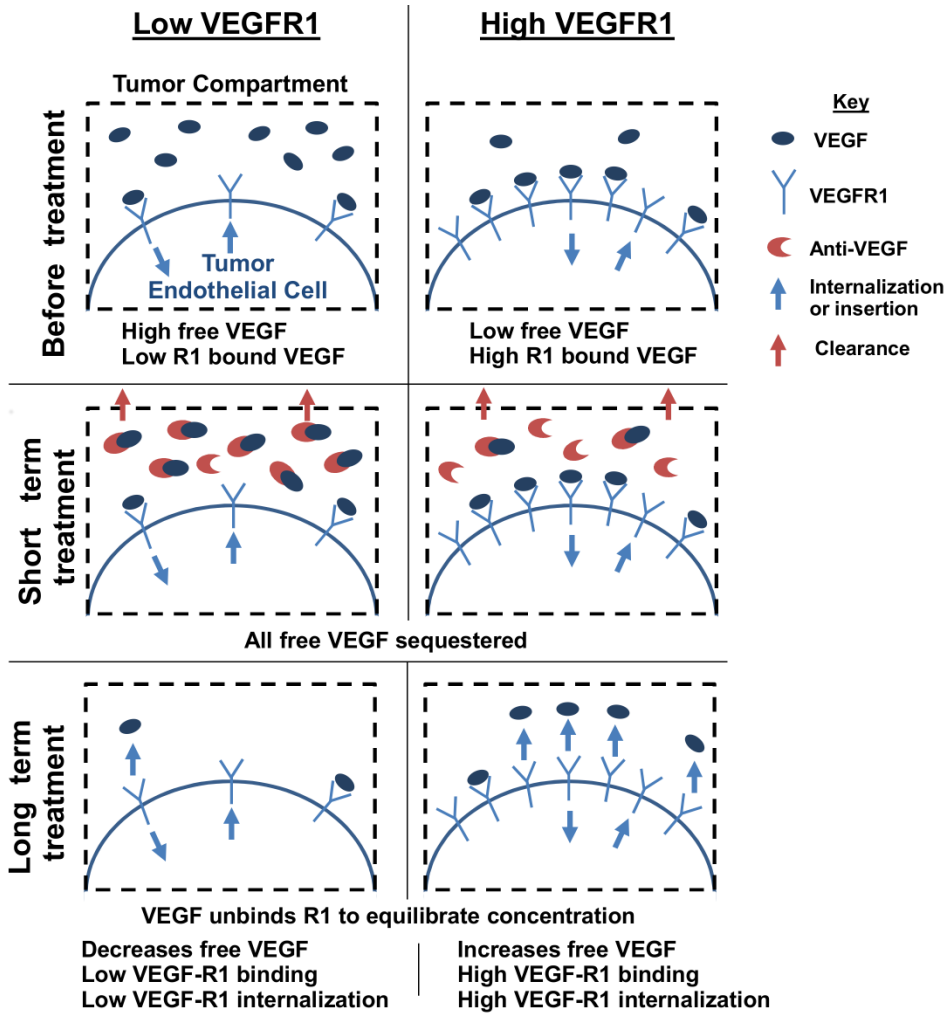

Figure 2.3: Tumor endothelial cell subpopulations with high VEGFR1 levels result in ineffective anti-VEGF treatment.

Tumor endothelial cell subpopulation responses to anti-VEGF treatment based on whether they express low (left) or high (right) VEGFR1 levels, derived from results found in [178]. High VEGFR1 subpopulations are resistanct to anti-VEGF treatment, as free VEGF increases following anti-VEGF treatment. Low VEGFR1 subpopulations conversely are not resistance to anti-VEGF treatment, as they exhibit reduced free VEGF following anti-VEGF treatment. High VEGFR1 subpopulations are additionally characterized by high VEGF-VEGFR1 binding and high VEGF-VEGFR1 internalization.

Table 2.1: The VEGF family proteins.

Protein	Isoform	Family Interactions	Primary Function	Discovery
VEGF-A		VEGFR1, VEGFR2 VEGF-A (homodimer) PlGF (heterodimer)	Pro-angiogenic	[48], [49]
	$VEGF\text{-}A_{110}$			[218]
	$VEGF\text{-}A_{121}$			[219]
	$VEGF\text{-}A_{145}$			[220]
	$VEGF\text{-}A_{148}$		Unknown	[221]
	$VEGF\text{-}A_{165}$		Pro-angiogenic	[219]
	$VEGF\text{-}A_{183}$			[222]
	$VEGF\text{-}A_{189}$			[219]
	$VEGF\text{-}A_{206}$			[223]
	$VEGF\text{-}A_{121b}$		Anti-angiogeneic	[61]
	$VEGF\text{-}A_{145b}$			[224]
	$VEGF\text{-}A_{165b}$			[225]
	$VEGF\text{-}A_{189b}$			[61]
VEGF-B		VEGFR1 VEGF-B (homodimer)	Neurogenesis and embryogenesis	[62]
	$VEGF\text{-}B_{167}$			[62]
	$VEGF\text{-}B_{186}$			[63]
VEGF-C		VEGFR3, VEGFR2 VEGF-C (homodimer)	Lymphangiogenesis	[226]
VEGF-D		VEGFR2, VEGFR3 VEGF-D (homodimer)	Lymphangiogenesis	[76]
PlGF		VEGFR1 PlGF (homodimer) VEGF-A (heterodimer)	Pro-angiogenic	[227]
	PlGF-1			[78]
	PlGF-2			[78]
	PlGF-3			[79]
	PlGF-4			[80]
VEGFR1		VEGF-A, VEGF-B, PlGF VEGFR1 (homodimer) VEGFR2 (heterodimer)	Angiogenesis	[228]
	sVEGFR1		Anti-angiogenic	[82]
VEGFR2		VEGF-A VEGFR2 (homodimer) VEGFR1, VEGFR3 (heterodimer)	Angiogenesis	[229], [230]
	sVEGFR2		Anti- angiogenic Anti-lymphangiogenic	[231]
VEGFR3		VEGF-C VEGFR3 (homodimer) VEGFR2 (heterodimer)	Lymphangiogenesis	[232]
	sVEGFR3		Anti-lymphangiogenic	[84]

Currently characterized ligands, receptors, and their isoforms in the VEGF family. Inter-family interactions, function, and discovery of each VEGF family protein are given. I list the general, primary function for each protein; note that specific function may differ depending on cell type or physiological context.

Table 2.2: Systems biology modeling approaches.

Computational Method	Scale	Functional Outputs	Angiogenesis applications	Reference
Kinetic: Deterministic	Molecules in continuum	Temporal concentration	Protein interactions Protein transport Drug PK/PD	[233]
Kinetic: Stochastic	Molecules	Temporal concentration	Protein interactions Protein transport Drug PK/PD	[233]
Agent-based	Molecular Cell	Spatiotemporal agent dynamics	Protein or cell motility Protein or cell interactions Cell proliferation	[96]
Molecular Modeling	Molecular	Binding potential	Structural analysis Inhibitor identification	[98]
Finite element	Tissue Fluids	Continuum mechanics	Hemodynamics Vessel sprouting Drug delivery	[100]
Multivariate	Cell Tissue	Signal-to-response	Stimuli to cell response	[234]

Typical computational models used in systems biology, the scale(s) of the quantities they model (i.e. molecules, cell, tissue), functional output(s) given by the model, specific applications to angiogenesis, and references describing the methods in detail.

CHAPTER 3

VEGFR1 PROMOTES CELL MIGRATION AND PROLIFERATION THROUGH PLC$_\gamma$ AND PI3K PATHWAYS

3.1 Introduction

Vascular endothelial growth factor (VEGF) is a potent angiogenesis promoter, and is therefore a promising target for many pathologies, including vascular disease and cancer [235]–[239]. Despite this promise, VEGF targeted therapies are not clinically effective for many patients [187], [188]. As such, there is an urgent need to develop a greater understanding of how VEGF-promoted angiogenesis can be controlled, mechanistically, to improve the efficiency and specificity of current angiogenic treatments.

VEGF receptor-1 (VEGFR1) has emerged as a predictive biomarker for anti-VEGF therapeutics in cancer [178], [240], [241], but its signaling mechanisms and function remain incompletely defined. VEGFR1 is conventionally described as a decoy receptor that does not produce intracellular signals [242], due to its high VEGF affinity but low phosphorylation compared to VEGFR2 [243]. However, emerging evidence suggests an active VEGFR1 signaling role in angiogenesis: membrane VEGFR1 is upregulated during vascular reperfusion stages in ischemic tissue [201]; and VEGFR1 tyrosine kinase-deficient mice exhibit reduced angiogenesis in both hypoxic tumor cells and tumor endothelial cells [202][203]. Furthermore, VEGFR1 demonstrates tumor activity via placental growth factor (PlGF) [204], [205]; wherein, inhibition of this VEGFR1 specific ligand, prevents tumor growth and metastasis [206]. Given this emerging evidence, and the VEGFR1 biomarker role in cancer, I believe that VEGFR1 must have an important signaling role, and I aim to delineate it.

VEGFR1 signaling can be determined by systems biology: mathematically defining receptor signaling. The power of a mechanistic approach is its faithfulness to the biological structure. Towards this end, the two key signaling mechanism post-VEGFR1 ligation include: (1) carboxy-terminal receptor phosphorylation at specific tyrosine sites and (2) adapter binding at these sites. I define these as the key steps, because they structurally facilitate the second messenger signaling that directs the angiogenic hallmarks of cell proliferation and migration [161], [244], [245]; as such, these steps may together predict those hallmarks. Indeed, there is evidence that tyrosine site phosphorylation is linked to cell response: cell proliferation results from phosphorylation at the VEGFR2 Tyr^{1175}; whereas, phosphorylation at the VEGFR2 Tyr^{1214} has been linked to cell migration [161]. Cell responses are similarly linked to adapter binding and adapter phosphorylation atRTK phosphor-tyrosine sites [246]–[250] While these tyrosine site-based and adapter-based approaches are useful to predict cell response, they are often analyzed separately, which does not enable a unified understanding of how RTK structure directs cell function [251], [252]. Therefore, computational models that integrate these key elements of receptor activation, would advance structure-based prediction of VEGFR1 signaling.

Here, I predict how VEGFR1 directs cell response by developing, comparing, and validating a structure-based model of carboxy-terminal VEGFR1 activation and a general VEGFR1 activation model. The models quantitatively rank adapter protein contributions to VEGFR1-mediated cell migration and cell proliferation. Model comparison reveals how degrees of model "sloppiness" affect predictions of receptor activation and cell response. Computational predictions of cell response to drug treatment are validated via functional assays. Together, my modeling approach provides a new, validated tool for structure-based prediction of cell signaling, applied to grant the exigent mapping of the angiogenic receptor VEGFR1.

3.2 Results

3.2.1 VEGFR1 primarily induces cell migration.

Following VEGF binding, the initial intracellular VEGFR1 signal transduction steps include: receptor dimerization; autophosphorylation, a post-translational modification (PTM) of carboxy-terminal tyrosines; adapter binding to phospho-tyrosine residues (Fig 3.1); and adapter phosphorylation. To identify how the aggregated cell response depends on such site-specific PTMs, I models where adapter binding and PTMs occur non-specifically (nonspecific model) and adapter binding and PTM processes represent known receptor binding specificity (specific model) (Fig 3.2A). Both the nonspecific and specific models predict that VEGFR1 primarily induces cell migration (Fig 3.2B). This is evidenced by migration exhibiting both the highest integrated cell response (Fig 3.2C) and the highest phosphorylation amplitude (Fig 3.2D). The specific model reveals mechanistic insight into the migratory cell response: the VEGFR1 tyrosine sites specify cell migration signaling. This is evidenced by the specific model exhibiting a greater contribution to migration signaling; the integrated migration response, relative to proliferation and degradation, increases 16% in the specific model, relative to the nonspecific model (Fig 3.2C). Furthermore, the migration phosphorylation amplitude increases 23% in the specific model, relative to the nonspecific model (Fig 3.2D). Therefore, I predict that VEGFR1 tyrosine sites are structured to specify cell migration signaling.

3.2.2 VEGFR1 tyrosine sites specify PLC_γ, and PI3K activation through adapter binding competition.

VEGFR1 tyrosine sites specify cell migration signaling through PLC_γ and PI3K phosphorylation (Fig 3.2E). PLC_γ and PI3K are the only adapters with increased integrated responses (Fig 3.2F) and phosphorylation amplitudes (Fig 3.2G) between nonspecific and

specific models. This unique increase in PLC_γ and PI3K activation is due to their binding preference with the VEGFR1 phospho-tyrosine sites (Fig 3.1A); only two adapters bind VEGFR1 simultaneously (Appendix A, Table A.4-A.5): one adapter at Tyr^{794} and a second adapter at another tyrosine site. PI3K and PLC_γ are the only adapters that bind Tyr^{794}, thus experiencing less VEGFR1-binding competition than the other adapters, resulting in greater activation. This is evidenced by PLC_γ and PI3K activation preferentially occurring at Tyr^{794} (Appendix A, Fig A.1).

3.2.3 VEGFR1-promoted cell responses are regulated by coordinated PLC_γ, PI3K, and Src activation.

To predict which adapters primarily direct VEGFR1 cell responses, I perform sensitivity analyses between adapter concentrations and cell responses with the specific site model. I predict that cell proliferation and migration are primarily mediated by PLC_γ and PI3K concentrations, in that order (Fig 3.3A-B, 3.3D-E). Conversely, degradation is primarily mediated by PLC_γ and Src concentrations, in that order (Fig 3.3C, F). These three adapters direct VEGFR1 signaling in a coordinated fashion: increasing the PLC_γ (Fig 3.4A-B), PI3K (Fig 3.4C-D), or Src (Fig 3.4E-F) concentration to $\sim 2 \cdot 10^4$ molecules/cell increases phosphorylation of the other two adapters. Increasing PI3K (Fig 3.4C) and Src (Fig 3.4E) concentrations above $\sim 2 \cdot 10^4$ molecules/cell increases the PLC_γ integrated response, indicating that PI3K and Src promote PLC_γ phosphorylation. Together with the result that VEGFR1 is structured to preferentially activate PLC_γ and PI3K, I predict that PLC_γ and PI3K mediate VEGFR1 cell responses through coordinated activation involving Src.

3.2.4 Specific tyrosine site modeling captures adapter phosphorylation dynamics.

The specific model accurately predicts PI3K phosphorylation dynamics and magnitude in VEGF-treated RAW 264.7 macrophages, evidenced by the X^2 goodness-of-fit test (Fig 3.5A) [253]. The specific model accurately predicts that PI3K phosphorylation is abrogated by the PI3K-specific inhibitor Wortmannin, while relatively unaffected by inhibiting other adapters (Fig 3.5A). Conversely, the nonspecific model accurately predicts relative phosphorylation trends (Appendix A, Fig A.2), but not phosphorylation magnitudes; the nonspecific model underestimates PI3K phosphorylation by 81% and fails the X^2 goodness-of-fit test (Fig 3.5A). Model predicted PLC_γ phosphorylation shows the same trend: the site-specific model accurately predicts PLC_γ phosphorylation given VEGF and inhibitor treatments, whereas the nonspecific model fails validation (Fig 3.5B). The specific model also accurately identifies which VEGFR1-associated adapters are not critical to VEGFR1 signaling: Abl phosphorylation is not detected as predicted (Fig 3.5C). This validation highlights that modeling specific receptor tyrosine sites is essential to capture adapter phosphorylation magnitudes, and is translatable across cell lines, whereas the conventional approach to model a nonspecific receptor tyrosine site fails physiological validation.

3.2.5 PI3K and PLC_γ are critical to VEGFR1-induced cell migration.

I validate the model prediction that VEGFR1 promotes cell migration, which is primarily regulated by PLC_γ, followed by PI3K. I find that VEGFR1 does promote cell migration: VEGF induces significant RAW migration in vitro (Fig 3.6A-B). Furthermore, VEGFR1-induced migration is primarily regulated by PLC_γ, followed by PI3K (Fig 3.6A-B). The specific VEGFR1 tyrosine site model accurately quantifies adapter contributions to RAW migration; RAW migration decreases 79% in vitro with PLC_γ inhibition (72% predicted) and 64% with PI3K

inhibition (64% predicted) (Fig 3.6B). Additionally, the model accurately identifies that Abl is insignificant to VEGFR1-induced migration (Fig 3.6B).

3.2.6 VEGFR1-induced cell proliferation is primarily mediated via PLC_γ.

I validate the model prediction that VEGFR1 promotes cell proliferation, primarily through PLC_γ activation. VEGFR1 promotes cell proliferation: VEGF induces significant RAW proliferation in vitro (Fig 3.6C). I validate the prediction that VEGFR1-induced migration is only significantly regulated by PLC_γ; RAW proliferation decreases 50% in vitro with PLC_γ inhibition (Fig 3.6C). Conversely, PI3K and Abl inhibition do not significantly affect cell proliferation, accurately predicted by the specific VEGFR1 site model.

3.3 Discussion

The VEGFR1 status as a decoy receptor may not fully capture its signaling role [178]; however, few studies have probed VEGFR1 signaling [242], which is difficult to map due to the low phosphorylation levels VEGFR1 exhibits. As VEGFR1 is a tyrosine kinase receptor, a receptor family known to signal through coupling with the SH2 domain of adapters [254], examining VEGFR1-adapter binding can offer new insight into VEGFR1 signal propagation. To this end, I developed and validated a receptor-adapter interaction modeling approach, which accurately predicts cell responses from adapter phosphorylation, and is translatable across receptor and cell types. Combining this modeling approach with experimental validation identified that VEGFR1 induces cell migration via PLC_γ and PI3K pathways, and induces proliferation via a PLC_γ pathway.

3.3.1 Novel modeling techniques allow prediction of receptor signaling roles.

My modeling approach quantifies adapter phosphorylation and cell responses simultaneously to map unknown receptor signaling pathways. My modeling approach refines the receptor signaling models by integrating the pioneered approaches that accurately predict select adapter-receptor interactions [158], [255]–[257] and cell responses [258]–[260] from external stimuli. I additionally advance receptor signaling models by providing the ability to map unknown receptor pathways. Furthermore, I show that this approach to model specific receptor tyrosine sites offers physiological relevancy; both nonspecific and specific VEGFR1 tyrosine site models are validated when only the shape of adapter phosphorylation over time is considered (Appendix A, Fig A.2), but only the specific tyrosine site model accurately predicts adapter phosphorylation magnitudes (Fig 3.5). My modeling approach presented here is advantageous as it maps unknown receptor signaling from adapter activation to cell response, simultaneously, with high physiological relevancy. Additionally, my receptor-adapter modeling approach can be easily integrated into pharmacokinetic/pharmacodynamic models, which accurately quantify extracellular VEGF concentration dynamics in response to anti-VEGF drugs [174], [179], [261], to provide a clinically relevant platform to explore how anti-VEGF drugs mediate VEGFR signaling: through altering extracellular VEGF concentrations, VEGF-VEGFR interactions, and subsequent intracellular VEGFR signaling. Such a model integration would overcome one of the major challenges for developing personalized, clinically relevant computational platforms reviewed in [211], [262]: providing a multiscale model to comprehensively investigate biological systems; in this case, comprehensively modeling receptor signaling at the tissue macroscale and intracellular microscale.

3.3.2 qFlow cytometry accurately quantifies membrane receptors.

My ability to accurately quantify VEGFR1 signaling highlights the power of integrating experiment and computation to provide new biology insight: empirical evidence defined VEGFR1-adapter reactions, kinetics, and concentrations for the model, which in turn provided testable VEGFR1 signaling predictions that I confirmed experimentally. This first step, model parameterization, is essential to develop physiologically relevant models, as previously described [91], [263], [264]. VEGFR concentration parameterization was achieved with quantitative flow (qFlow) cytometry [201], [265], [266], a recently established high-throughput approach that detects receptor expression with a fluorescent affinity probe and quantifies absolute receptor levels using fluorescent calibration standards [267]. While qFlow cytometry is becoming an essential tool for parameterizing receptor concentrations in computational models [158], [159], [163], [174], [176]–[179], analogous methods for quantifying other receptor signaling parameters, such as adapter phosphorylation rates, are not well established. As such, most computational models contain parameters that are estimated or generalized across multiple species or interactions [268]computational models; Bose and Janes recently developed one such method for high-throughput characterization of signal molecule dephosphorylation kinetics via phosphatase activity [269]. Development of such high-throughput methods to completely parameterize receptor signaling models, from species concentrations to specific kinetics for every interaction, would unlock additional options for tuning receptor signaling, such as by targeting specific phosphatases, while maintaining high physiological relevancy.

3.3.3 VEGFR1 preferentially activates PLC_γ in burst activation to induce cell migration, possibly through Ca^{2+} signaling.

I show that VEGFR1-induced PLC_γ activation is required for cell migration, and hypothesize this VEGFR1-PLC_γ-mediated migration involves Ca^{2+} signaling. PLC_γ

phosphorylation is known to activate Ca^{2+} influx [270], [271] in oscillatory bursts [272]–[275]. Furthermore, directed cell migration requires Ca^{2+} pulses near the leading edge of the cell [276]–[278]. From this prior knowledge, combined with the delta function-like PLC_γ activation observed in the model, I hypothesize that VEGFR1 phosphorylates PLC_γ in quick bursts to induce Ca^{2+} pulses and direct cell migration. This burst PLC_γ activation could explain how cells migrate towards a VEGF gradient, with a possible mechanism being as follows: (1) VEGF binds plasma membrane VEGFR1 on the cell facing the gradient; (2) VEGFR1 recruits and phosphorylates PLC_γ; and (3) phosphorylated PLC_γ causes Ca^{2+} pulses by activating Ca^{2+} channels, a well-established mechanism [279]–[281] reviewed by Mikoshiba [282], initiating migration towards the VEGF gradient. This mechanism is further supported by experimental data showing that Ca^{2+} pulse following VEGF simulation is required for HUVEC migration [280]. As the extent of directed cell migration is dependent on growth factor gradient patterns [283], I hypothesize that VEGFR1-PLC_γ activation acts as a VEGF gradient sensor to determine both cell migration direction and magnitude. Future work experimentally probing PLC_γ-mediated migration, is necessary to validate this mechanism.

3.3.4 Ca^{2+} signaling may indirectly regulate PI3K activation by VEGFR1.

I identified PI3K as a primary adapter directing VEGFR1-mediated cell migration. Primarily, PI3K is known to promote cell migration through Akt activation [284], [285], which also involves Ca^{2+} signaling; PI3K/Akt activation translocates Ca^{2+} channels to the cell membrane, inducing Ca^{2+} entry into cells, and subsequent cell migration [286]. However, PI3K activation does not induce Ca^{2+} signaling in HUVECs [287]; rather, PI3K is activated by Ca^{2+} to promote HUVEC migration [288]. Thus, PI3K may play an important role in indirectly activating Ca^{2+} signaling and HUVEC migration.

3.3.5 The PLC_γ, PI3K, and Src dependent relationship may form a Ca^{2+} signaling regulatory loop.

I observed a dependent relationship between VEGFR1-induced PLC_γ, PI3K, and Src phosphorylation. As PI3K and PLC_γ cooperate to initiate Ca^{2+} signaling [289], I hypothesize that PI3K, PLC_γ, and Ca^{2+} have a dependent relationship to robustly mediate VEGFR1-induced cell migration. Furthermore, PLC_γ induced Ca^{2+} signaling phosphorylates Src [290], and Src phosphorylates PLC_γ [287], [290], [291] and PI3K [292]–[294]. Thus, I hypothesize from these studies and my results that VEGFR1 is structured to preferentially activate a PLC_γ, PI3K, and Src regulatory loop mediating Ca^{2+} signaling (Fig 3.7), and subsequent cell migration.

3.3.6 VEGFR1-promoted hematopoietic progenitor cell migration may be required for tumor cell metastasis.

The strong VEGFR1 migratory signal I identify here indicates VEGFR1 signaling may be required for hematopoietic progenitor cell (HPC) migration to form pre-metastatic niche clusters. Metastasis from the primary tumor site requires circulating tumor cells to extravaste into secondary sites [295]. Prior to this process, the tumor primes pre-metastatic niches, sites receptive to recruiting circulating tumor cells, to direct at which secondary sites metastasis occurs [296]. These pre-metastatic niches are characterized by clustering of VEGFR1 positive HPCs; inhibiting VEGFR1 on HPCs prevents pre-metastatic niche formation and tumor cell metastasis [297]. This effect of pre-metastatic niche formation being prevented with VEGFR1 inhibition may be explained by HPC migration requiring VEGFR1 signaling; thus, inhibiting VEGFR1 would prevent HPC migration, HPC clustering, and subsequent tumor cell metastasis. Furthermore, Akt activation has been implicated in macrophage-assisted cancer cell invasion [298], supporting my hypothesis that VEGFR1-PI3K-Ca^{2+} signaling (Fig 3.7) promotes

macrophage migration. Therefore, targeting VEGFR1-induced HPC migration may be a therapeutic option to prevent tumor cell metastasis.

3.3.7 VEGFR1 can be comprehensively modeled by incorporating adapter-adapter interactions and specific phosphatases.

My modeling approach accurately predicted adapter phosphorylation and cell responses by quantifying complex formation between specific VEGFR1 tyrosine sites and single adapters, with adapter dephosphorylation occurring through a generalized phosphatase. Building upon this validated model to include adapter-adapter interactions and specific phosphatases would comprehensively represent VEGFR1 signaling. Modeling adapter-adapter interactions would identify how VEGFR1 signaling is directed through adapter cooperativity; adapter-adapter interactions occur via adapter SH3 domains [299] to form larger signaling complexes that direct differential cell outcomes [300], [301]. The ability to accurately model multi-adapter complex formation with VEGFR1 is currently limited however, as no known experimental or computational studies have mapped the adapter-adapter interactions downstream VEGFR1. This limitation may be overcome by identifying VEGFR1-associated adapter-adapter interactions from VEGF-induced protein phosphorylation dynamics, a predictive approach validated with the epidermal growth factor receptor signaling axis [302].

Modeling specific phosphatases would identify additional VEGFR1-targeting therapeutics; since different phosphatases bind specific adapters to dynamically regulate receptor signaling [303], VEGFR1-induced adapter phosphorylation and cell responses could be directed by targeting specific phosphatases. The ability to model specific phosphatases is currently limited however, as the specific phosphatases involved in VEGFR1 signaling, and their adapter interaction kinetics, have not been determined. This limitation may be overcome using the high-

throughput assay for identifying phosphoprotein-specific phosphatases and kinetics developed by the Janes lab [269]. Overall, incorporating adapter-adapter interactions and phosphatase specificity into the VEGFR1 model would provide further insight into how VEGFR1 signaling is directed systemically, and identify additional proteins or interactions that can targeted to tune VEGFR1 signaling.

3.3.8 Conclusions.

My modeling approach has identified that VEGFR1 actively promotes cell migration and proliferation primarily via the PLC_{γ} and PI3K pathways, and has posited a new hypothesis that adapter coordination and Ca^{2+} signaling may be regulate this VEGFR1-mediated migratory response. These findings critically advance our understanding of angiogenesis by providing a structurally-based mechanism for VEGFR1 function. These findings and my modeling platform also offer mechanistic guidance for developing therapeutics targeting VEGFR1 signaling. This also represents a paradigm shift, since VEGF, generally, and VEGFR2 are primary targets for drug discovery. This modeling approach provides a foundation to fully understand receptor signaling mechanisms, an essential step to develop effective angiogenic therapeutics for vascular diseases and cancers.

3.4 Materials and Methods

3.4.1 Computational models.

VEGFR-adapter interaction models are defined by ordinary differential equations and solved with the SimBiology toolbox in MATLAB. In general, the VEGFR-adapter scheme interaction scheme follows:

$$
\begin{aligned}
&\mathrm{VEGF+VEGFR} \underset{\mathrm{koff_{VEGF}}}{\overset{\mathrm{kon_{VEGF}}}{\rightleftarrows}} \mathrm{pVEGFR} \\
&\mathrm{pVEGFR+A} \underset{\mathrm{koff_{A}}}{\overset{\mathrm{kon_{A}}}{\rightleftarrows}} \mathrm{[pVEGFR{:}A]} \\
&\mathrm{[pVEGFR{:}A]} \xrightarrow{\mathrm{kp}} \mathrm{[pVEGFR{:}pA]} \\
&\mathrm{[pVEGFR{:}pA] + PTPN} \underset{\mathrm{koff_{PTPN}}}{\overset{\mathrm{kon_{PTPN}}}{\rightleftarrows}} \mathrm{[pVEGFR{:}pA{:}PTPN]} \\
&\mathrm{[pVEGFR{:}pA{:}PTPN]} \xrightarrow{\mathrm{kd_{PTPN}}} \mathrm{pVEGFR + [A{:}PTPN]}
\end{aligned}
\tag{3.1}
$$

for each adapter A and both VEGFRs, where PTPN are phosphatases. Model predicted adapter phosphorylation in HUVECs shows good agreement to previous experimental data (Appendix A, Fig A.2). VEGFR1 and VEGFR2 are both modeled for this validation (Fig 3.1), as HUVECs express both receptors. Following this validation, I examine adapter-VEGFR1 interactions specifically to determine the VEGFR1 function. See Appendix A for details.

3.4.2 Protein concentrations.

HUVEC protein concentrations are determined by Western blot intensity, relative to a known protein concentration, assuming a linear relationship between protein band intensities (Appendix A, Table A.1). I assume PTPN acts as an “infinite reservoir”; the PTPN concentration is sufficiently high to not be a limiting species in any reaction.

3.4.3 Kinetics parameters.

Each adapter is assumed to have the same interaction kinetics (on-rate and off-rate) for both VEGFR1 and VEGFR2, and is the same for all tyrosine sites (Appendix A, Table A.2). Adapter-VEGFR interaction kinetics are assumed identical to adapter-EGFR interaction kinetics. If adapter-VEGFR or adapter-EGFR interaction rates are unavailable, I assume the rates between the SH2 domain of the adapter and a phosphorylated tyrosine kinase fragment is identical to the

adapter-VEGFR rates. (4) I assume a 1 pL cell volume, to convert rates from M to molecules/cell.

3.4.4 Adapter phosphorylation.

All adapter phosphorylation rates (kp) are 0.01 s^{-1}, so adapter phosphorylation is only dependent on VEGFR interaction kinetics. Adapters do not undergo auto-dephosphorylation, and are only dephosphorylated by phosphatases. A generalized phosphatase (PTPN) binds and dephosphorylates all adapters, with the same interaction kinetics and dephosphorylation rate.

3.4.5 Predicting cell response from adapter phosphorylation.

The degradation cell response is identical to c-Cbl phosphorylation; only c-Cbl contributes to a degradation cell response. Proliferation and migration cell responses are determined by a weighed sum of adapter phosphorylation. Weights are calculated by the contribution each adapter provides towards the specific cell response, as determined experimentally (Appendix A, Table A.3).

3.4.6 Tyrosine site specificity.

Multiple adapters can bind a single receptor if the combined size of the adapters is smaller than the available space between tyrosine sites (Appendix A, Table A.4-A.5). Adapters bind the receptor in 1-dimension (the y-direction). Total adapter sizes are determined by measuring the maximal space the adapter crystal structure occupies in the y-direction. The center of an adapter binds a VEGFR tyrosine site; thus, the amount of space a receptor occupies between VEGFR tyrosine sites is half the total adapter size. I measure the average distance between VEGFR amino acids, and use that distance to determine the space between VEGFR tyrosine sites. For example, the distance between individual amino acids in VEGFR1 was

measured as 0.171 Å/amino acid, so the distance between tyrosine sites Tyr^{1242} and Tyr^{1333} is 15.6 Å.

3.4.7 Experimental Methods.

Experiments were performed using murine RAW 264.7 macrophages due to their high VEGFR1 expression (Appendix A, Fig A.3), making them an ideal cell line to study VEGFR1 signaling. RAW 264.7 macrophages were cultured in Dulbecco's Modified Eagle's Medium (DMEM) supplemented with 10% fetal bovine serum (FBS) and 1% penicillin-streptomycin (PS). Cells were maintained in a humidified incubator at 37 ^{o}C and 5% CO_2. Murine VEGF-A_{164} was purchased from BioLegend, and all inhibitors (Wortmannin, U73122, and Imatinib Mesylate) were purchased from Selleckchem. ELISA kits were purchased from Assay Biotechnology. The MTT cell proliferation assay kit was purchased from Thermo Fisher Scientific.

3.4.8 Quantifying protein phosphorylation.

RAWs were seeded into a 96-well plate, stimulated with VEGF or any inhibitors for specified times, and the phosphorylated and total proteins of interest (PLC_{γ}, PI3K, and Abl) were measured using ELISAs. See SI Materials and Methods for details.

3.4.9 Cell migration assays.

RAWs were seeded into a 12-well plate, scratched with a pipette tip, treated with VEGF or any inhibitors, and imaged at 0 h and 24 h to characterize migration. See SI Materials and Methods for details.

3.4.10 Cell proliferation assays.

RAWS were seeded into a 96-well plate, stimulated with VEGF or any inhibitors, and cell proliferation was measured after 24 h using a MTT assay. See SI Materials and Methods for details.

3.4.11 Flow cytometry.

RAWs were labeled with Phycoerythrin (PE)-conjugated monoclonal antibodies specific to VEGFR1 or VEGFR2. Fluorescence given off by PE was captured in flow cytometry, and converted to VEGFR level per cell (Appendix A, Fig A.3). See SI Materials and Methods for details.

3.5 Figures

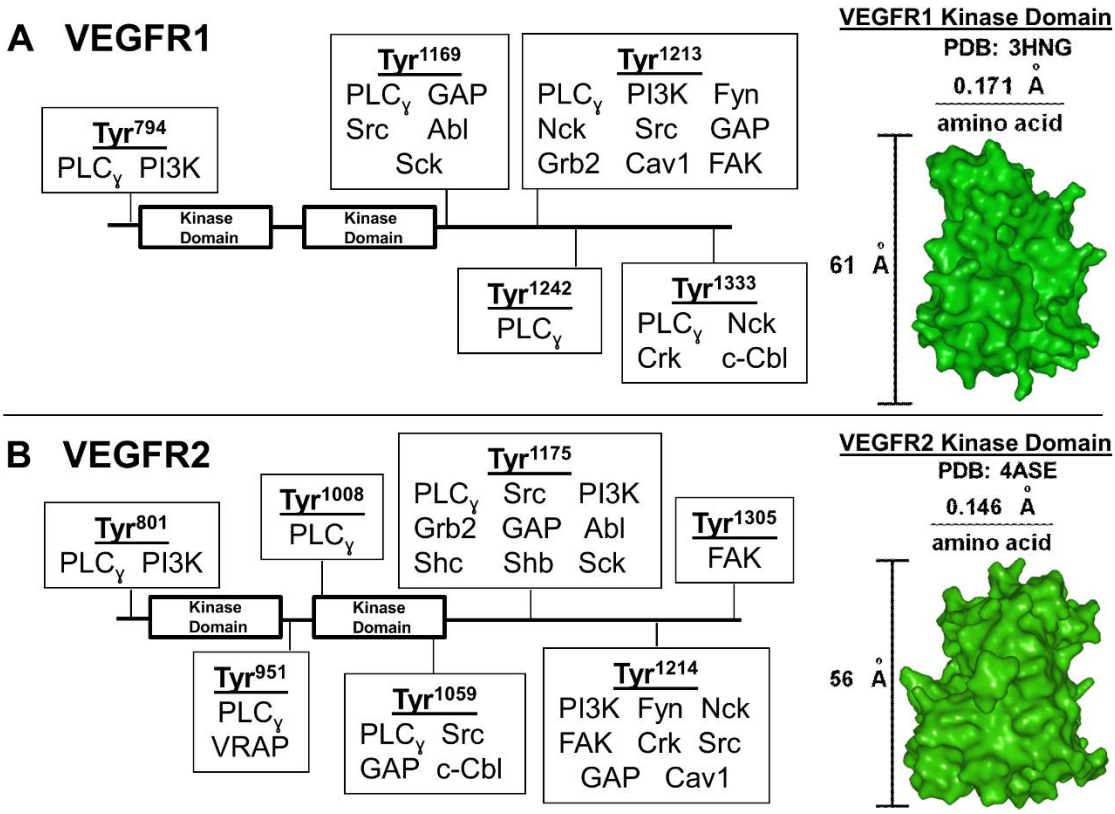

Fig 3.1: VEGFR-adapter interaction schematics.

Adapters bind specific tyrosine (Tyr) sites on (A) VEGFR1 and (B) VEGFR2 (Appendix A, Table A.4). VEGFR1 and VEGFR2 kinase domain crystal structures were used to measure the distance between individual VEGFR amino acids. This measurement, along with adapter size measurements (Appendix A, Table A.5), were used to map the adapters and Tyr sites that allow multiple adapters to bind a VEGFR simultaneously.

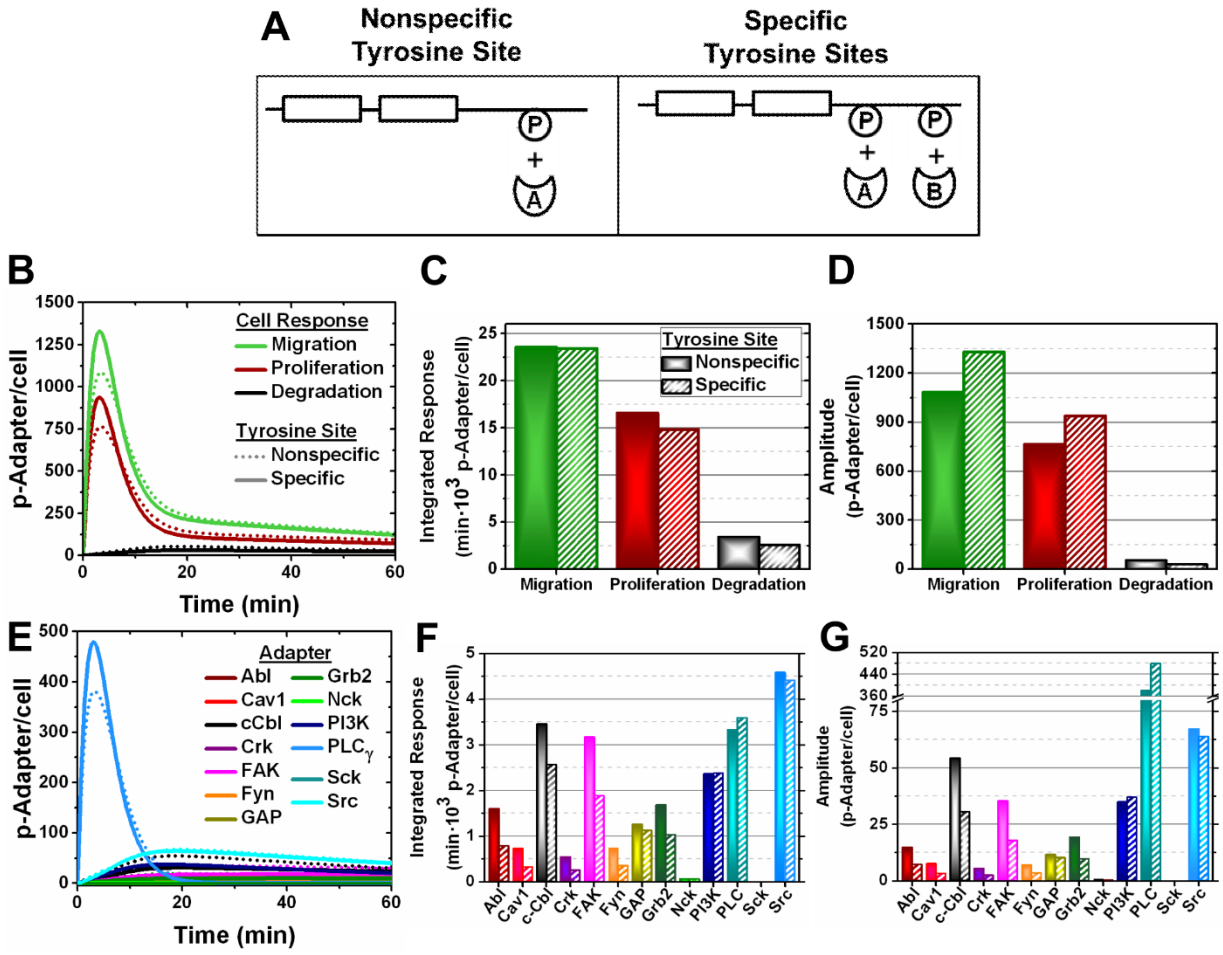

Fig 3.2: The VEGFR1 structure preferentially activates PLC$_\gamma$ and PI3K.

(A) Schematics for the VEGFR1-adapter interaction models: (left) adapters bind a single nonspecific VEGFR1 tyrosine site versus (right) adapters binding specific VEGFR1 tyrosine sites. Here adapters are shown in a generalized form, labeled A and B, P represents a phosphorylated receptor Tyr site, and the plus symbol indicates an adapter binding the phosphorylated receptor Tyr site. VEGFR1 signaling was modeled in HUVECs to determine (B) VEGFR1-induced cell response dynamics, (C) the integrated cell responses, and (D) cell response phosphorylation amplitudes. Likewise, (E) VEGFR1-mediated adapter phosphorylation dynamics in HUVECs are analyzed to quantify (F) integrated adapter responses and (G) adapter phosphorylation amplitudes.

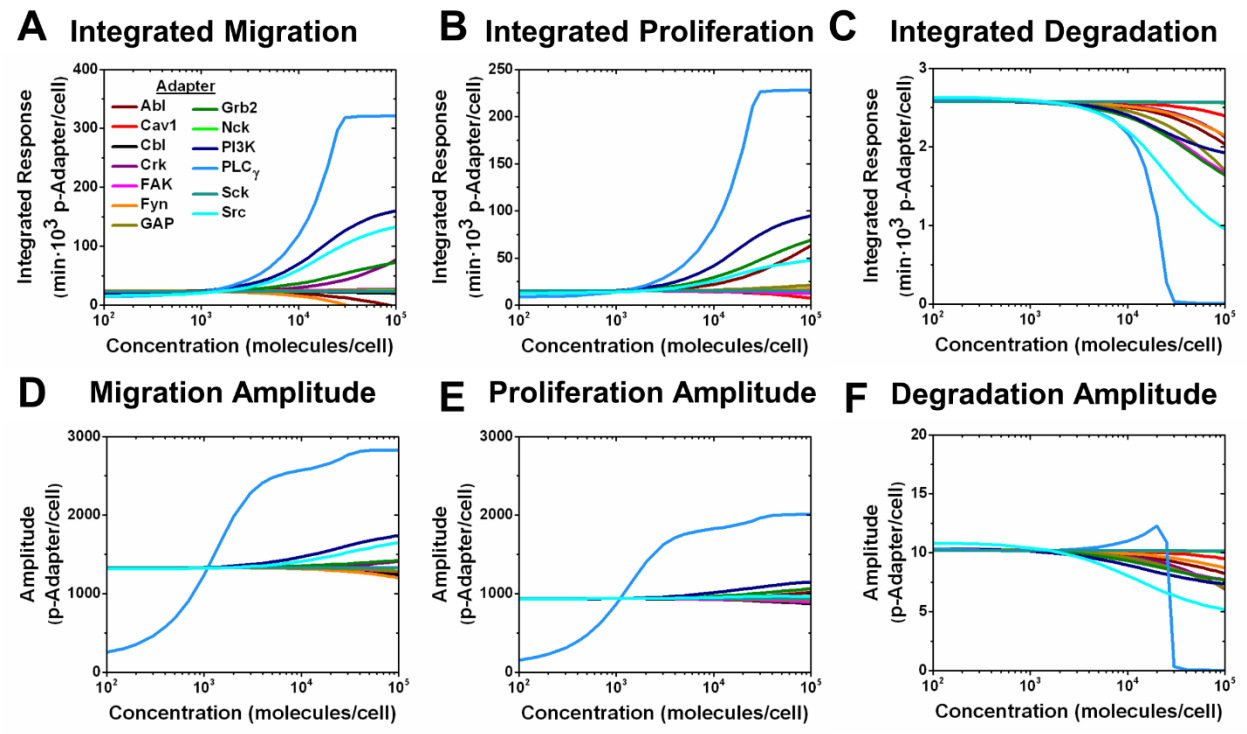

Fig 3.3: VEGFR1-induced cell migration and proliferation are primarily directed by PLC_γ and PI3K concentrations.

(A-C) Integrated responses and (D-F) phosphorylation amplitudes for each cell response were quantified with respect to adapter concentration, using the specific VEGFR1 tyrosine site model.

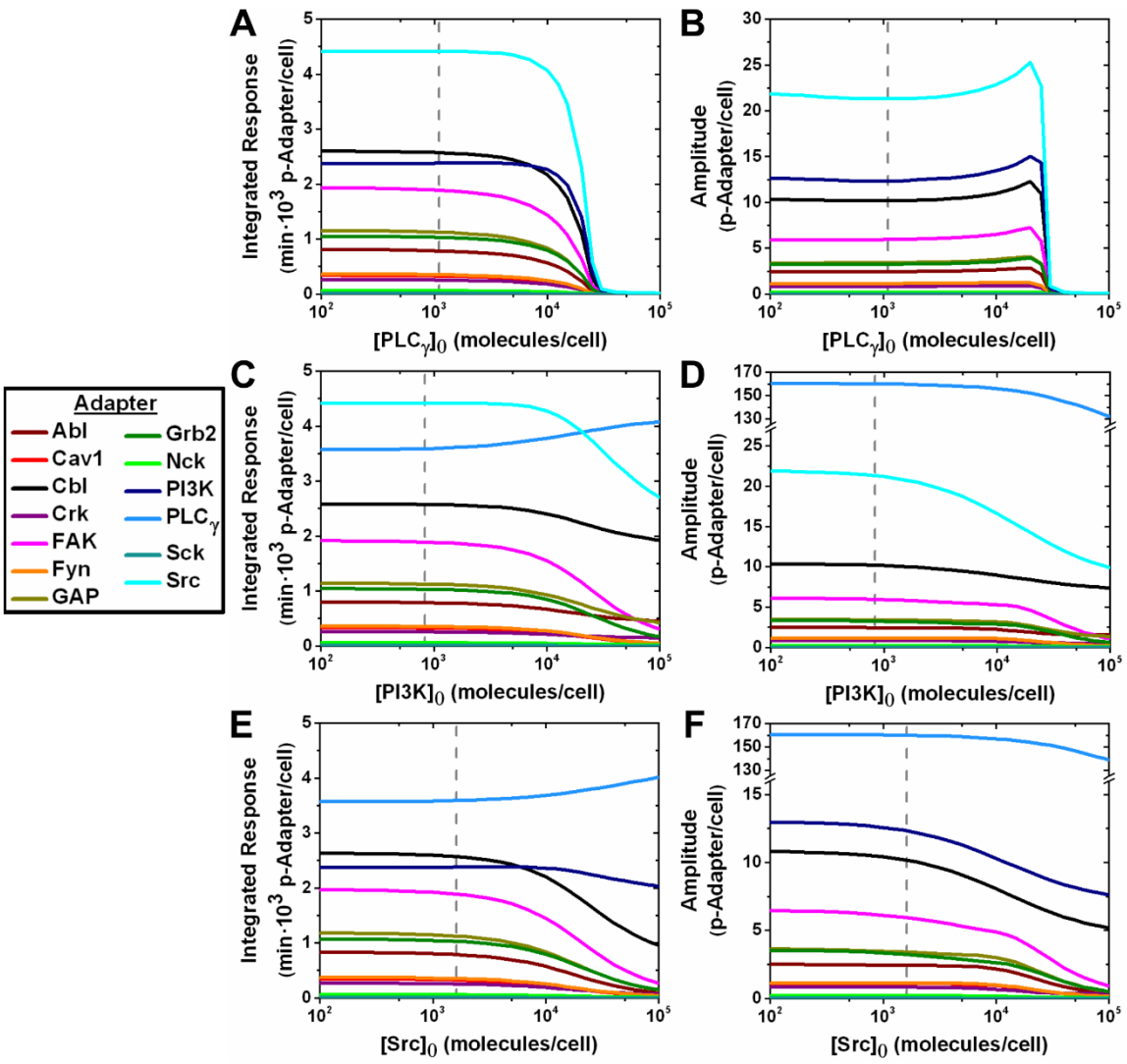

Fig 3.4: PLC$_\gamma$, PI3K, and Src form a coordinated activation loop with one another.

The integrated responses and phosphorylation amplitudes of all adapters were examined with altering (A-B) PLC$_\gamma$ concentration, (C-D) PI3K concentration, and (E-F) Src concentration, using the specific VEGFR1 tyrosine site model. Adapter concentrations were ranged between 10^2 - 10^5 molecules/cell. The vertical gray dashed lines indicate the physiological adapter concentration in HUVECs (Appendix A, Table A.1).

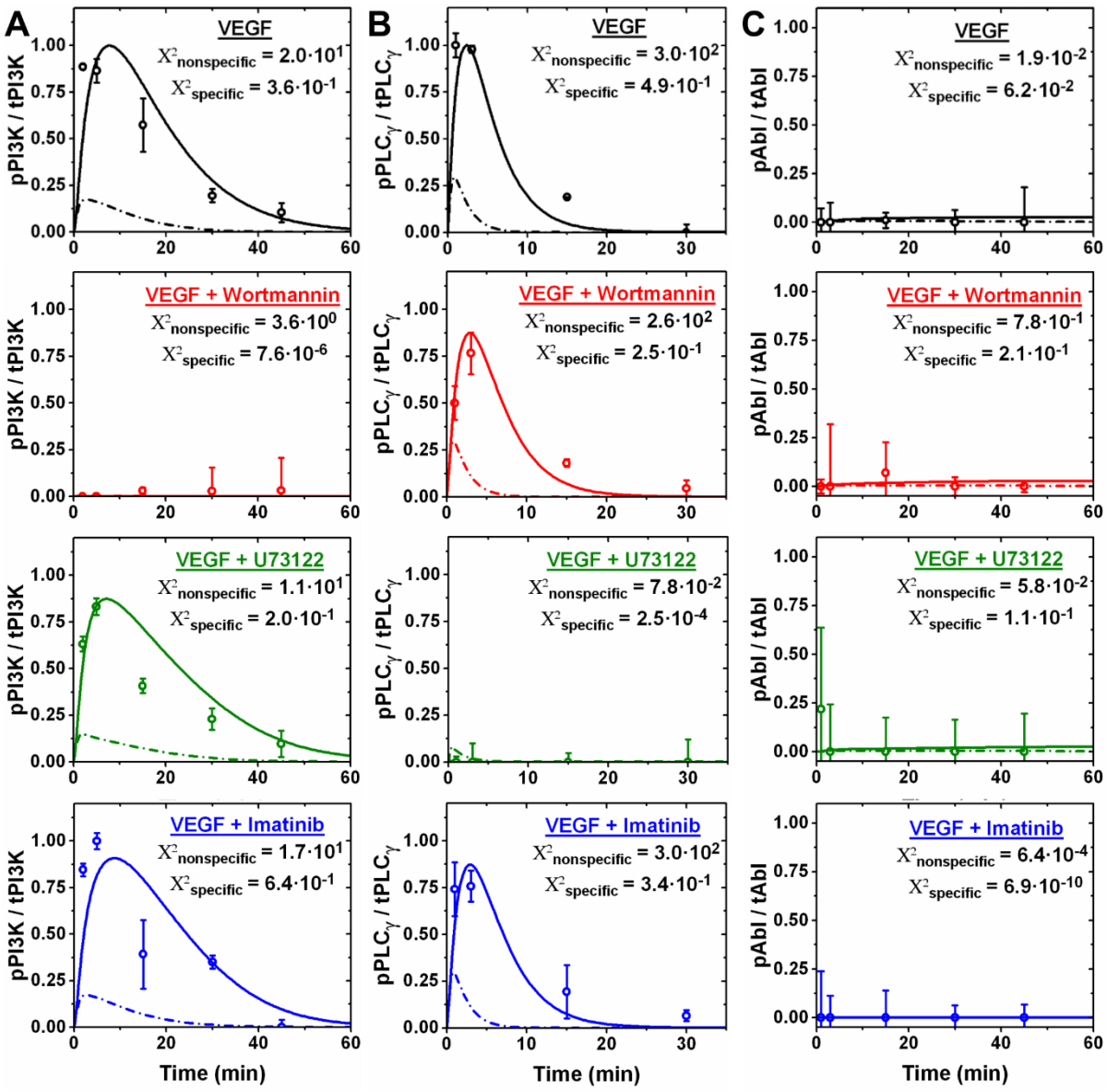

Fig 3.5: VEGFR1 phosphorylates PI3K and PLC$_\gamma$ with model predicted dynamics.

(A) PI3K, (B) PLC$_\gamma$, and (C) Abl phosphorylation in RAWs were quantified with ELISAs at multiple time points given treatment with VEGF-A$_{164}$ (50 ng/mL), 100 nM Wortmannin (PI3K inhibitor), 10 μM U73122 (PLC$_\gamma$ inhibitor), and 6 μM Imatinib Mesylate (Abl inhibitor). Data is represented as the mean phosphorylated over mean total protein (p/t) ratio ± standard error of the mean (SEM) for each treatment type and treatment time; here SEM is the sum of the phosphorylated and total protein SEMs. The p/t ratio given inhibitor treatment specific to the protein of interest was subtracted as background for each treatment time. Predicted adapter phosphorylation with a nonspecific (dashed line) and specific (solid line) VEGFR1 tyrosine sites are shown compared to experimental data (open circles). Goodness of fit is tested by the X^2 goodness-of-fit test [253].

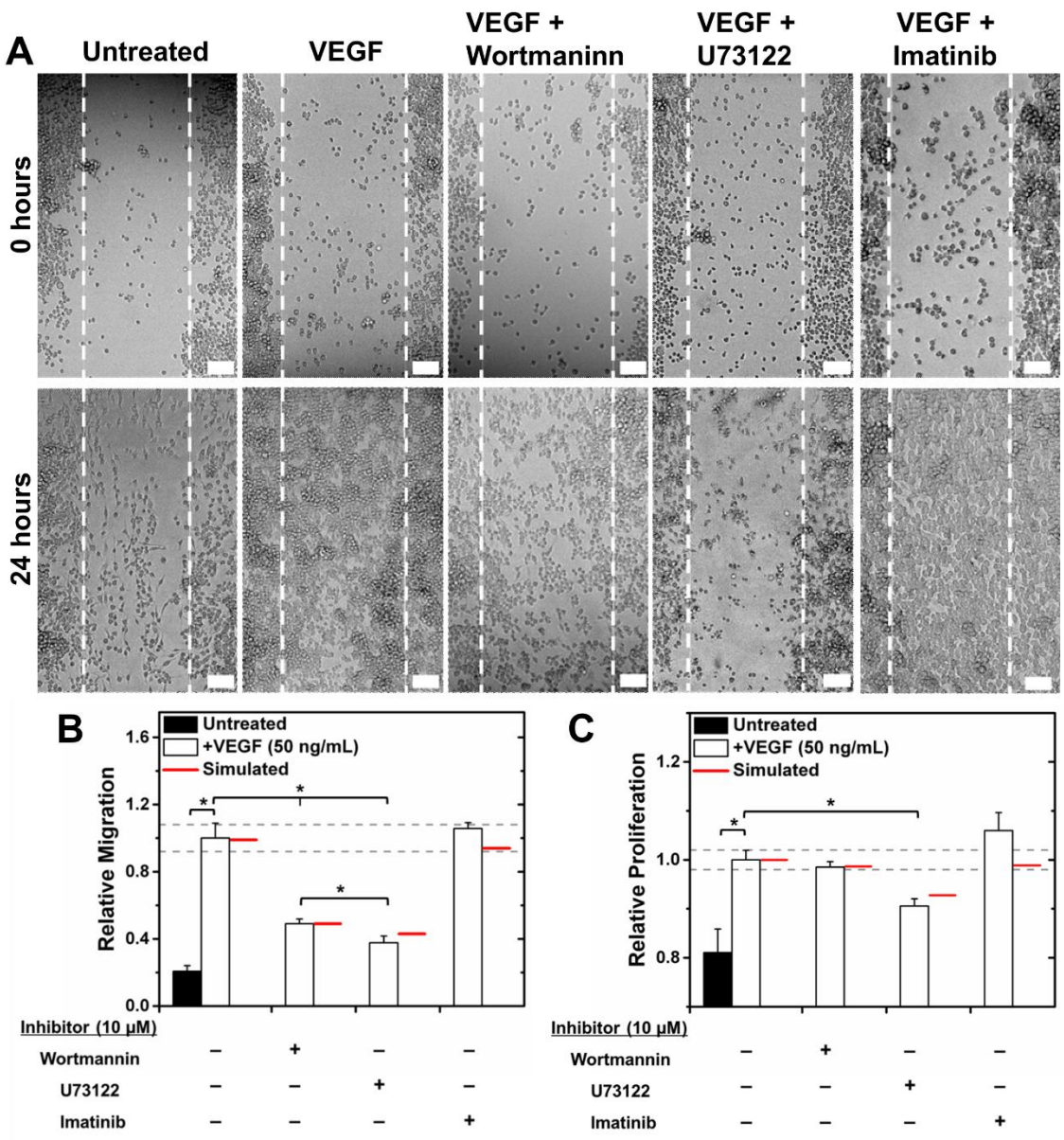

Fig 3.6: PLC$_\gamma$ and PI3K regulate VEGFR1-induced cell responses in vitro.

(A) RAW migration was measured in wound healing assays at 0 h and 24 h post scratch. Scale bars represent 50 μm. (B) Analyzed wound healing assays show that inhibiting PLC$_\gamma$ or PI3K significantly decreases VEGF-induced RAW migration. (C) PLC$_\gamma$ inhibition significantly decreases VEGF-induced RAW proliferation, measured with MTT assays. Treatments for all experiments were: 50 ng/mL VEGF-A$_{164}$, 10 μM Wortmannin (PI3K inhibitor), 10 μM U73122 (PLC$_\gamma$ inhibitor), and 10 μM Imatinib Mesylate (Abl inhibitor). All experiments were performed in triplicate, and data is represented as mean ± SEM. Experimental significance is given at $p < 0.05$. (B-C) The predicted maximum reduction in cell response from the model is given for each inhibitor treatment (red line). Dashed grey lines outline the range corresponding to 10% variation in cell migration given VEGF treatment alone; inhibitor treatments are predicted to be significant by the model if the predicted cell migration lies outside this range.

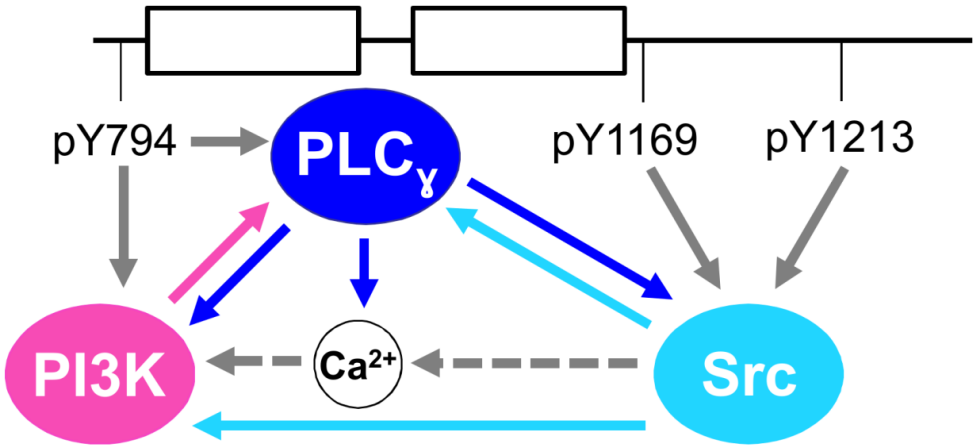

Fig 3.7: VEGFR1 preferentially activates PLC_γ, PI3K, and Src, possibly to form a Ca^{2+} signaling regulatory loop.

My simulations predict that VEGFR1 tyrosine sites are structured to preferentially associate with PLC_γ or PI3K at Tyr^{794} and Src at Tyr^{1169} or Tyr^{1213}, simultaneously. I theorize that this PLC_γ, PI3K, and Src activation scheme by VEGFR1 forms a Ca^{2+} signaling regulatory loop, as depicted. Arrow color indicates adapter or Ca^{2+} signal activation by VEGFR1 (solid gray), PLC_γ (blue), PI3K (pink), Src (cyan), or through Ca^{2+} signaling (dashed gray). Additional VEGFR1 binding sites and adapter association are not shown.

CHAPTER 4

INTEGRATIVE META-MODELING IDENTIFIES ENDOCYTIC VESICLES, LATE ENDOSOMES, AND THE NUCLEUS AS THE CELLULAR COMPARTMENTS PRIMARILY DIRECTING RTK SIGNALING

4.1 Introduction

Receptor signal transduction is critical to many pathologies, including cancers [304], [305] and vascular diseases [306], [307]. Typically, membrane receptors are targeted to control signal transduction, as they are the initial mediators of eliciting cell responses from extracellular signal transducers (e.g., ligands) [301], [308]. While signal transduction pathways have been established for specific membrane receptors [309]–[312], how cell physiology directs signal transduction fundamentally, for any receptor in general, remains undefined. Delineating cell physiology effects on receptor signaling would result in a "signaling template" that both governs signaling fundamentals and may be tuned to account for receptor-specific spatiotemporal dynamics [313], [314]. Engineering such a signaling template would offer improved signal mapping, while enabling receptor-based signaling control, critical for treating pathological conditions.

Systems biology allows for this delineation between cell physiology and receptor signaling. Systems biology studies have identified that endocytosis directs receptor signaling to primarily occur intracellularly [195], [315]: cells exhibiting prolonged receptor signaling and enhanced cell responses exhibit less receptor recycling, leading to intracellular ligand-receptor accumulation, [316], [317]. Experimental studies validated these computational predictions; high epidermal growth factor receptor (EGFR) phosphorylation, along with phosphorylated Shc,

Grb2, and mSOS signaling molecules, were identified within endosomes [318]. Such studies advanced early views that endocytosis only functioned to terminate membrane receptor signaling [315], derived from experimental findings that while ligand-bound receptors traffic to lysosomes, where protein degradation occurs, ~10-fold faster than unligated receptors [319]–[321]. Thus, computational systems biology provides valuable insight into receptor signaling; extending these studies to model how cell physiology and endocytosis direct intracellular-based receptor signaling, fundamentally, would further refine the knowledge of receptor signaling mechanisms.

Understanding how endocytosis fundamentally directs intracellular receptor signaling requires receptor-specific endocytosis mechanisms to be delineated. This delineation requires identifying the signaling mechanisms common to all receptor types. However, the ability to identify these common receptor signaling mechanisms from experimental observations is limited; intracellular-based receptor signaling studies have examined EGFR almost exclusively [196], [310], [322], providing insights that may not be extendable to other receptor types. Therefore, conducting a computational meta-analysis across multiple receptor families will allow the signaling mechanisms common to different receptors to be identified.

I develop a computational endocytosis signaling template to conduct a meta-analysis across eight tyrosine kinase receptors (RTKs): EGFR, FGFR1, IGFR1, PDGFRα, PDGFRβ, VEGFR1, VEGFR2, and Tie2. I delineate the complex endocytosis mechanisms to understand intracellular RTK signaling in general, by examining how cell (compartment volume, trafficking kinetics, and pH; Table 1) and ligand-receptor physiology (ligand/receptor concentration and interaction kinetics; Table 2) direct signaling. Specifically, I model RTK translocation post-ligand simulation: internalization and trafficking through intracellular compartments (Fig 4.1). I weigh receptor phosphorylation, a post-translational modification, across each endocytic

compartment. I predict that RTK signaling primarily occurs within endocytic vesicles, due to their low volume potentiating ligand concentrations. I also predict that all RTKs undergo nuclear translocation dependent on extracellular ligand concentration, requiring a late endosome pathway. Overall, this study provides fundamental insights into RTK signaling, and an endocytosis signaling template that can be applied to probe specific RTK signaling, or test RTK therapeutics.

4.2 Results

4.2.1 RTK phosphorylation primarily occurs intracellularly.

Quantifying compartmentalized receptor signaling reveals that RTKs primarily signal within endocytic vesicles, comprising > 43% the total receptor signaling within the cell, for all eight RTKs modeled (Table 2). Conversely, membrane signaling is relatively low, giving < 1% the total receptor signaling for all eight RTKs (Table 2). This indicates that essentially all RTK signaling within a cell stems from intracellular receptors.

4.2.2 Absolute membrane signaling is dependent on the RTK.

While these eight RTKs follow the same signaling trend, receptor signaling primarily occurring intracellularly, absolute receptor signaling, given by integrated response, is highly variable. Nuclear signaling ranges between 3.3% - 27% the total receptor signaling within the cell, given by FGFR1 and EGFR, respectively.(Table 2). Absolute receptor signaling is directed by the RTK complex level, which is defined as $\frac{[R][L]}{K_d}$, where [R] is receptor level, [L] is ligand concentration, and K_d is the ligand-receptor dissociation constant. FGFR1 has the lowest nuclear signaling since it has the lowest complex level amongst the eight RTKs. Conversely, EGFR has a large complex level, leading to high nuclear signaling (Table 2). This computational signaling

template thus allows receptor signaling importance to be weighed relative to other receptors within each cellular compartment; amongst these eight RTKs, nuclear signaling is ranked as: EGFR > IGFR1 > PDGFRα > VEGFR1 > VEGFR2 > PDGFRβ > Tie2 > FGFR1.

4.2.3 Endocytic compartmentalization leads to two primary receptor signaling trends.

To understand how receptor signaling is dynamically regulated by endocytic compartmentalization, I examine Ang2-Tie2 signaling, as a representative axis for these eight RTKs. I find that receptors associated with the membrane (Fig 4.2A), endocytic vesicles (Fig 4.2B), early endosomes (Fig 4.2C), and recycling endosomes (Fig 4.2D) have similar activation and decay constants, implying these compartments promote similar receptor signaling dynamics. Likewise, receptors associated with late endosomes (Fig 4.2E) and lysosomes (Fig 4.2F) have the same activation and decay constants. The nucleus is the only compartment that does not follow one of these two signaling dynamics (Fig 4.2G). These activation and decay constants define two receptor dynamic trends: the membrane, endocytic vesicles, early endosomes, and recycling endosomes promote rapid receptor signaling, whereas late endosomes and lysosomes promote slow receptor signaling.

4.2.4 Phosphorylated receptors primarily associate with endocytic vesicles and late endosomes after ligand stimulation.

Receptor signaling compartmentalization reveals that receptor phosphorylation primarily occurs within endocytic vesicles early, and late endosomes late, after ligand stimulus. Within 5 minutes after ligand stimulus, ~22% the total cell receptors are phosphorylated within endocytic vesicles, whereas < 1% are within all other compartments (Fig 4.2H). Conversely, 3 hours after ligand stimulus, ~11% the total cell receptors are phosphorylated within late endosomes, whereas

< 5% are within all other compartments (Fig 4.2H). Thus, phosphorylated receptors preferentially associate with endocytic vesicles immediately following ligand stimulation, switching to late endosomes at later time points.

4.2.5 Membrane receptors facilitate burst signaling whereas endocytic receptors facilitate sustained signaling.

From these results that receptor phosphorylation primarily occurs within endocytic vesicles, I hypothesize that the small endocytic vesicle volume (Table 4.1) facilitates high ligand concentration and strong ligand-receptor interactions, causing high receptor phosphorylation. To test this hypothesis, I compare receptor phosphorylation within endocytic vesicle to membrane receptor phosphorylation (Fig 4.3A). At the membrane, less than 1% the total receptors are phosphorylated 60 minutes after ligand stimulation (Fig 4.3B). Conversely, ~80% the total receptors within a single endocytic vesicle are phosphorylated at equilibrium, reached within 5 minutes after ligand stimulation (Fig 4.3C). Subsequently, the same number of receptors within endocytic vesicles produces substantially greater signaling than at the membrane: 5 orders of magnitude higher at 2 hours after ligand stimulation (Fig 4.3D). This implies that the low endocytic vesicle volume does concentrate ligand signaling, facilitating strong ligand-receptor interactions, and presenting endocytic vesicles as the chief signaling compartment.

4.2.6 Nuclear translocation requires a late endosome pathway.

To understand how receptors undergo nuclear translocation, I observe how nuclear signaling is affected by blocking endocytic pathways (Fig 4.4). Nuclear translocation is most effectively inhibited by blocking receptor trafficking from late endosomes to the nucleus, decreasing nuclear signaling 96% (Fig 4.4). Likewise, nuclear translocation is most effectively

promoted by blocking receptor trafficking from late endosomes to lysosomes, increasing nuclear signaling 133% (Fig 4.4). Interestingly, blocking the early to late endosomes pathway has a lesser effect on nuclear translocation, despite this pathway being required for receptor association with late endosomes. Therefore, late endosome trafficking directs nuclear translocation.

4.2.7 Compartmentalized receptor signaling is best regulated by the extracellular ligand concentration.

To identify how the RTK parameters (receptor level, ligand concentration, and ligand-receptor kinetics) mediate compartmentalization and signaling for a single RTK, I examine Ang2-Tie2 signaling in response to altering RTK parameters (Fig 4.5). While ligand-receptor kinetics direct membrane signaling (Fig 4.5A), receptor signaling in all intracellular compartments are unaffected by altering ligand-receptor kinetics (Fig 4.5B-E). Receptor level only affects nuclear and endocytic vesicle receptor signaling, evidenced by an eight order of magnitude increase in receptor increasing nuclear signaling from 3% to 22% (Fig 4.5E). Conversely, ligand concentration highly regulates receptor signaling in all intracellular compartments (Fig 4.5B-E), evidenced by increasing the ligand concentration eight orders of magnitude reducing endocytic vesicle signaling from 73% to 43% (Fig 4.5B). Thus, compartmentalized signaling for a single RTK is directed by the extracellular ligand concentration.

4.2.8 Nuclear based receptor signaling is best regulated by ligand concentration.

To test if extracellular ligand concentration directs intracellular signaling across all eight RTKs, I perform a correlation analysis between nuclear signaling and RTK parameters (Fig 4.6).

Nuclear signaling has low correlation with the receptor level (Fig 4.6A, $R^2 = 0.08$) and the ligand-receptor dissociation constant (Fig 4.6B, $R^2 = 0.17$), implying that these parameters have low weight in determining nuclear-based RTK signaling. Conversely, extracellular ligand concentration better characterizes nuclear signaling (Fig 4.6C, $R^2 = 0.47$), indicating the highest weight amongst the three RTK parameters. This correlation analysis predicts that increasing the extracellular ligand concentration one order of magnitude will increase nuclear signaling 3.2-fold. Furthermore, the complex level, which comprises the other three parameters, provides a good overall predictor of nuclear signaling (Fig 4.6D, $R^2 = 0.75$), confirming that nuclear signaling is mediated by these three RTK parameters. This trend that receptor level and ligand-receptor dissociation constant have low weight, versus extracellular ligand concentration having high weight, in mediating receptor signaling holds for all endocytic compartments (Appendix B, Fig B.2-B.5). Thus, the extracellular ligand concentration regulates compartmentalized receptor signaling across all eight RTKs.

4.3 Discussion

My integrative RTK meta-modeling approach is the first time that these eight RTKs, all of which are critical to disease (e.g., cancer [304], [305], [323], [324], cardiovascular disease [306], [307], stroke [325], [326]) have been comparatively modeled. This meta-modeling led to five important findings: (1) RTK signaling primarily stems from endocytic vesicles, whereas membrane signaling is relatively low; (2) high receptor activation within endocytic vesicles is due to their low volume, facilitating ligand enrichment; (3) all RTKs exhibit nuclear translocation, requiring a late endosome pathway; (4) signaling between RTK type and cellular compartments can be ranked; (5) the extracellular ligand concentration directs compartmentalized RTK signaling. These findings can be applied to quantify receptor signaling,

understand how RTK signaling directs cell response, and optimize RTK therapeutics targeting endocytic pathways.

4.3.1 Targeting intracellular-based signaling is critical to direct RTK signaling.

My signaling template predicts that RTK signaling primarily occurs within endocytic vesicles. This trend holds for all eight RTKs tested, regardless of receptor level or ligand-receptor interaction kinetics: receptor level varies 29-fold, and ligand-receptor dissociation constant varies $1.0 \cdot 10^3$-fold, across these eight RTKs [178], [327]–[334]. Experimental studies have shown that intracellular-based signaling is important for the RTKs tested here, without identifying which specific compartment signaling stems from: ERK phosphorylation is reduced by inhibiting EGFR [335], FGFR1 [336], IGFR1 [337], PDGFRβ [338], or VEGFR2 [339] endocytosis. Similarly, PDGFRα accumulation in endocytic vesicles increases ERK phosphorylation [340]. Additionally, experimental studies show that RTK inhibitors that penetrate the plasma membrane are more effective at reducing signaling [341], [342]. While no experimental studies have currently investigated intracellular Tie2 signaling to my knowledge, my simulations indicate intracellular-based Tie2 is important to Tie2 signaling. My results and these previous experimental studies indicate that targeting endocytic vesicle receptors is necessary to effectively regulate RTK signaling.

4.3.2 Application to understanding cancer drug resistance.

My finding that RTK phosphorylation primarily occurs within endocytic vesicles is also useful for understanding cancer cell drug resistance. In particular, I predict that drugs target membrane receptors, but not endocytic vesicle receptors, would be sub-optimal. Literature offers an example of such failed-targeting in gefitinib, a small molecule inhibitor that blocks the EGFR

ATP binding site and is used to treat non-small cell lung cancer (NSCLC). This drug is only effective in cell types where it inhibits intracellular-based EGFR signaling [343], [344], such as in NSCLC PC9 cells where gefitinib inhibits endocytosis. Conversely, QG56 cells have aberrant endocytosis natively and are thus gefitinib-resistant; gefitinib can only inhibit membrane-EGFR in QG56 cells [343]. Thus, my simulations offer guidance in RTK inhibition, suggesting improved efficacy when inhibiting intracellular receptor phosphorylation, while offering insight into reduced drug efficacy.

4.3.3 Temporal implications for therapeutics.

I identified two distinct receptor phosphorylation dynamics across endocytic compartments, characterized by (1) rapid receptor phosphorylation and (2) slow receptor phosphorylation dynamics. These intracellular signaling dynamics have also been observed in experimental studies [315], [345]–[347]. PDGFRs [347] and VEGFR2 [348] are primarily phosphorylated within endosomal compartments early, 30 minutes, then shift to downstream endocytic compartments late, 2 hours, following ligand stimulation. However, these studies do not differentiate receptor phosphorylation at different endocytic compartments, which is a fundamental advancement of my model. This pattern highlighted by my model is particularly useful for optimizing time-dependent drug delivery [349]–[351]. Specifically, drug regimens targeting endocytic vesicle signaling would need to be initiated and effective within 30 minutes following ligand stimulus, when receptor signaling occurs. Thus, these identified compartment receptor signaling dynamics can be applied to optimize drug delivery regimes.

4.3.4 Receptor signaling can be controlled by targeting endocytic vesicles or late endosomes.

The results that receptor signaling primarily occurs from endocytic vesicles implies that receptor signaling can be regulated by directing receptor trafficking. Endocytic vesicle signaling could be prevented by treating cells with dynasore to inhibit dynamin, preventing receptor endocytosis and retaining receptors at the membrane [352], [353]. Conversely, phorbol esters could be used to increase RTK signaling [354], [355]; stimulating BHK-21 cells with phorbol esters increases the number of endocytic vesicles up to 2-fold [356]. Alternatively, neomycin prevents endocytic vesicle fusion into early endosomes, retaining receptors within endocytic vesicles [357], [358]. Similarly, nuclear translocation can be directed by targeting Rab GTPases to block late endosome pathways [359]–[362]; mutating Rab7 prevents VEGFR2 endocytosis to late endosomes [359]. Directing nuclear trafficking is desirable as nuclear translocated receptors potentiate cell responses by promoting gene expression [363]–[368]. Thus, directing receptor trafficking, rather than directly alter receptor signaling, may be a viable therapeutic option.

4.3.5 Application to RTKs based primarily intracellularly.

My signaling template not only provides insight into generalized RTK signaling, but can also be applied to specific cases, such as targeting RTKs that are primarily localized intracellularly. Approximately half the cellular VEGFR2, often targeted to inhibit tumor angiogenesis [369], [370], is localized within endosomes [371], [372]. This intracellular pool is critical to VEGFR2 function, as facilitating cell uptake of a VEGFR2 antibody, by loading it into liposomes, decreased tumor volume 77% after compared to extracellularly applying the VEGFR2 antibody alone [373]. My signaling template easily allows this intracellular VEGFR2 pool to be modeled, allowing additional optimization and testing for VEGFR2 therapeutics.

4.3.6 Conclusions.

Here I present a computational meta-analysis tracking RTK endocytosis and phosphorylation. I find that across eight RTKs, receptor phosphorylation primarily occurs intracellularly, directed primarily by the extracellular ligand concentration. Furthermore, I find significant nuclear translocation of membrane receptors through a late endosome pathway, indicating that preventing endocytosis through late endosomes, such as with Rab7 inhibition, will prevent nuclear translocation and subsequent gene expression. Overall, this study provides a signaling template for studying specific RTKs or endocytic pathways, allowing therapeutic investigation and drug delivery optimization.

4.4 Materials and Methods

4.4.1 Computational RTK endocytosis model.

Cell compartment volumes (Table 4.1), pH (Table 4.1), and trafficking kinetics (Appendix B, Table B.1) are held the same for all RTKs. Ligand concentrations, receptor concentrations, and interaction kinetics are RTK specific (Table 4.2) [177], [327], [328], [330]–[334], [374]. Trafficking kinetics are determined by fitting to experimental data that quantify receptor localization to the membrane (Appendix B, Fig B.1A), nucleus (Appendix B, Fig B.1B), endosomes (Appendix B, Fig B.1C-D), and lysosomes (Appendix B, Fig B.1E-F). The best fit parameters were found by minimizing the global Chi-square between experimental data and simulation:

$$\min\left[\sum_{i=1}^{n}\frac{(\bar{y}_i-\hat{y}_i)^2}{\bar{y}_i}\right] \tag{4.1}$$

where $\bar{y}_i$ is the mean value of experimental data point i, $\hat{y}_i$ is the simulated value, and n is the total number of experimental data points. With this computational signaling template, I quantify

the integrated response, total receptor phosphorylation over time [375], [376], at each compartment, normalized to the membrane integrated response (Table 4.2).

4.4.2 Model compartmentalization.

The model contains eight compartments representing standard receptor endocytosis [377]–[380]: (i) ligand-membrane receptor binding, (ii) ligand and receptor internalization via endocytic vesicles, (iii) endocytic vesicle fusion into early endosomes, (iv) early endosome recycling to the membrane, (v) early endosomal maturation into late endosomes, (vi) late endosome trafficking to lysosomes for degradation, (vii) early endosome and lysosome trafficking to the nucleus. I assume all compartments, except for the extracellular space, are spherical (Table 4.1). I assume that recycling endosomes are the same size as endocytic vesicles. Furthermore, I assume that lysosomes are the same size as late endosomes. I model the extracellular space volume as 0.5 cm^3, shared equally between $2 \cdot 10^5$ cells, based on typical culture conditions in 24-well plates [381]. The cytoplasm volume is included for reference only; I assume no ligands or receptors are available within the cytoplasm (Table 4.1).

4.4.3 Ligand-receptor interactions.

In all model compartments (Fig 4.1), I employ generalized ligand-receptor interactions using the following chemical reactions:

$$L + R \underset{koff_{L\text{-}R}}{\overset{kon_{L\text{-}R}}{\rightleftarrows}} L{:}R \tag{4.2}$$

$$L{:}R \underset{kdp}{\overset{kp}{\rightleftarrows}} L{:}pR \tag{4.3}$$

$$L{:}pR \xrightarrow{koff_{L\text{-}R}} L + R \tag{4.4}$$

where L is the ligand (M), R is the unphosphorylated receptor (M), pR is the phosphorylated receptor (M), semicolon indicates bound proteins, $kon_{L\text{-}R}$ is the ligand-receptor on-rate, $koff_{L\text{-}R}$ is the ligand-receptor off-rate, kp is the receptor phosphorylation rate ($1 \cdot 10^{-2}$ s^{-1} [159]), and kdp is the receptor dephosphorylation rate ($1 \cdot 10^{-3}$ s^{-1} [159]). I assume the receptor phosphorylation and dephosphorylation rate are the same for all eight RTKs, and remain the same across all model compartments. Each compartment has additional trafficking or degradation reactions (Appendix B, Table B.1).

4.4.4 Ligand-receptor interaction kinetics.

The ligand-receptor dissociation constant depends on compartment pH (Table 4.1) [378], [382], [383]. Ligand-receptor interactions are strongest at pH 7.4, typical pH of the extracellular space, cytoplasm, and nucleus [384], but weaken as pH decreases [385]. Ligand-receptor dissociation constants typically increase 2- to 3-fold as pH decreases from 7.4 to 6.0 [385], [386], corresponding to early endosome pH [378]. At pH 5.0 in late endosomes [378], dissociation constants increase ~10-fold [386]. Ligand-receptor interactions no longer occur below pH 5.0, corresponding to lysosomes [378]. I fit the ligand-receptor off-rate as an exponential function to these average pH values by

$$k_{off} = 1.21 \cdot e^{-0.96 \cdot pH} \tag{4.5}$$

where pH < 5.0 has an infinite off-rate allowing no ligand-receptor interactions (Table 1). Similar pH mediated ligand-receptor kinetics have been constructed for EGF-EGFR interactions in early endosomes [327], [387].

4.4.5 Defining ligand and receptor concentrations.

All cell receptors are initially localized to the cell membrane and all ligands are localized extracellularly (Table 4.2). Receptor and ligand concentrations are in units of molecules/cell, using concentration conversions from mass/volume to moles/volume as necessary using the ligand molecular weight: Ang2: 70 kDa [388], EGF: 74 kDa [389], FGF-2: 18 kDa [390], IGF-1: 7.6 kDa [391], PDGF-AA: 30 kDa [392], PDGF-BB: 24 kDa [392], VEGF-A: 45 kDa [393].

4.4.6 Comparing receptor phosphorylation within endocytic vesicles to membrane.

To compare endocytic vesicle to membrane receptor signaling, I model endocytic vesicles and membranes in isolation: no ligand, receptor, or ligand-receptor complex trafficking occurs. This ensures receptor phosphorylation is solely dependent on compartment volume. I assume one ligand for each receptor; for Tie2, which has 1,800 membrane receptors (Table 4.2) [328], this equates to 1,800 (84 pg/mL or 1.2 pM) extracellular Ang2 molecules, within the measured serum range (Table 4.2). I assume a single endocytic vesicle contains 5 receptors [394]–[396], giving 5 ligand molecules (1.1 mg/mL or 16 μM) in a single endocytic vesicle. When simulating all 1,800 receptors associated within endocytic vesicles, I model 5 receptors per endocytic vesicle, giving 360 endocytic vesicles total.

4.4.7 Correlation analyses.

The correlation analyses between compartment receptor signaling and RTK parameters is performed in OriginLab. I assume a lognormal fit between receptor signaling and RTK parameter to calculate the R^2 fit, for all compartments. I focus on nuclear signaling for this correlation analysis as it provides the most variable compartment receptor signaling across the eight RTKs (Table 4.2), thus best representing how the RTK parameters mediate receptor signaling

4.5 Figures and Tables

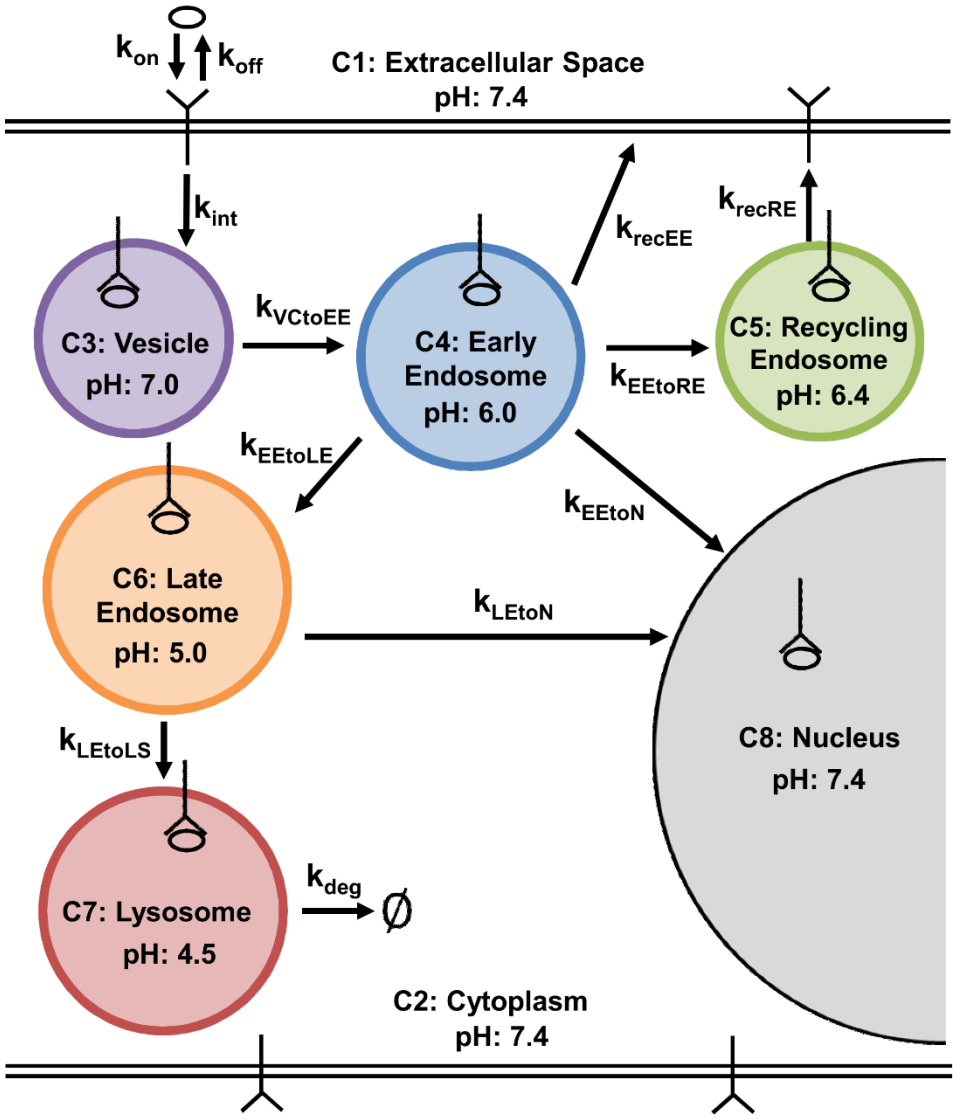

Figure 4.1: RTK endocytosis signaling template.

Ligand-receptor interactions and trafficking occur across seven compartments (C1-C8), defined by their volume, pH, and ligand-receptor kinetics (Table 4.1). Rate parameters describing the transitions between intracellular compartments are also given.

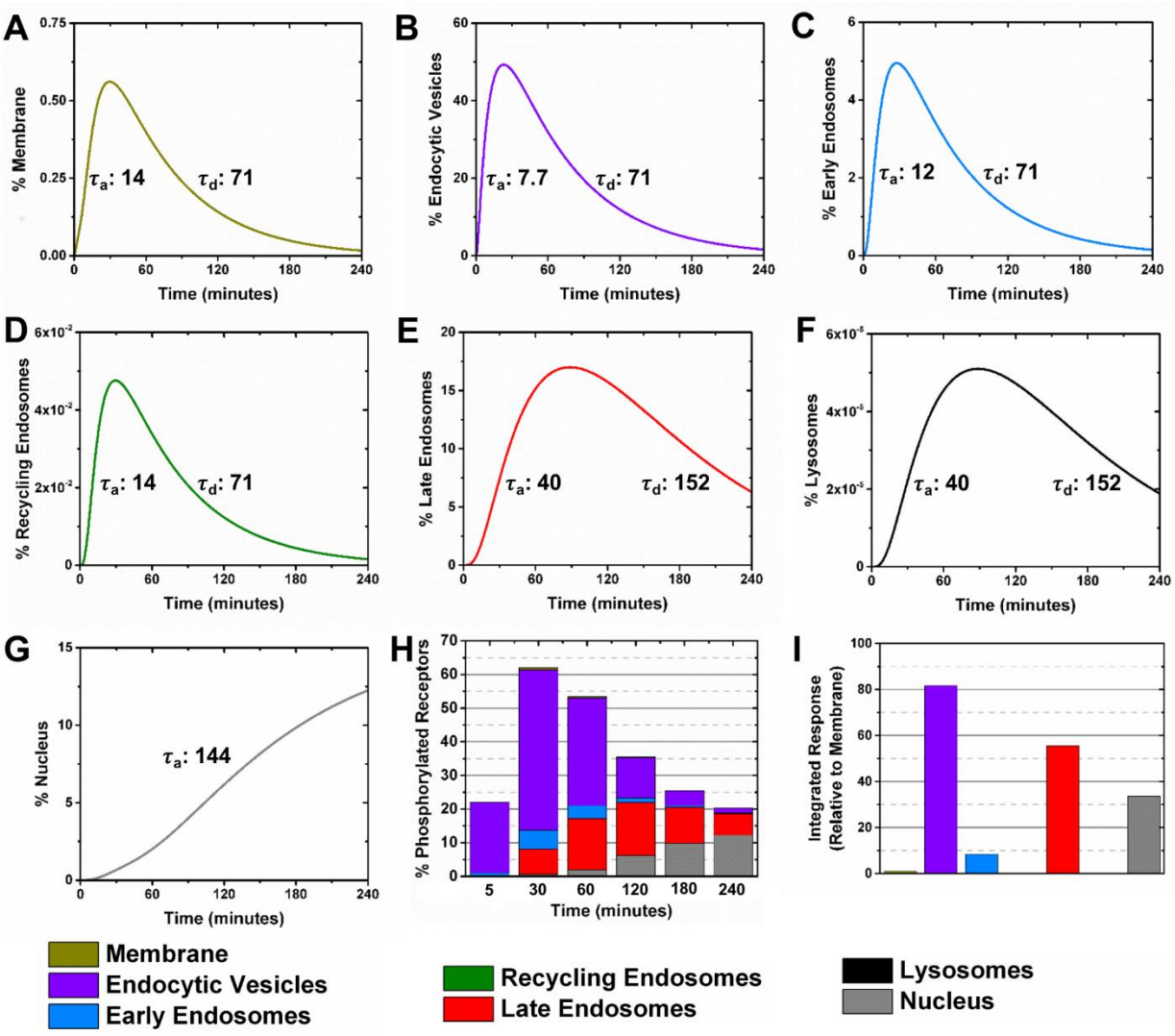

Figure 4.2: RTK phosphorylation primarily occurs within endocytic vesicles early, and late endosomes late, after ligand stimulus.

The percent of phosphorylated receptors relative to total cell receptors are given on (A) the cell membrane, (B) endocytic vesicles, (C) early endosomes, (D) recycling endosomes, (E) late endosomes, (F) lysosomes, and (G) in the nucleus. The activation time constant (τ_a, time from ligand stimulus to 63.2% max phosphorylation) and decay time constant (τ_d, time from max phosphorylation to 36.8% max phosphorylation) in minutes are also given for each compartment. (H) Phosphorylated receptor localization relative to total cell receptors at 5, 60, 120, 180, and 240 minutes after ligand stimulus.

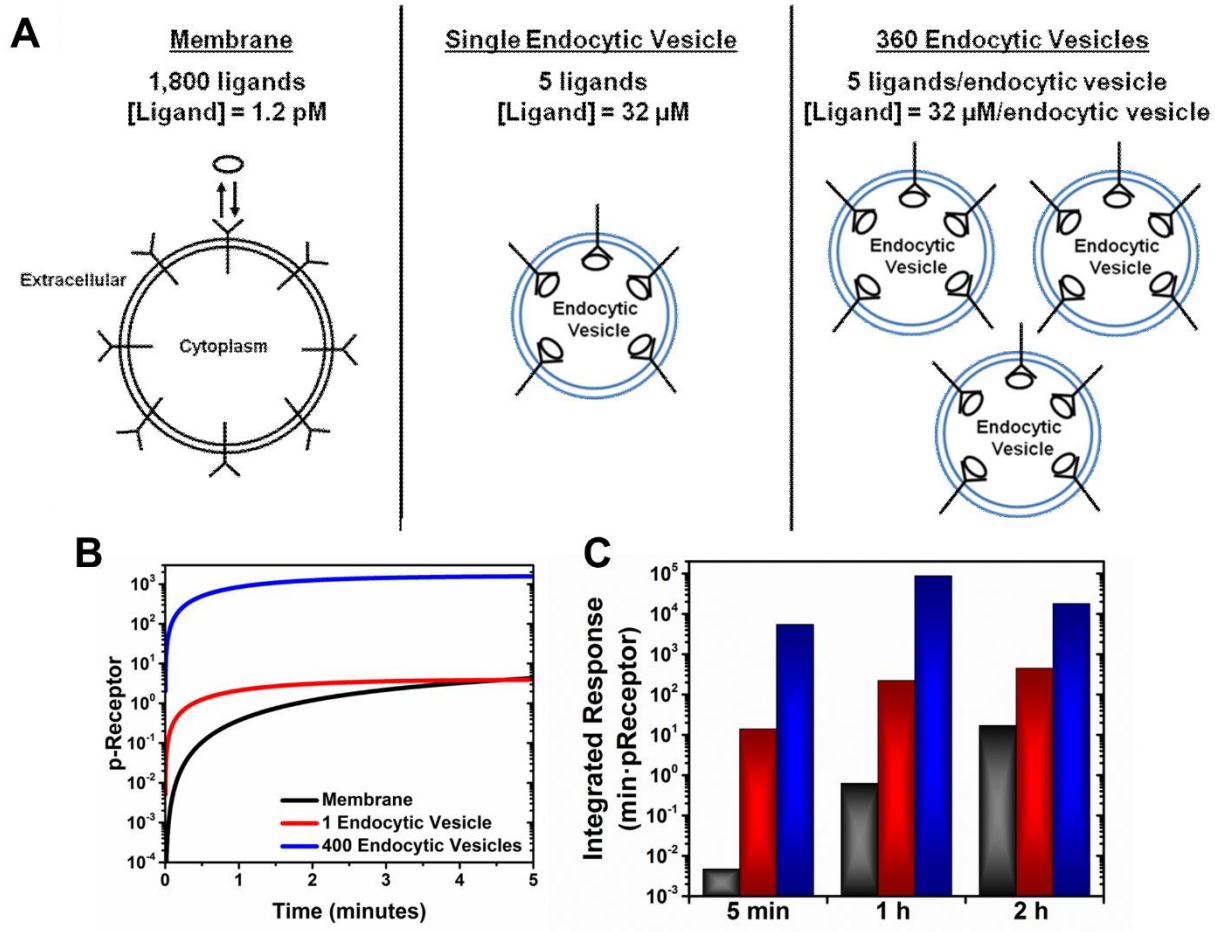

Figure 4.3: Endocytic vesicles facilitate high, sustained receptor phosphorylation.

(A) Schematic showing the three simulations cases. (B) Receptor phosphorylation versus time was simulated on the cell membrane, on a single endocytic vesicle, or when all receptors were contained on endocytic vesicles. (C) The integrated responses, area under the curve, at 5 minutes, 1 hour and 2 hours are given for each case.

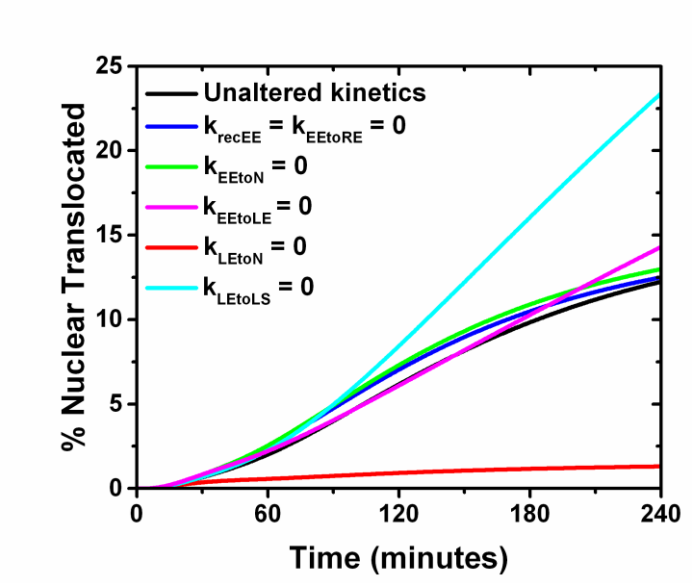

Figure 4.4: Nuclear translocation requires a late endosome pathway.

Percent total cell receptors translocated to the nucleus when endocytic pathways are blocked for 4 hours following ligand stimulus. Inhibited pathways involve receptor movement from the early endosomes and late endosomes (Fig 4.1). These pathways are the recycling pathway (blue line), early endosomes to nucleus (green line), early endosomes to late endosomes (magenta line), late endosome to nucleus (red line), and the degradation pathway (cyan line).

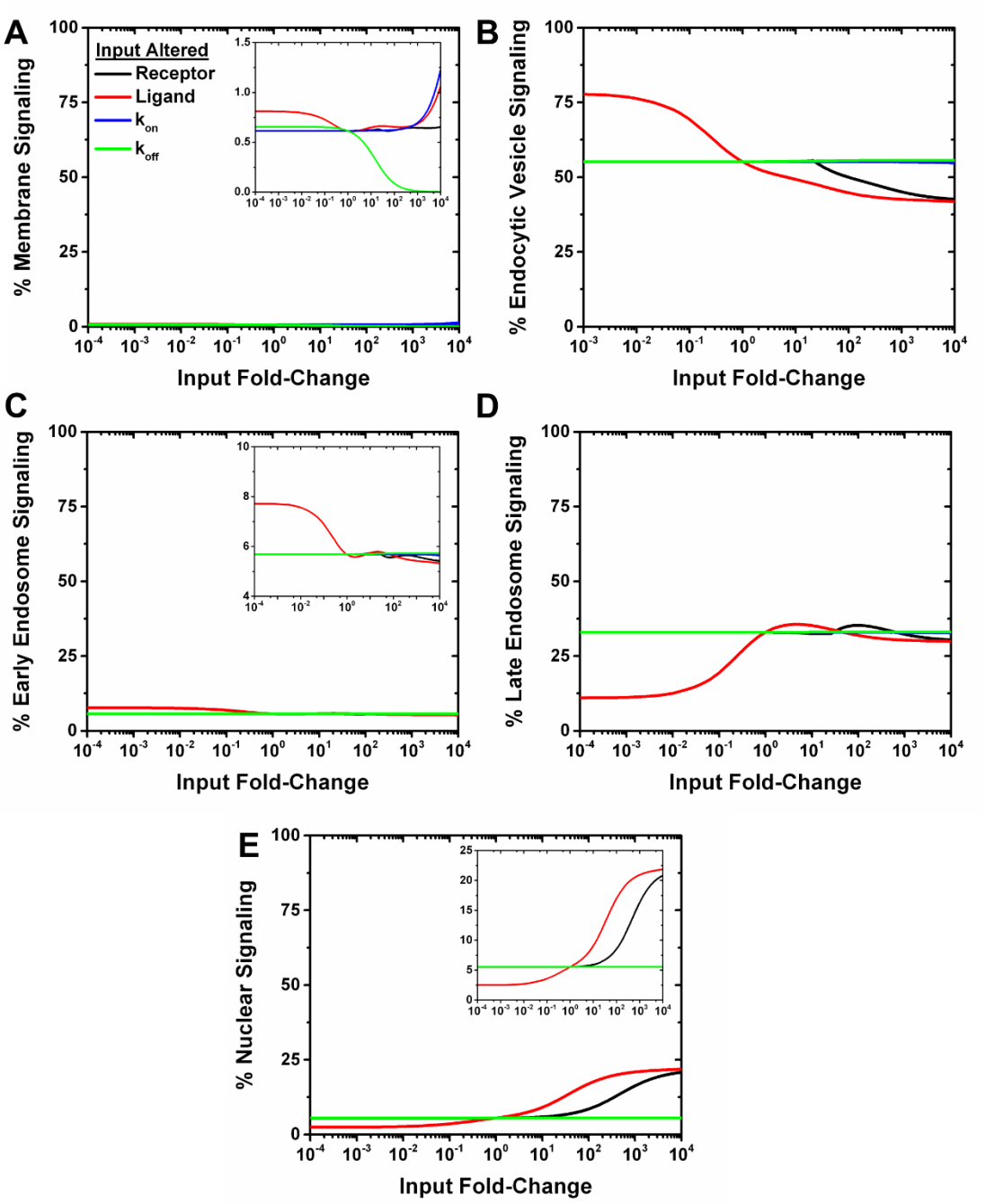

Figure 4.5: Signaling compartmentalization is directed by extracellular ligand concentration.

The percents of total receptor signaling associated with (A) the membrane, (B) endocytic vesciles, (C) early endosomes, (D) late endosomes, and (E) nucleus were quantified with altered Ang2-Tie2 parameters, chosen as representative for all RTKs. Recycling endosome and lysosome based receptor signaling are not included as they account for < 0.01% total receptor signaling. The four parameters changed are: receptor level (black line), ligand concentration (red line), ligand-receptor on-rate (blue), and ligand-receptor off-rate (green).

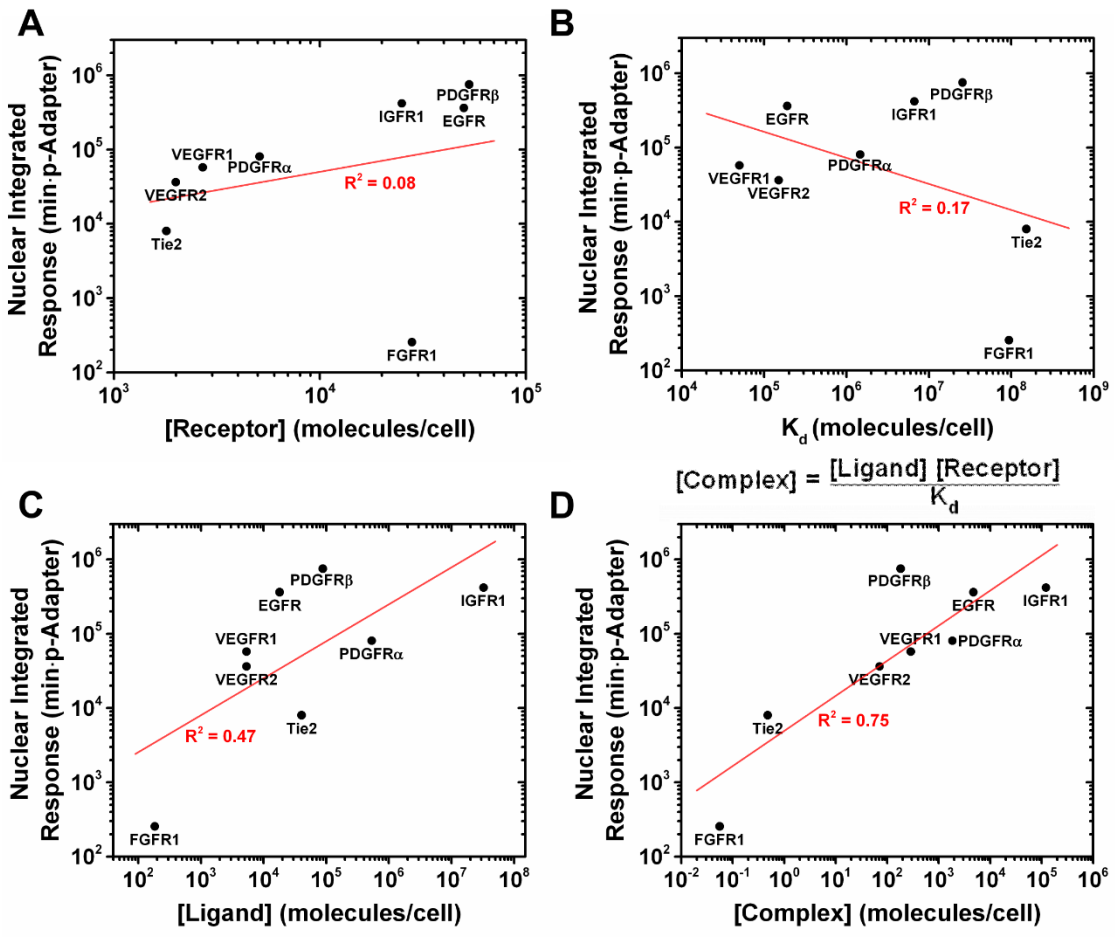

Figure 4.6: Nuclear signaling across RTKs is directed by extracellular ligand concentration.

Nuclear signaling amongst the 8 RTKs was fit to the following RTK parameters: (A) receptor level, (B) extracellular ligand concentration, (C) ligand-receptor dissociation constant, and (D) complex level, defined as the product of extracellular ligand concentration and membrane receptor level divided by the ligand-receptor dissociation constant. The R^2 goodness of fit, using a lognormal fit assumption, is given for each RTK parameter.

Table 4.1: Model compartment parameters.

Compartment	Spherical Diameter	Volume (cm^3)	pH	k_{on} (1/molecules·s)	k_{off} (1/s)
Extracellular Space	-	$2.5 \cdot 10^{-6}$	7.4	$6.6 \cdot 10^{-9}$	$1.0 \cdot 10^{-3}$
Cytoplasm	18 µm[a]	$1.6 \cdot 10^{-9}$	7.4	-	-
Endocytic Vesicle	100 nm[b]	$5.2 \cdot 10^{-16}$	7.0	$3.2 \cdot 10^{1}$	$1.5 \cdot 10^{-3}$
Early Endosome	1 µm[c]	$5.2 \cdot 10^{-13}$	6.0	$3.2 \cdot 10^{-2}$	$3.8 \cdot 10^{-3}$
Recycling Endosome	100 nm[d]	$5.2 \cdot 10^{-16}$	6.4	$3.2 \cdot 10^{-2}$	$2.6 \cdot 10^{-3}$
Late Endosome	2 µm[e]	$4.2 \cdot 10^{-12}$	5.0	$4.0 \cdot 10^{-3}$	$1.0 \cdot 10^{-2}$
Lysosome	2 µm[e]	$4.2 \cdot 10^{-12}$	4.5	0	$1.0 \cdot 10^{2}$
Nucleus	14 µm[f]	$1.4 \cdot 10^{-9}$	7.4	$1.2 \cdot 10^{-5}$	$1.0 \cdot 10^{-3}$

Compartments are defined by their spherical diameter, volume, pH, and ligand-receptor kinetics as shown. All compartments are assumed spherical except for the extracellular space. Note that k_{off} rates are regulated by pH and the k_{on} rates by compartment volume. References for diameters are given in the footnotes.

[a][397]; [b][398], [399]; [c] [400]; [d][398], [399]; [e][400]; [f][401].

Table 4.2: Compartment integrated responses for various RTKs.

		Ang2-Tie2	EGF-EGFR	FGF2-FGFR1	IGF1-IGFR1	PDGFAA-PDGFRβ	PDGFBB-PDGFRα	VEGFA-VEGFR1	VEGFA-VEGFR2
Parameters	Receptors/cell	[a] $1.8 \cdot 10^3$	[d] $5.0 \cdot 10^4$	[f] $2.8 \cdot 10^4$	[i] $2.5 \cdot 10^4$	[a] $5.3 \cdot 10^4$	[a] $5.1 \cdot 10^3$	[o] $2.7 \cdot 10^3$	[o] $2.0 \cdot 10^3$
	k_{on} ($M^{-1}s^{-1}$)	[b] $6.0 \cdot 10^3$	[d] $3.0 \cdot 10^7$	[g] $9.6 \cdot 10^4$	[j] $2.7 \cdot 10^5$	[l] $8.8 \cdot 10^3$	[l] $7.8 \cdot 10^6$	[o] $3.0 \cdot 10^7$	[o] $1.0 \cdot 10^7$
	k_{off} (s^{-1})	[b] $6.1 \cdot 10^{-4}$	[d] $3.8 \cdot 10^{-3}$	[g] $5.9 \cdot 10^{-3}$	[j] $1.2 \cdot 10^{-3}$	[l] $1.5 \cdot 10^{-4}$	[l] $7.6 \cdot 10^{-3}$	[o] $1.0 \cdot 10^{-3}$	[o] $1.0 \cdot 10^{-3}$
	Ligand in Serum (pg/mL)	[c] 1865	[e] 917	[h] 2.2	[k] $1.65 \cdot 10^5$	[m] 1769	[n] 8506	[h] 160	[h] 160
Integrated response relative to membrane	Membrane	1.0	1.0	1.0	1.0	1.0	1.0	1.0	1.0
	Endocytic Vesicle	90	84	386	75	57	73	76	80
	Early Endosome	9.2	4.2	10	2.7	8.9	2.4	8.0	8.4
	Recycling Endosome	$8.8 \cdot 10^{-2}$	$3.8 \cdot 10^{-2}$	$9.8 \cdot 10^{-2}$	$2.3 \cdot 10^{-2}$	$8.7 \cdot 10^{-2}$	$1.9 \cdot 10^{-2}$	$7.6 \cdot 10^{-2}$	$8.0 \cdot 10^{-2}$
	Late Endosome	54	39	108	27	41	23	52	55
	Lysosome	$1.6 \cdot 10^{-4}$	$1.2 \cdot 10^{-4}$	$3.2 \cdot 10^{-4}$	$8.1 \cdot 10^{-5}$	$1.2 \cdot 10^{-4}$	$6.8 \cdot 10^{-5}$	$1.6 \cdot 10^{-4}$	$1.6 \cdot 10^{-4}$
	Nucleus	9	47	17	38	16	35	36	33
	Total membrane integrated response (p-Receptor·time)	$8.9 \cdot 10^2$	$7.7 \cdot 10^3$	$1.5 \cdot 10^1$	$1.1 \cdot 10^4$	$4.7 \cdot 10^4$	$2.3 \cdot 10^3$	$1.6 \cdot 10^3$	$1.1 \cdot 10^3$

Integrated responses in each compartment, relative to the membrane, in addition to interaction kinetics and receptor levels, are given for various RTKs. Interaction kinetics are given for pH = 7.4. Trafficking kinetics are kept the same for every RTK. Ligand concentrations are taken from serum levels. The total membrane integrated response over 4 hours after ligand stimulus is given for each RTK.

[a][328]; [b][332]; [c][402]; [d][327]; [e][403]; [f][333]; [g][334]; [h][404]; [i][330]; [j][331]; [k][405]; [l][329]; [m][406]; [n][407]; [o][178]

References

[1] D. Ribatti and E. Crivellato, "'Sprouting angiogenesis', a reappraisal," *Dev. Biol.*, vol. 372, no. 2, pp. 157–165, Dec. 2012.

[2] V. Djonov, M. Schmid, S. A. Tschanz, and P. H. Burri, "Intussusceptive Angiogenesis," *Circ. Res.*, vol. 86, no. 3, p. 286 LP-292, Feb. 2000.

[3] A. HELISCH and W. SCHAPER, "Arteriogenesis The Development and Growth of Collateral Arteries," *Microcirculation*, vol. 10, no. 1, pp. 83–97, 2003.

[4] M. Heil, I. Eitenmüller, T. Schmitz-Rixen, and W. Schaper, "Arteriogenesis versus angiogenesis: similarities and differences," *J. Cell. Mol. Med.*, vol. 10, no. 1, pp. 45–55, Jan. 2006.

[5] A. A. Ucuzian, A. A. Gassman, A. T. East, and H. P. Greisler, "Molecular Mediators of Angiogenesis," *J. Burn Care Res.*, vol. 31, no. 1, p. 158, 2010.

[6] H. M. Eilken and R. H. Adams, "Dynamics of endothelial cell behavior in sprouting angiogenesis," *Curr. Opin. Cell Biol.*, vol. 22, no. 5, pp. 617–625, Oct. 2010.

[7] T. M. Honnegowda, P. Kumar, E. G. P. Udupa, S. Kumar, U. Kumar, and P. Rao, "Role of angiogenesis and angiogenic factors in acute and chronic wound healing," *Plast. Aesthetic Res. Vol 2, No 5*, Sep. 2015.

[8] J. Welti, S. Loges, S. Dimmeler, and P. Carmeliet, "Recent molecular discoveries in angiogenesis and antiangiogenic therapies in cancer," *J. Clin. Invest.*, vol. 123, no. 8, pp. 3190–3200.

[9] P. H. Burri, R. Hlushchuk, and V. Djonov, "Intussusceptive angiogenesis: Its emergence, its characteristics, and its significance," *Dev. Dyn.*, vol. 231, no. 3, pp. 474–488, 2004.

[10] S. J. Mentzer and M. A. Konerding, “Intussusceptive Angiogenesis: Expansion and Remodeling of Microvascular Networks,” *Angiogenesis*, vol. 17, no. 3, pp. 499–509, Jul. 2014.

[11] A. N. Makanya, R. Hlushchuk, and V. G. Djonov, “Intussusceptive angiogenesis and its role in vascular morphogenesis, patterning, and remodeling,” *Angiogenesis*, vol. 12, no. 2, p. 113, 2009.

[12] B. Styp-Rekowska, R. Hlushchuk, A. R. Pries, and V. Djonov, “Intussusceptive angiogenesis: pillars against the blood flow,” *Acta Physiol.*, vol. 202, no. 3, pp. 213–223, 2011.

[13] R. K. Jain, J. D. Martin, and T. Stylianopoulos, “The role of mechanical forces in tumor growth and therapy,” *Annu. Rev. Biomed. Eng.*, vol. 16, pp. 321–346, Jul. 2014.

[14] S. Egginton, “Angiogenesis – may the force be with you!,” *J. Physiol.*, vol. 588, no. Pt 23, pp. 4615–4616, Dec. 2010.

[15] P. Carmeliet and R. K. Jain, “Angiogenesis in cancer and other diseases,” *Nature*, vol. 407, no. 6801, pp. 249–257, Sep. 2000.

[16] J. Folkman, “Tumor Angiogenesis: Therapeutic Implications,” *N Engl J Med*, vol. 285, pp. 1182–6, 1971.

[17] J. Folkman, “The intestine as an organ culture,” in *Carcinoma of the Colon and Antecedent Epithelium*, 1970, pp. 113–127.

[18] M. A. GIMBRONE, R. H. ASTER, R. S. COTRAN, J. CORKERY, J. H. JANDL, and J. FOLKMAN, “Preservation of Vascular Integrity in Organs perfused in vitro with a Platelet-rich Medium,” *Nature*, vol. 222, no. 5188, pp. 33–36, Apr. 1969.

[19] H. S. N. Greene, “HETEROLOGOUS TRANSPLANTATION OF MAMMALIAN TUMORS,” *J. Exp. Med.*, vol. 73, no. 4, p. 461 LP-474, Apr. 1941.

[20] T. Cavallo, R. Sade, J. Folkman, and R. S. Cotran, “TUMOR ANGIOGENESIS : Rapid Induction of Endothelial Mitoses Demonstrated by Autoradiography,” *J. Cell Biol.*, vol. 54, no. 2, pp. 408–420, Aug. 1972.

[21] B. A. Warren and P. Shubik, “The growth of the blood supply to melanoma transplants in the hamster cheek pouch,” *Lab Invest*, vol. 15, pp. 464–78, 1966.

[22] B. A. WARREN, “The ultrastructure of capillary sprouts induced by melanoma transplants in the golden hamster,” *J. R. Microsc. Soc.*, vol. 86, no. 2, pp. 177–187, 1966.

[23] G. H. Algire, H. W. Chalkley, F. Y. Legallais, and H. D. Park, “Vasculae Reactions of Normal and Malignant Tissues in Vivo. I. Vascular Reactions of Mice to Wounds and to Normal and Neoplastic Transplants,” *J. Natl. Cancer Inst.* , vol. 6, no. 1, pp. 73–85, Aug. 1945.

[24] I. F. Tannock, “The relation between cell proliferation and the vascular system in a transplanted mouse mammary tumour,” *Br J Cancer*, vol. 22, no. 2, pp. 258–273, Jun. 1968.

[25] I. F. Tannock, “Population Kinetics of Carcinoma Cells, Capillary Endothelial Cells, and Fibroblasts in a Transplanted Mouse Mammary Tumor,” *Cancer Res.*, vol. 30, no. 10, p. 2470 LP-2476, Oct. 1970.

[26] F. Hillen and A. W. Griffioen, “Tumour vascularization: sprouting angiogenesis and beyond,” *Cancer Metastasis Rev.*, vol. 26, no. 3–4, pp. 489–502, Dec. 2007.

[27] S. M. Weis and D. A. Cheresh, “Tumor angiogenesis: molecular pathways and therapeutic

targets," *Nat Med*, vol. 17, no. 11, pp. 1359–1370, Nov. 2011.

[28] R. S. Samant and L. A. Shevde, "Recent Advances in Anti-Angiogenic Therapy of Cancer," *Oncotarget*, vol. 2, no. 3, pp. 122–134, Mar. 2011.

[29] I. S. Moreira and P. A. F. and M. J. Ramos, "Vascular Endothelial Growth Factor (VEGF) Inhibition - A Critical Review," *Anti-Cancer Agents in Medicinal Chemistry*, vol. 7, no. 2. pp. 223–245, 2007.

[30] R. K. Jain, "Normalization of tumor vasculature: an emerging concept in antiangiogenic therapy," *Science (80-.).*, vol. 307, pp. 58–62, 2005.

[31] R. K. Jain, "Vascular and interstitial biology of tumors," in *Clinical Oncology 3rd ed*, 2004, pp. 153–72.

[32] D. M. McDonald and P. L. Choyke, "Imaging of angiogenesis: from microscope to clinic," *Nat Med*, vol. 9, no. 6, pp. 713–725, Jun. 2003.

[33] P. Baluk, S. Morikawa, A. Haskell, M. Mancuso, and D. M. McDonald, "Abnormalities of Basement Membrane on Blood Vessels and Endothelial Sprouts in Tumors," *Am. J. Pathol.*, vol. 163, no. 5, pp. 1801–1815, Nov. 2003.

[34] R. K. Jain, "The next frontier of molecular medicine: delivery of therapeutics," *Nat. Med.*, vol. 4, no. 6, pp. 655–657, 1998.

[35] J. Ma, S. Pulfer, S. Li, J. Chu, K. Reed, and J. M. Gallo, "Pharmacodynamic-mediated Reduction of Temozolomide Tumor Concentrations by the Angiogenesis Inhibitor TNP-470," *Cancer Res.*, vol. 61, no. 14, p. 5491 LP-5498, Jul. 2001.

[36] T. P. Padera, B. R. Stoll, J. B. Tooredman, D. Capen, E. di Tomaso, and R. K. Jain, "Pathology: Cancer cells compress intratumour vessels," *Nature*, vol. 427, no. 6976, p.

695, Feb. 2004.

[37] R. T. Tong, Y. Boucher, S. V Kozin, F. Winkler, D. J. Hicklin, and R. K. Jain, "Vascular Normalization by Vascular Endothelial Growth Factor Receptor 2 Blockade Induces a Pressure Gradient Across the Vasculature and Improves Drug Penetration in Tumors," *Cancer Res.*, vol. 64, no. 11, p. 3731 LP-3736, Jun. 2004.

[38] H. Wildiers, G. Guetens, G. De Boeck, E. Verbeken, B. Landuyt, W. Landuyt, E. A. de Bruijn, and A. T. van Oosterom, "Effect of antivascular endothelial growth factor treatment on the intratumoral uptake of CPT-11," *Br J Cancer*, vol. 88, no. 12, pp. 1979–1986.

[39] F. Winkler, S. V Kozin, R. T. Tong, S.-S. Chae, M. F. Booth, I. Garkavtsev, L. Xu, D. J. Hicklin, D. Fukumura, E. di Tomaso, L. L. Munn, and R. K. Jain, "Kinetics of vascular normalization by VEGFR2 blockade governs brain tumor response to radiation: Role of oxygenation, angiopoietin-1, and matrix metalloproteinases," *Cancer Cell*, vol. 6, no. 6, pp. 553–563, Dec. 2004.

[40] Y. Huang, S. Goel, D. G. Duda, D. Fukumura, and R. K. Jain, "Vascular normalization as an emerging strategy to enhance cancer immunotherapy," *Cancer Res.*, vol. 73, no. 10, pp. 2943–2948, May 2013.

[41] S. Goel, A. H.-K. Wong, and R. K. Jain, "Vascular Normalization as a Therapeutic Strategy for Malignant and Nonmalignant Disease," *Cold Spring Harb. Perspect. Med.*, vol. 2, no. 3, p. a006486, Mar. 2012.

[42] S. M. Tolaney, Y. Boucher, D. G. Duda, J. D. Martin, G. Seano, M. Ancukiewicz, W. T. Barry, S. Goel, J. Lahdenrata, S. J. Isakoff, E. D. Yeh, S. R. Jain, M. Golshan, J. Brock,

M. Snuderl, E. P. Winer, I. E. Krop, and R. K. Jain, “Role of vascular density and normalization in response to neoadjuvant bevacizumab and chemotherapy in breast cancer patients,” *Proc. Natl. Acad. Sci. U. S. A.*, vol. 112, no. 46, pp. 14325–14330, Nov. 2015.

[43] Y. Cao, “Future options of anti-angiogenic cancer therapy,” *Chin. J. Cancer*, vol. 35, no. 1, p. 21, 2016.

[44] N. S. Vasudev and A. R. Reynolds, “Anti-angiogenic therapy for cancer: current progress, unresolved questions and future directions,” *Angiogenesis*, vol. 17, no. 3, pp. 471–494, 2014.

[45] G. Peach, M. Griffin, K. G. Jones, M. M. Thompson, and R. J. Hinchliffe, “Diagnosis and management of peripheral arterial disease,” *BMJ Br. Med. J.*, vol. 345, Aug. 2012.

[46] J. S. Berger and W. R. Hiatt, “Medical Therapy in Peripheral Artery Disease,” *Circulation*, vol. 126, no. 4, p. 491 LP-500, Jul. 2012.

[47] H. S. Rasmussen, C. S. Rasmussen, and J. Macko, “VEGF gene therapy for coronary artery disease and peripheral vascular disease,” *Cardiovasc. Radiat. Med.*, vol. 3, no. 2, pp. 114–117, Apr. 2002.

[48] D. R. Senger, S. J. Galli, A. M. Dvorak, C. A. Perruzzi, V. S. Harvey, and H. F. Dvorak, “Tumor cells secrete a vascular permeability factor that promotes accumulation of ascites fluid,” *Science (80-.).*, vol. 219, no. 4587, p. 983 LP-985, Feb. 1983.

[49] D. W. Leung, G. Cachianes, W. J. Kuang, D. V Goeddel, and N. Ferrara, “Vascular endothelial growth factor is a secreted angiogenic mitogen,” *Science (80-.).*, vol. 246, no. 4935, p. 1306 LP-1309, Dec. 1989.

[50] P. J. Keck, S. D. Hauser, G. Krivi, K. Sanzo, T. Warren, J. Feder, and D. T. Connolly,

"Vascular permeability factor, an endothelial cell mitogen related to PDGF," *Science (80-.).*, vol. 246, no. 4935, p. 1309 LP-1312, Dec. 1989.

[51] K. J. Kim, B. Li, J. Winer, M. Armanini, N. Gillett, H. S. Phillips, and N. Ferrara, "Inhibition of vascular endothelial growth factor-induced angiogenesis suppresses tumour growth in vivo," *Nature*, vol. 362, pp. 841–844, 1993.

[52] M. W. Majesky, "A Little VEGF Goes a Long Way," *Circulation*, vol. 94, no. 12, p. 3062 LP-3064, Dec. 1996.

[53] N. Ferrara and A. P. Adamis, "Ten years of anti-vascular endothelial growth factor therapy," *Nat Rev Drug Discov*, vol. 15, no. 6, pp. 385–403, Jun. 2016.

[54] N. Ferrara, G. H-P, J. LeCouter, F. N, G. H-P, L. J, H.-P. Gerber, and J. LeCouter, "The biology of VEGF and its receptors," *Nat Med*, vol. 9, no. 6, pp. 669–676, Jun. 2003.

[55] S. Ogawa, A. Oku, A. Sawano, S. Yamaguchi, Y. Yazaki, and M. Shibuya, "A Novel Type of Vascular Endothelial Growth Factor, VEGF-E (NZ-7 VEGF), Preferentially Utilizes KDR/Flk-1 Receptor and Carries a Potent Mitotic Activity without Heparin-binding Domain," *J. Biol. Chem.* , vol. 273, no. 47, pp. 31273–31282, Nov. 1998.

[56] H. Takahashi, S. Hattori, A. Iwamatsu, H. Takizawa, and M. Shibuya, "A Novel Snake Venom Vascular Endothelial Growth Factor (VEGF) Predominantly Induces Vascular Permeability through Preferential Signaling via VEGF Receptor-1," *J. Biol. Chem.* , vol. 279, no. 44, pp. 46304–46314, Oct. 2004.

[57] B. A. Keyt, L. T. Berleau, H. V Nguyen, H. Chen, H. Heinsohn, R. Vandlen, and N. Ferrara, "The Carboxyl-terminal Domain(111 165) of Vascular Endothelial Growth Factor Is Critical for Its Mitogenic Potency," *J. Biol. Chem.*, vol. 271, no. 13, pp. 7788–7795,

Mar. 1996.

[58] N. Ferrara, G. H-P, J. LeCouter, F. N, G. H-P, and L. J, “The biology of VEGF and its receptors,” *Nat Med*, vol. 9, pp. 669–676, 2003.

[59] Y. Qiu, C. Hoareau-Aveilla, S. Oltean, S. J. Harper, and D. O. Bates, “The anti-angiogenic isoforms of VEGF in health and disease,” *Biochem. Soc. Trans.*, vol. 37, no. Pt 6, pp. 1207–1213, Dec. 2009.

[60] C. Hilmi, M. Guyot, and G. Pages, “VEGF Spliced Variants: Possible Role of Anti-Angiogenesis Therapy,” *J Nucleic Acids*, vol. 2012, p. 162692, 2012.

[61] J. Woolard, W.-Y. Wang, H. S. Bevan, Y. Qiu, L. Morbidelli, R. O. Pritchard-Jones, T.-G. Cui, M. Sugiono, E. Waine, R. Perrin, R. Foster, J. Digby-Bell, J. D. Shields, C. E. Whittles, R. E. Mushens, D. A. Gillatt, M. Ziche, S. J. Harper, and D. O. Bates, “VEGF165b, an Inhibitory Vascular Endothelial Growth Factor Splice Variant,” *Cancer Res.*, vol. 64, no. 21, p. 7822 LP-7835, Nov. 2004.

[62] B. Olofsson, K. Pajusola, A. Kaipainen, G. von Euler, V. Joukov, O. Saksela, A. Orpana, R. F. Pettersson, K. Alitalo, and U. Eriksson, “Vascular endothelial growth factor B, a novel growth factor for endothelial cells.,” *Proc. Natl. Acad. Sci. U. S. A.*, vol. 93, no. 6, pp. 2576–2581, Mar. 1996.

[63] B. Olofsson, K. Pajusola, G. von Euler, D. Chilov, K. Alitalo, and U. Eriksson, “Genomic Organization of the Mouse and Human Genes for Vascular Endothelial Growth Factor B (VEGF-B) and Characterization of a Second Splice Isoform,” *J. Biol. Chem.* , vol. 271, no. 32, pp. 19310–19317, Aug. 1996.

[64] T. Falk, S. Zhang, and S. J. Sherman, “Vascular endothelial growth factor B (VEGF-B) is

up-regulated and exogenous VEGF-B is neuroprotective in a culture model of Parkinson's disease," *Mol. Neurodegener.*, vol. 4, no. 1, p. 49, 2009.

[65] R. Kivelä, M. Bry, M. R. Robciuc, M. Räsänen, M. Taavitsainen, J. M. U. Silvola, A. Saraste, J. J. Hulmi, A. Anisimov, M. I. Mäyränpää, J. H. Lindeman, L. Eklund, S. Hellberg, R. Hlushchuk, Z. W. Zhuang, M. Simons, V. Djonov, J. Knuuti, E. Mervaala, and K. Alitalo, "VEGF-B-induced vascular growth leads to metabolic reprogramming and ischemia resistance in the heart," *EMBO Mol. Med.*, vol. 6, no. 3, p. 307 LP-321, Jan. 2014.

[66] D. Bellomo, J. P. Headrick, G. U. Silins, C. A. Paterson, P. S. Thomas, M. Gartside, A. Mould, M. M. Cahill, I. D. Tonks, S. M. Grimmond, S. Townson, C. Wells, M. Little, M. C. Cummings, N. K. Hayward, and G. F. Kay, "Mice Lacking the Vascular Endothelial Growth Factor-B Gene (Vegfb) Have Smaller Hearts, Dysfunctional Coronary Vasculature, and Impaired Recovery From Cardiac Ischemia," *Circ. Res.*, vol. 86, no. 2, p. e29 LP-e35, Feb. 2000.

[67] C. E. Hagberg, A. Falkevall, X. Wang, E. Larsson, J. Huusko, I. Nilsson, L. A. van Meeteren, E. Samen, L. Lu, M. Vanwildemeersch, J. Klar, G. Genove, K. Pietras, S. Stone-Elander, L. Claesson-Welsh, S. Yla-Herttuala, P. Lindahl, and U. Eriksson, "Vascular endothelial growth factor B controls endothelial fatty acid uptake," *Nature*, vol. 464, no. 7290, pp. 917–921, Apr. 2010.

[68] X. Li, "VEGF-B: a thing of beauty," *Cell Res.*, vol. 20, no. 7, pp. 741–744, Jul. 2010.

[69] M. Bry, R. Kivelä, V.-M. Leppänen, and K. Alitalo, "Vascular Endothelial Growth Factor-B in Physiology and Disease," *Physiol. Rev.*, vol. 94, no. 3, p. 779 LP-794, Jul. 2014.

[70] X. Li, K. Aase, H. Li, G. von Euler, and U. Eriksson, “Isoform-specific expression of VEGF-B in normal tissues and tumors,” *Growth Factors*, vol. 19, no. 1, pp. 49–59, 2001.

[71] J. L. Su, C. J. Yen, P. S. Chen, S. E. Chuang, C. C. Hong, I. H. Kuo, H. Y. Chen, M. C. Hung, and M. L. Kuo, “The role of the VEGF-C/VEGFR-3 axis in cancer progression,” *Br. J. Cancer*, vol. 96, no. 4, pp. 541–545, Feb. 2007.

[72] Y. Kodera, Y. Katanasaka, Y. Kitamura, H. Tsuda, K. Nishio, T. Tamura, and F. Koizumi, “Sunitinib inhibits lymphatic endothelial cell functions and lymph node metastasis in a breast cancer model through inhibition of vascular endothelial growth factor receptor 3,” *Breast Cancer Res.*, vol. 13, no. 3, pp. R66–R66, Jun. 2011.

[73] Y. Deng, X. Zhang, and M. Simons, “Molecular controls of lymphatic VEGFR3 signaling,” *Arterioscler. Thromb. Vasc. Biol.*, vol. 35, no. 2, pp. 421–429, Feb. 2015.

[74] S. Nakao, S. Zandi, Y. Hata, S. Kawahara, R. Arita, A. Schering, D. Sun, M. I. Melhorn, Y. Ito, N. Lara-Castillo, T. Ishibashi, and A. Hafezi-Moghadam, “Blood vessel endothelial VEGFR-2 delays lymphangiogenesis: an endogenous trapping mechanism links lymph- and angiogenesis,” *Blood*, vol. 117, no. 3, pp. 1081–1090, Jan. 2011.

[75] R. Krebs and M. Jeltsch, “The lymphangiogenic growth factors VEGF-C and VEGF-D Part 1 : Fundamentals and embryonic development,” *LymphForsch*, vol. 17, pp. 30–7, 2013.

[76] M. G. Achen, M. Jeltsch, E. Kukk, T. Mäkinen, A. Vitali, A. F. Wilks, K. Alitalo, and S. A. Stacker, “Vascular endothelial growth factor D (VEGF-D) is a ligand for the tyrosine kinases VEGF receptor 2 (Flk1) and VEGF receptor 3 (Flt4),” *Proc. Natl. Acad. Sci. U. S. A.*, vol. 95, no. 2, pp. 548–553, Jan. 1998.

[77] M. E. Baldwin, M. M. Halford, S. Roufail, R. A. Williams, M. L. Hibbs, D. Grail, H. Kubo, S. A. Stacker, and M. G. Achen, "Vascular Endothelial Growth Factor D Is Dispensable for Development of the Lymphatic System," *Mol. Cell. Biol.*, vol. 25, no. 6, pp. 2441–2449, Mar. 2005.

[78] D. Maglione, V. Guerriero, G. Viglietto, M. G. Ferraro, O. Aprelikova, K. Alitalo, S. Del Vecchio, K. J. Lei, J. Y. Chou, and M. G. Persico, "Two alternative mRNAs coding for the angiogenic factor, placenta growth factor (PlGF), are transcribed from a single gene of chromosome 14," *Oncogene*, vol. 8, no. 4, pp. 925–31, 1993.

[79] Y. Y. Cao, W.-R. Ji, P. Qi, Å. Rosin, and Y. Y. Cao, "Placenta Growth Factor: Identification and Characterization of a Novel Isoform Generated by RNA Alternative Splicing," *Biochem. Biophys. Res. Commun.*, vol. 235, no. 3, pp. 493–498, 1997.

[80] W. Yang, H. Ahn, M. Hinrichs, R. J. Torry, and D. S. Torry, "Evidence of a novel isoform of placenta growth factor (PlGF-4) expressed in human trophoblast and endothelial cells," *J. Reprod. Immunol.*, vol. 60, no. 1, pp. 53–60, Oct. 2003.

[81] S. De Falco, "The discovery of placenta growth factor and its biological activity," *Exp Mol Med*, vol. 44, pp. 1–9, Jan. 2012.

[82] R. L. Kendall and K. A. Thomas, "Inhibition of vascular endothelial cell growth factor activity by an endogenously encoded soluble receptor," *Proc. Natl. Acad. Sci.* , vol. 90, no. 22, pp. 10705–10709, Nov. 1993.

[83] H. Pavlakovic, J. Becker, R. Albuquerque, J. Wilting, and J. Ambati, "Soluble VEGFR-2: an Anti-lymphangiogenic Variant of VEGF Receptors," *Ann. N. Y. Acad. Sci.*, vol. 1207, no. Suppl 1, pp. E7-15, Oct. 2010.

[84] N. Singh, M. Tiem, R. Watkins, Y. K. Cho, Y. Wang, T. Olsen, H. Uehara, C. Mamalis, L. Luo, Z. Oakey, and B. K. Ambati, "Soluble vascular endothelial growth factor receptor 3 is essential for corneal alymphaticity," *Blood*, vol. 121, no. 20, pp. 4242–4249, May 2013.

[85] C. Hornig, B. Barleon, S. Ahmad, P. Vuorela, A. Ahmed, and H. A. Weich, "Release and Complex Formation of Soluble VEGFR-1 from Endothelial Cells and Biological Fluids," *Lab Invest*, vol. 80, no. 4, pp. 443–454.

[86] R. L. Kendall, G. Wang, and K. A. Thomas, "Identification of a Natural Soluble Form of the Vascular Endothelial Growth Factor Receptor, FLT-1, and Its Heterodimerization with KDR," *Biochem. Biophys. Res. Commun.*, vol. 226, no. 2, pp. 324–328, 1996.

[87] B. Mezquita, J. Mezquita, M. Pau, and C. Mezquita, "A novel intracellular isoform of VEGFR-1 activates Src and promotes cell invasion in MDA-MB-231 breast cancer cells.," *J. Cell. Biochem.*, vol. 110, no. 3, pp. 732–42, Jun. 2010.

[88] B. Mezquita, P. Mezquita, M. Pau, J. Mezquita, and C. Mezquita, "Unlocking Doors without Keys: Activation of Src by Truncated C-terminal Intracellular Receptor Tyrosine Kinases Lacking Tyrosine Kinase Activity," *Cells*, vol. 3, no. 1, pp. 92–111, Mar. 2014.

[89] R. Blanco and H. Gerhardt, "VEGF and Notch in tip and stalk cell selection," *Cold Spring Harb. Perspect. Med.*, vol. 3, no. 1, pp. 1–20, 2013.

[90] S. Chen, A. Ansari, W. Sterrett, K. Hurley, K. Kemball, J. C. Weddell, and P. I. Imoukhuede, "Current state-of-the-art and future directions in systems biology," *Prog. Commun. Sci.*, vol. 1, pp. 12–26, 2014.

[91] K. A. Janes and D. A. Lauffenburger, "Models of signalling networks – what cell

biologists can gain from them and give to them," *J. Cell Sci.*, vol. 126, no. 9, p. 1913 LP-1921, May 2013.

[92] M. Buiatti and G. Longo, "Randomness and multilevel interactions in biology," *Theory Biosci.*, vol. 132, no. 3, pp. 139–158, 2013.

[93] Y. Pilpel, "Noise in Biological Systems: Pros, Cons, and Mechanisms of Control BT - Yeast Systems Biology: Methods and Protocols," I. J. Castrillo and G. S. Oliver, Eds. Totowa, NJ: Humana Press, 2011, pp. 407–425.

[94] D. J. Wilkinson, "Stochastic modelling for quantitative description of heterogeneous biological systems.," *Nat. Rev. Genet.*, vol. 10, no. fEbruAry, pp. 122–133, 2009.

[95] R. Kerr, T. Bartol, B. Kaminsky, M. Dittrich, J. Chang, S. Baden, T. Sejnowski, and J. Stiles, "Fast Monte Carlo Simulation Methods for Biological Reaction-Diffusion Systems in Solution and on Surfaces," *SIAM J. Sci. Comput.*, vol. 30, no. 6, pp. 3126–3149, Jan. 2008.

[96] G. An, Q. Mi, J. Dutta-Moscato, and Y. Vodovotz, "Agent-based models in translational systems biology," *Wiley Interdiscip. Rev. Syst. Biol. Med.*, vol. 1, no. 2, pp. 159–171, 2009.

[97] J. Cosgrove, J. Butler, K. Alden, M. Read, V. Kumar, L. Cucurull-Sanchez, J. Timmis, and M. Coles, "Agent-Based Modeling in Systems Pharmacology," *CPT Pharmacometrics Syst. Pharmacol.*, vol. 4, no. 11, pp. 615–629, 2015.

[98] P. Aloy and R. B. Russell, "Structural systems biology: modelling protein interactions," *Nat Rev Mol Cell Biol*, vol. 7, no. 3, pp. 188–197, Mar. 2006.

[99] P. M. Hoi, S. Li, C. T. Vong, H. H. L. Tseng, Y. W. Kwan, and S. M.-Y. Lee, "Recent

advances in structure-based drug design and virtual screening of VEGFR tyrosine kinase inhibitors," *Methods*, vol. 71, pp. 85–91, Jan. 2015.

[100] J. C. Vanegas-Acosta and D. A. Garzón-Alvarado, "Biological modelling and computational implementation using the finite elements method," *Comput. Appl. Math.*, vol. 33, no. 3, pp. 621–640, 2014.

[101] J. C. Weddell, J. Kwack, P. I. Imoukhuede, and A. Masud, "Hemodynamic Analysis in an Idealized Artery Tree: Differences in Wall Shear Stress between Newtonian and Non-Newtonian Blood Models," *PLoS One*, vol. 10, no. 4, p. e0124575, Apr. 2015.

[102] P. K. Kreeger, "Using Partial Least Squares Regression to Analyze Cellular Response Data," *Sci. Signal.*, vol. 6, no. 271, p. tr7-tr7, Apr. 2013.

[103] E. Bartocci and P. Lió, "Computational Modeling, Formal Analysis, and Tools for Systems Biology," *PLoS Comput Biol*, vol. 12, no. 1, p. e1004591, Jan. 2016.

[104] S. R. Eddy, "What is Bayesian statistics?," *Nat Biotech*, vol. 22, no. 9, pp. 1177–1178, Sep. 2004.

[105] A. K. M. Azad, A. Lawen, and J. M. Keith, "Prediction of signaling cross-talks contributing to acquired drug resistance in breast cancer cells by Bayesian statistical modeling," *BMC Syst. Biol.*, vol. 9, no. 1, p. 2, 2015.

[106] A. L. Tarca, V. J. Carey, X. Chen, R. Romero, and S. Drăghici, "Machine Learning and Its Applications to Biology," *PLoS Comput Biol*, vol. 3, no. 6, p. e116, Jun. 2007.

[107] C. Sommer and D. W. Gerlich, "Machine learning in cell biology – teaching computers to recognize phenotypes," *J. Cell Sci.*, vol. 126, no. 24, p. 5529 LP-5539, Dec. 2013.

[108] L. A. Liotta, G. M. Saidel, and J. Kleinerman, "Diffusion model of tumor vascularization

and growth," *Bull. Math. Biol.*, vol. 39, no. 1, pp. 117–128, 1977.

[109] A. A. Qutub and A. S. Popel, "Angiogenesis, Computational Modeling Perspective BT - Encyclopedia of Applied and Computational Mathematics," B. Engquist, Ed. Berlin, Heidelberg: Springer Berlin Heidelberg, 2015, pp. 58–67.

[110] A. S. Deakin, "Model for initial vascular patterns in melanoma transplants," *Growth*, vol. 40, pp. 191–201, 1976.

[111] C. L. Stokes, D. A. Lauffenburger, and S. K. Williams, "Endothelial Cell Chemotaxis in Angiogenesis - Biological Motion," in *Lecture Notes in Biomathematics Vol 89*, W. Alt and G. Hoffmann, Eds. Berlin, Heidelberg: Springer Berlin Heidelberg, 1990, pp. 442–452.

[112] C. L. Stokes and D. a Lauffenburger, "Analysis of the roles of microvessel endothelial cell random motility and chemotaxis in angiogenesis.," *J. Theor. Biol.*, vol. 152, no. 3, pp. 377–403, Oct. 1991.

[113] M. A. Chaplain and A. R. Anderson, "Mathematical modelling, simulation and prediction of tumour-induced angiogenesis.," *Invasion Metastasis*, vol. 16, pp. 222–34, 1996.

[114] A. R. A. Anderson and M. A. J. Chaplain, "Continuous and discrete mathematical models of tumor-induced angiogenesis," *Bull. Math. Biol.*, vol. 60, no. 5, pp. 857–899, 1998.

[115] A. J. Connor, R. P. Nowak, E. Lorenzon, M. Thomas, F. Herting, S. Hoert, T. Quaiser, E. Shochat, J. Pitt-Francis, J. Cooper, P. K. Maini, and H. M. Byrne, "An integrated approach to quantitative modelling in angiogenesis research," *J. R. Soc. Interface*, vol. 12, no. 110, Aug. 2015.

[116] X. Zheng, G. Y. Koh, and T. Jackson, "A continuous model of angiogenesis: initiation,

extension, and maturation of new blood vessels modulated by vascular endothelial growth factor, angiopoietins, platelet-derived growth factor-B, and pericytes," *Discret. continous Dyn. Syst. Ser. B*, vol. 18, pp. 1109–54, 2013.

[117] L. T. Edgar, J. B. Hoying, U. Utzinger, C. J. Underwood, L. Krishnan, B. K. Baggett, S. A. Maas, J. E. Guilkey, and J. A. Weiss, "Mechanical Interaction of Angiogenic Microvessels With the Extracellular Matrix," *J. Biomech. Eng.*, vol. 136, no. 2, pp. 210011–2100115, Feb. 2014.

[118] S. M. Peirce, F. Mac Gabhann, and V. L. Bautch, "Integration of experimental and computational approaches to sprouting angiogenesis," *Curr. Opin. Hematol.*, vol. 19, no. 3, pp. 184–191, 2012.

[119] H. Gerhardt, M. Golding, M. Fruttiger, C. Ruhrberg, A. Lundkvist, A. Abramsson, M. Jeltsch, C. Mitchell, K. Alitalo, D. Shima, and C. Betsholtz, "VEGF guides angiogenic sprouting utilizing endothelial tip cell filopodia," *J. Cell Biol.*, vol. 161, no. 6, pp. 1163–1177, Jun. 2003.

[120] V. L. Bautch, "VEGF-Directed Blood Vessel Patterning: From Cells to Organism," *Cold Spring Harb. Perspect. Med.*, vol. 2, no. 9, p. a006452, Sep. 2012.

[121] M. Hellstrom, L.-K. Phng, J. J. Hofmann, E. Wallgard, L. Coultas, P. Lindblom, J. Alva, A.-K. Nilsson, L. Karlsson, N. Gaiano, K. Yoon, J. Rossant, M. L. Iruela-Arispe, M. Kalen, H. Gerhardt, and C. Betsholtz, "Dll4 signalling through Notch1 regulates formation of tip cells during angiogenesis," *Nature*, vol. 445, no. 7129, pp. 776–780, 2007.

[122] M. Hellström, L.-K. Phng, and H. Gerhardt, "VEGF and Notch Signaling: The Yin and Yang of Angiogenic Sprouting," *Cell Adh. Migr.*, vol. 1, no. 3, pp. 133–136, Jul. 2007.

[123] K. Bentley, H. Gerhardt, and P. A. Bates, “Agent-based simulation of notch-mediated tip cell selection in angiogenic sprout initalisation,” *J Theor Biol*, vol. 250, no. 1, pp. 25–36, Jan. 2008.

[124] K. Bentley, G. Mariggi, H. Gerhardt, P. a. Bates, B. PA, B. K, M. G, G. H, and B. PA, “Tipping the balance: robustness of tip cell selection, migration and fusion in angiogenesis,” *PLoS Comput Biol*, vol. 5, no. 10, p. e1000549, 2009.

[125] L. Jakobsson, C. A. Franco, K. Bentley, R. T. Collins, B. Ponsioen, I. M. Aspalter, I. Rosewell, M. Busse, G. Thurston, A. Medvinsky, S. Schulte-Merker, and H. Gerhardt, “Endothelial cells dynamically compete for the tip cell position during angiogenic sprouting,” *Nat Cell Biol*, vol. 12, no. 10, pp. 943–953, 2010.

[126] M. J. Siemerink, I. Klaassen, I. M. C. Vogels, A. W. Griffioen, C. J. F. Van Noorden, and R. O. Schlingemann, “CD34 marks angiogenic tip cells in human vascular endothelial cell cultures,” *Angiogenesis*, vol. 15, no. 1, pp. 151–163, Mar. 2012.

[127] E. Kur, J. Kim, A. Tata, C. H. Comin, K. I. Harrington, L. da F. Costa, K. Bentley, and C. Gu, “Temporal modulation of collective cell behavior controls vascular network topology,” *Elife*, vol. 5, p. e13212, Feb. 2016.

[128] R. McLennan, L. Dyson, K. W. Prather, J. A. Morrison, R. E. Baker, P. K. Maini, and P. M. Kulesa, “Multiscale mechanisms of cell migration during development: theory and experiment,” *Development*, vol. 139, no. 16, p. 2935 LP-2944, Jul. 2012.

[129] R. McLennan, L. J. Schumacher, J. A. Morrison, J. M. Teddy, D. A. Ridenour, A. C. Box, C. L. Semerad, H. Li, W. McDowell, D. Kay, P. K. Maini, R. E. Baker, and P. M. Kulesa, “VEGF signals induce trailblazer cell identity that drives neural crest migration,” *Dev.*

Biol., vol. 407, no. 1, pp. 12–25, Nov. 2015.

[130] S. E. M. Boas and R. M. H. Merks, "Tip cell overtaking occurs as a side effect of sprouting in computational models of angiogenesis," *BMC Syst. Biol.*, vol. 9, no. 1, pp. 1–17, 2015.

[131] P. Santos-Oliveira, A. Correia, T. Rodrigues, T. M. Ribeiro-Rodrigues, P. Matafome, J. C. Rodríguez-Manzaneque, R. Seiça, H. Girão, and R. D. M. Travasso, "The Force at the Tip - Modelling Tension and Proliferation in Sprouting Angiogenesis," *PLoS Comput Biol*, vol. 11, no. 8, p. e1004436, Aug. 2015.

[132] H. V Jain and T. L. Jackson, "A Hybrid Model of the Role of VEGF Binding in Endothelial Cell Migration and Capillary Formation," *Front. Oncol.*, vol. 3, p. 102, May 2013.

[133] G. I. BELL, "Model for the binding of multivalent antigen to cells," *Nature*, vol. 248, no. 5447, pp. 430–431, Mar. 1974.

[134] F. Mac Gabhann and A. S. Popel, "Model of competitive binding of vascular endothelial growth factor and placental growth factor to VEGF receptors on endothelial cells," *Am J Physiol Hear. Circ Physiol*, vol. 286, pp. H153–H164, 2004.

[135] M. Marcellini, N. De Luca, T. Riccioni, A. Ciucci, A. Orecchia, P. M. Lacal, F. Ruffini, M. Pesce, F. Cianfarani, G. Zambruno, A. Orlandi, and C. M. Failla, "Increased Melanoma Growth and Metastasis Spreading in Mice Overexpressing Placenta Growth Factor," *Am. J. Pathol.*, vol. 169, no. 2, pp. 643–654, Aug. 2006.

[136] H. Roy, S. Bhardwaj, M. Babu, S. Jauhiainen, K. H. Herzig, A. R. Bellu, H. J. Haisma, P. Carmeliet, K. Alitalo, and S. Yla-Herttuala, "Adenovirus-Mediated Gene Transfer of

Placental Growth Factor to Perivascular Tissue Induces Angiogenesis via Upregulation of the Expression of Endogenous Vascular Endothelial Growth Factor-A," *Hum Gene Ther*, vol. 16, pp. 1422–8, 2005.

[137] G. N. Masoud and W. Li, "HIF-1α pathway: role, regulation and intervention for cancer therapy," *Acta Pharm. Sin. B*, vol. 5, no. 5, pp. 378–389, Sep. 2015.

[138] J. E. Ziello, I. S. Jovin, and Y. Huang, "Hypoxia-Inducible Factor (HIF)-1 Regulatory Pathway and its Potential for Therapeutic Intervention in Malignancy and Ischemia," *Yale J. Biol. Med.*, vol. 80, no. 2, pp. 51–60, Jun. 2007.

[139] R. Du, K. V Lu, C. Petritsch, P. Liu, R. Ganss, E. Passegué, H. Song, S. VandenBerg, R. S. Johnson, Z. Werb, and G. Bergers, "HIF1α Induces the Recruitment of Bone Marrow-Derived Vascular Modulatory Cells to Regulate Tumor Angiogenesis and Invasion," *Cancer Cell*, vol. 13, no. 3, pp. 206–220, Mar. 2008.

[140] A. A. Qutub and A. S. Popel, "A computational model of intracellular oxygen sensing by hypoxia-inducible factor HIF1α," *J. Cell Sci.*, vol. 119, no. 16, p. 3467 LP-3480, Aug. 2006.

[141] M. A. Yucel and I. A. Kurnaz, "An in silico model for HIF-α regulation and hypoxia response in tumor cells," *Biotechnol. Bioeng.*, vol. 97, no. 3, pp. 588–600, 2007.

[142] C. Zhao and A. S. Popel, "Computational Model of MicroRNA Control of HIF-VEGF Pathway: Insights into the Pathophysiology of Ischemic Vascular Disease and Cancer," *PLoS Comput Biol*, vol. 11, no. 11, p. e1004612, Nov. 2015.

[143] R. Roskoski Jr., "VEGF receptor protein–tyrosine kinases: Structure and regulation," *Biochem. Biophys. Res. Commun.*, vol. 375, no. 3, pp. 287–291, Oct. 2008.

[144] F. Mac Gabhann, M. T. Yang, and A. S. Popel, "Monte Carlo simulations of VEGF binding to cell surface receptors in vitro," *Biochim. Biophys. Acta - Mol. Cell Res.*, vol. 1746, no. 2, pp. 95–107, Dec. 2005.

[145] F. Mac Gabhann and A. S. Popel, "Dimerization of VEGF receptors and implications for signal transduction: A computational study," *Biophys Chem*, vol. 128, no. 2–3, pp. 125–139, 2007.

[146] M. J. Cudmore, P. W. Hewett, S. Ahmad, K.-Q. Wang, M. Cai, B. Al-Ani, T. Fujisawa, B. Ma, S. Sissaoui, W. Ramma, M. R. Miller, D. E. Newby, Y. Gu, B. Barleon, H. Weich, and A. Ahmed, "The role of heterodimerization between VEGFR-1 and VEGFR-2 in the regulation of endothelial cell homeostasis," *Nat. Commun.*, vol. 3, p. 972, 2012.

[147] F. Mac Gabhann and A. S. Popel, "Interactions of VEGF isoforms with VEGFR-1, VEGFR-2, and neuropilin in vivo: a computational model of human skeletal muscle.," *Am. J. Physiol. Heart Circ. Physiol.*, vol. 292, no. 1, pp. H459-74, Jan. 2007.

[148] M. O. Stefanini, F. T. H. Wu, F. Mac Gabhann, and A. S. Popel, "The Presence of VEGF Receptors on the Luminal Surface of Endothelial Cells Affects VEGF Distribution and VEGF Signaling," *PLoS Comput Biol*, vol. 5, p. e1000622, 2009.

[149] J. Grunstein, J. J. Masbad, R. Hickey, F. Giordano, and R. S. Johnson, "Isoforms of Vascular Endothelial Growth Factor Act in a Coordinate Fashion To Recruit and Expand Tumor Vasculature," *Mol. Cell. Biol.*, vol. 20, no. 19, pp. 7282–7291, Oct. 2000.

[150] C. Ruhrberg, H. Gerhardt, M. Golding, R. Watson, S. Ioannidou, H. Fujisawa, C. Betsholtz, and D. T. Shima, "Spatially restricted patterning cues provided by heparin-binding VEGF-A control blood vessel branching morphogenesis," *Genes Dev.*, vol. 16,

no. 20, pp. 2684–2698, Oct. 2002.

[151] P. Vempati, A. S. Popel, and F. Mac Gabhann, “Formation of VEGF isoform-specific spatial distributions governing angiogenesis: computational analysis,” *BMC Syst Biol*, vol. 5, no. May, p. 59, Jan. 2011.

[152] M. G. F. Vempati P Popel AS and P. A. S. Vempati P Mac Gabhann F, “Quantifying the Proteolytic Release of Extracellular Matrix-Sequestered VEGF with a Computational Model,” *PLoS One*, vol. 5, p. e11860, 2010.

[153] M. Simons, E. Gordon, and L. Claesson-Welsh, “Mechanisms and regulation of endothelial VEGF receptor signalling,” *Nat Rev Mol Cell Biol*, vol. 17, no. 10, pp. 611–625, Oct. 2016.

[154] L. Claesson-Welsh, “VEGF receptor signal transduction – A brief update,” *Vascul. Pharmacol.*, 2016.

[155] T. Alarcón and K. M. Page, “Mathematical models of the VEGF receptor and its role in cancer therapy,” *J. R. Soc. Interface*, vol. 4, no. 13, pp. 283–304, Apr. 2007.

[156] L. Y. Mi, D. S. Ettenson, and E. R. Edelman, “Phospholipase C-delta extends intercellular signalling range and responses to injury-released growth factors in non-excitable cells,” *Cell Prolif.*, vol. 41, no. 4, pp. 671–690, Aug. 2008.

[157] L. Napione, S. Pavan, A. Veglio, A. Picco, G. Boffetta, A. Celani, G. Seano, L. Primo, A. Gamba, and F. Bussolino, “Unraveling the influence of endothelial cell density on VEGF-A signaling.,” *Blood*, vol. 119, no. 23, pp. 5599–607, Jun. 2012.

[158] W. H. Tan, A. S. Popel, and F. Mac Gabhann, “Computational Model of Gab1/2-Dependent VEGFR2 Pathway to Akt Activation.,” *PLoS One*, vol. 8, no. 6, p. e67438,

Jan. 2013.

[159] W. H. Tan, F. Mac Gabhann, and A. S. Popel, “Computational model of VEGFR2 pathway to ERK activation and modulation through receptor trafficking,” *Cell Signal*, vol. 25, pp. 2496–2510, 2013.

[160] S. M. Anderson, B. Shergill, Z. T. Barry, E. Manousiouthakis, T. T. Chen, E. Botvinick, M. O. Platt, M. L. Iruela-Arispe, and T. Segura, “VEGF internalization is not required for VEGFR-2 phosphorylation in bioengineered surfaces with covalently linked VEGF,” *Integr. Biol.*, vol. 3, no. 9, pp. 887–896, 2011.

[161] L. W. Clegg and F. Mac Gabhann, “Site-Specific Phosphorylation of VEGFR2 Is Mediated by Receptor Trafficking: Insights from a Computational Model,” *PLoS Comput Biol*, vol. 11, no. 6, p. e1004158, Jun. 2015.

[162] F. T. H. Wu, M. O. Stefanini, F. Mac Gabhann, and A. S. Popel, “Modeling of Growth Factor-Receptor Systems:: From Molecular-Level Protein Interaction Networks to Whole-Body Compartment Models,” *Method Enzym.*, vol. 467, pp. 461–497, 2009.

[163] P. Yen, S. D. Finley, M. O. Engel-Stefanini, and A. S. Popel, “A Two-Compartment Model of VEGF Distribution in the Mouse,” *PLoS One*, vol. 6, no. 11, p. e27514, Nov. 2011.

[164] F. T. H. Wu, M. O. Stefanini, F. Mac Gabhann, and A. S. Popel, “A Compartment Model of VEGF Distribution in Humans in the Presence of Soluble VEGF Receptor-1 Acting as a Ligand Trap,” *PLoS One*, vol. 4, no. 4, p. e5108, Apr. 2009.

[165] Y. Cao, “Therapeutic Angiogenesis for Ischemic Disorders: What Is Missing for Clinical Benefits?,” *Discov Med*, vol. 9, pp. 179–84, 2010.

[166] F. Mac Gabhann, A. A. a. Qutub, B. H. B. Annex, and A. S. A. Popel, "Systems biology of pro-angiogenic therapies targeting the VEGF system," *Wiley Interdiscip Rev Syst Biol Med*, vol. 2, no. 6, pp. 694–707, Nov. 2010.

[167] J. Ji, F. Mac Gabhann, and A. Popel, "Skeletal muscle VEGF gradients in peripheral arterial disease: simulations of rest and exercise," *Am J Physiol Hear. Circ Physiol*, vol. 293, pp. H3740-49, 2007.

[168] F. Mac Gabhann, J. W. Ji, and A. S. Popel, "VEGF gradients, receptor activation, and sprout guidance in resting and exercising skeletal muscle," *J Appl Physiol*, vol. 102, pp. 722–734, 2007.

[169] J. Myers, "Exercise and Cardiovascular Health," *Circulation*, vol. 107, no. 1, p. e2 LP-e5, Jan. 2003.

[170] F. Mac Gabhann, J. Ji, and A. Popel, "Multi-scale computational models of pro-angiogenic treatments in peripheral arterial disease," *Ann Biomed Eng*, vol. 35, pp. 982–94, 2007.

[171] F. Mac Gabhann, J. W. Ji, and A. S. Popel, "Computational Model of Vascular Endothelial Growth Factor Spatial Distribution in Muscle and Pro-Angiogenic Cell Therapy," *PLoS Comput. Biol.*, vol. 2, no. 9, p. e127, Sep. 2006.

[172] M. O. Stefanini, F. T. H. Wu, F. Mac Gabhann, and A. S. Popel, "A compartment model of VEGF distribution in blood, healthy and diseased tissues.," *BMC Syst. Biol.*, vol. 2, no. 1, p. 77, Jan. 2008.

[173] W. F. T. Stefanini MO Mac Gabhann F, Popel AS and M. G. F. P. A. S. Stefanini MO Wu FT, "Increase of plasma VEGF after intravenous administration of bevacizumab is

predicted by a pharmacokinetic model.," *Cancer Res*, vol. 70, no. 23, pp. 9886–9894, 2010.

[174] S. D. Finley, M. Dhar, and A. S. Popel, "Compartment model predicts VEGF secretion and investigates the effects of VEGF trap in tumor-bearing mice," *Front Oncol*, vol. 3, p. 196, 2013.

[175] T. Wilde and V. Damian, "In Silico Mechanistic Model for Understanding Intravitreal Dosing Frequency of Anti-VEGF Therapies," *ARVO Annu. Meet.*, vol. 55, p. 601, 2014.

[176] S. D. Finley and A. S. Popel, "Predicting the effects of anti-angiogenic agents targeting specific VEGF isoforms.," *AAPS J.*, vol. 14, no. 3, pp. 500–9, Sep. 2012.

[177] S. D. Finley, M. O. Engel-Stefanini, P. Imoukhuede, and A. S. Popel, "Pharmacokinetics and pharmacodynamics of VEGF-neutralizing antibodies," *BMC Syst. Biol.*, vol. 5, p. 193, Jan. 2011.

[178] J. C. Weddell and P. I. Imoukhuede, "Quantitative characterization of cellular membrane-receptor heterogeneity through statistical and computational modeling.," *PLoS One*, vol. 9, no. 5, p. e97271, Jan. 2014.

[179] S. D. Finley, P. Angelikopoulos, P. Koumoutsakos, and A. S. Popel, "Pharmacokinetics of Anti-VEGF Agent Aflibercept in Cancer Predicted by Data-Driven, Molecular-Detailed Model," *CPT Pharmacometrics Syst. Pharmacol.*, vol. 4, no. 11, pp. 641–649, 2015.

[180] R. Ragno, F. Ballante, A. Pirolli, R. B. Wickersham, A. Patsilinakos, S. Hesse, E. Perspicace, and G. Kirsch, "Vascular endothelial growth factor receptor-2 (VEGFR-2) inhibitors: development and validation of predictive 3-D QSAR models through extensive ligand- and structure-based approaches," *J. Comput. Aided. Mol. Des.*, vol. 29, no. 8, pp.

757–776, 2015.

[181] U. Schmidt, J. Ahmed, E. Michalsky, M. Hoepfner, and R. Preissner, “Comparative VEGF receptor tyrosine kinase modeling for the development of highly specific inhibitors of tumor angiogenesis.,” *Genome Inf.*, vol. 20, pp. 243–51, 2008.

[182] B. Nitzsche, C. Gloesenkamp, M. Schrader, M. Ocker, R. Preissner, M. Lein, A. Zakrzewicz, B. Hoffmann, and M. Hopfner, “Novel compounds with antiangiogenic and antiproliferative potency for growth control of testicular germ cell tumours,” *Br J Cancer*, vol. 103, no. 1, pp. 18–28, Jun. 2010.

[183] B. Gautier, M. A. Miteva, V. Goncalves, F. Huguenot, P. Coric, S. Bouaziz, B. Seijo, J.-F. Gaucher, I. Broutin, C. Garbay, A. Lesnard, S. Rault, N. Inguimbert, B. O. Villoutreix, and M. Vidal, “Targeting the Proangiogenic VEGF-VEGFR Protein-Protein Interface with Drug-like Compounds by In Silico and In Vitro Screening,” *Cell Chem. Biol.*, vol. 18, no. 12, pp. 1631–1639, Sep. 2016.

[184] J. Kankanala, A. M. Latham, A. P. Johnson, S. Homer-Vanniasinkam, C. W. G. Fishwick, and S. Ponnambalam, “A combinatorial in silico and cellular approach to identify a new class of compounds that target VEGFR2 receptor tyrosine kinase activity and angiogenesis,” *Br. J. Pharmacol.*, vol. 166, no. 2, pp. 737–748, May 2012.

[185] A. M. Latham, J. Kankanala, G. W. Fearnley, M. C. Gage, M. T. Kearney, S. Homer-Vanniasinkam, S. B. Wheatcroft, C. W. G. Fishwick, and S. Ponnambalam, “In Silico Design and Biological Evaluation of a Dual Specificity Kinase Inhibitor Targeting Cell Cycle Progression and Angiogenesis,” *PLoS One*, vol. 9, no. 11, p. e110997, Nov. 2014.

[186] L. Shi, J. Zhou, J. Wu, Y. Shen, and X. Li, “Anti-Angiogenic Therapy: Strategies to

Develop Potent VEGFR-2 Tyrosine Kinase Inhibitors and Future Prospect," *Curr Med Chem*, vol. 23, pp. 1000–40, 2016.

[187] K. L. Meadows and H. I. Hurwitz, "Anti-VEGF therapies in the clinic.," *Cold Spring Harb. Perspect. Med.*, vol. 2, no. 10, Oct. 2012.

[188] Y. Kubota, "Tumor Angiogenesis and Anti-angiogenic Therapy," *Keio J. Med.*, vol. 61, no. 2, pp. 47–56, 2012.

[189] K. V Lu and G. Bergers, "Mechanisms of evasive resistance to anti-VEGF therapy in glioblastoma," *CNS Oncol.*, vol. 2, no. 1, pp. 49–65, Jan. 2013.

[190] W. C. Aird, "Endothelial Cell Heterogeneity," *Cold Spring Harb. Perspect. Med.*, vol. 2, no. 1, p. a006429, Jan. 2012.

[191] T. F. Paiva, V. H. F. de Jesus, R. A. Marques, A. A. B. A. da Costa, M. P. de Macedo, P. M. Peresi, A. Damascena, B. M. Rossi, M. D. Begnami, and V. C. C. de Lima, "Angiogenesis-related protein expression in bevacizumab-treated metastatic colorectal cancer: NOTCH1 detrimental to overall survival," *BMC Cancer*, vol. 15, p. 643, Sep. 2015.

[192] H. P. Dhakal, B. Naume, M. Synnestvedt, E. Borgen, R. Kaaresen, E. Schlichting, G. Wiedswang, A. Bassarova, R. Holm, K.-E. Giercksky, and J. M. Nesland, "Expression of vascular endothelial growth factor and vascular endothelial growth factor receptors 1 and 2 in invasive breast carcinoma: prognostic significance and relationship with markers for aggressiveness," *Histopathology*, vol. 61, no. 3, pp. 350–364, Sep. 2012.

[193] D. Lambrechts, H.-J. Lenz, S. de Haas, P. Carmeliet, and S. J. Scherer, "Markers of Response for the Antiangiogenic Agent Bevacizumab," *J. Clin. Oncol.* , vol. 31, no. 9, pp.

1219–1230, Mar. 2013.

[194] J. R. van Beijnum, P. Nowak-Sliwinska, E. J. M. Huijbers, V. L. Thijssen, and A. W. Griffioen, “The Great Escape; the Hallmarks of Resistance to Antiangiogenic Therapy,” *Pharmacol. Rev.*, vol. 67, no. 2, p. 441 LP-461, Mar. 2015.

[195] R. Irannejad, N. G. Tsvetanova, B. T. Lobingier, and M. von Zastrow, “Effects of endocytosis on receptor-mediated signaling,” *Curr. Opin. Cell Biol.*, vol. 35, pp. 137–143, Aug. 2015.

[196] A. Tomas, C. E. Futter, and E. R. Eden, “EGF receptor trafficking: consequences for signaling and cancer,” *Trends Cell Biol.*, vol. 24, no. 1, pp. 26–34, Aug. 2015.

[197] Z. Zhang, K. G. Neiva, M. W. Lingen, L. M. Ellis, and J. E. Nor, “VEGF-dependent tumor angiogenesis requires inverse and reciprocal regulation of VEGFR1 and VEGFR2,” *Cell Death Differ*, vol. 17, pp. 499–512, 2010.

[198] X. Ye, Y. Abou-Rayyah, J. Bischoff, A. Ritchie, N. J. Sebire, P. Watts, A. J. Churchill, and D. O. Bates, “Altered ratios of pro- and anti-angiogenic VEGF-A variants and pericyte expression of DLL4 disrupt vascular maturation in infantile haemangioma,” *J. Pathol.*, vol. 239, no. 2, pp. 139–151, Jun. 2016.

[199] A. Briot and M. L. Iruela-Arispe, “Blockade of specific Notch ligands: A new promising approach in cancer therapy,” *Cancer Discov.*, vol. 5, no. 2, pp. 112–114, Feb. 2015.

[200] D.-K. Lim, R. G. Wylie, R. Langer, and D. S. Kohane, “Selective binding of C-6 OH sulfated hyaluronic acid to the angiogenic isoform of VEGF165,” *Biomaterials*, vol. 77, pp. 130–138, Jan. 2016.

[201] P. I. Imoukhuede, A. O. Dokun, B. H. Annex, and A. S. Popel, “Endothelial cell-by-cell

profiling reveals the temporal dynamics of VEGFR1 and VEGFR2 membrane localization after murine hindlimb ischemia," *Am J Physiol Hear. Circ Physiol*, vol. 304, no. 8, pp. H1085–H1093, 2013.

[202] P. I. Imoukhuede and A. S. Popel, "Quantitative fluorescent profiling of VEGFRs reveals tumor cell and endothelial cell heterogeneity in breast cancer xenografts.," *Cancer Med.*, vol. 3, pp. 225–44, Jan. 2014.

[203] M. Murakami, Y. Zheng, M. Hirashima, T. Suda, Y. Morita, J. Ooehara, H. Ema, G. H. Fong, and M. Shibuya, "VEGFR1 tyrosine kinase signaling promotes lymphangiogenesis as well as angiogenesis indirectly via macrophage recruitment.," *Arterioscler. Thromb. Vasc. Biol.*, vol. 28, no. 4, pp. 658–64, Apr. 2008.

[204] C. Fischer, M. Mazzone, B. Jonckx, and P. Carmeliet, "FLT1 and its ligands VEGFB and PlGF: drug targets for anti-angiogenic therapy?," *Nat Rev Cancer*, vol. 8, no. 12, pp. 942–956, Dec. 2008.

[205] A. Adini, T. Kornaga, F. Firoozbakht, and L. E. Benjamin, "Placental Growth Factor Is a Survival Factor for Tumor Endothelial Cells and Macrophages," *Cancer Res.*, vol. 62, no. 10, p. 2749 LP-2752, May 2002.

[206] C. Fischer, B. Jonckx, M. Mazzone, S. Zacchigna, S. Loges, L. Pattarini, E. Chorianopoulos, L. Liesenborghs, M. Koch, M. De Mol, M. Autiero, S. Wyns, S. Plaisance, L. Moons, N. van Rooijen, M. Giacca, J.-M. Stassen, M. Dewerchin, D. Collen, and P. Carmeliet, "Anti-PlGF Inhibits Growth of VEGF(R)-Inhibitor-Resistant Tumors without Affecting Healthy Vessels," *Cell*, vol. 131, no. 3, pp. 463–475, Nov. 2007.

[207] K. M. Naegle, R. E. Welsch, M. B. Yaffe, F. M. White, and D. A. Lauffenburger,

"MCAM: Multiple Clustering Analysis Methodology for Deriving Hypotheses and Insights from High-Throughput Proteomic Datasets," *PLoS Comput Biol*, vol. 7, no. 7, p. e1002119, Jul. 2011.

[208] A. S. Holehouse and K. M. Naegle, "Reproducible Analysis of Post-Translational Modifications in Proteomes—Application to Human Mutations," *PLoS One*, vol. 10, no. 12, p. e0144692, Dec. 2015.

[209] M. L. Neal and R. Kerckhoffs, "Current progress in patient-specific modeling," *Brief. Bioinform.*, vol. 11, no. 1, pp. 111–126, Jan. 2010.

[210] R. Chen and M. Snyder, "Systems Biology: Personalized Medicine for the Future?," *Curr. Opin. Pharmacol.*, vol. 12, no. 5, pp. 623–628, Oct. 2012.

[211] J. Walpole, J. a Papin, and S. M. Peirce, "Multiscale computational models of complex biological systems.," *Annu. Rev. Biomed. Eng.*, vol. 15, pp. 137–54, Jan. 2013.

[212] P. A. Galie, D.-H. T. Nguyen, C. K. Choi, D. M. Cohen, P. A. Janmey, and C. S. Chen, "Fluid shear stress threshold regulates angiogenic sprouting," *Proc. Natl. Acad. Sci. U. S. A.*, vol. 111, no. 22, pp. 7968–7973, Jun. 2014.

[213] N. Baeyens, S. Nicoli, B. G. Coon, T. D. Ross, K. Van den Dries, J. Han, H. M. Lauridsen, C. O. Mejean, A. Eichmann, J.-L. Thomas, J. D. Humphrey, and M. A. Schwartz, "Vascular remodeling is governed by a VEGFR3-dependent fluid shear stress set point," *Elife*, vol. 4, p. e04645, 2015.

[214] N. G. dela Paz, T. E. Walshe, L. L. Leach, M. Saint-Geniez, and P. A. D'Amore, "Role of shear-stress-induced VEGF expression in endothelial cell survival," *J. Cell Sci.*, vol. 125, no. 4, pp. 831–843, Feb. 2012.

[215] G. A. Anderson, R. S. Udan, M. E. Dickinson, and R. M. Henkelman, “Cardiovascular Patterning as Determined by Hemodynamic Forces and Blood Vessel Genetics,” *PLoS One*, vol. 10, no. 9, p. e0137175, Sep. 2015.

[216] C.-L. E. Helm, M. E. Fleury, A. H. Zisch, F. Boschetti, and M. A. Swartz, “Synergy between interstitial flow and VEGF directs capillary morphogenesis in vitro through a gradient amplification mechanism,” *Proc. Natl. Acad. Sci. U. S. A.*, vol. 102, no. 44, pp. 15779–15784, Nov. 2005.

[217] S. Chen, J. C. Weddell, P. Gupta, G. Conard, J. Parkin, and P. I. Imoukhuede, “qFlow cytometry-based receptoromic screening: a high-throughput quantification approach informing biomarker selection and nanosensor development,” *Methods Mol Biol*, vol. (in press), 2016.

[218] M. Burchardt, T. Burchardt, M.-W. Chen, A. Shabsigh, A. de la Taille, R. Buttyan, and R. Shabsigh, “Expression of Messenger Ribonucleic Acid Splice Variants for Vascular Endothelial Growth Factor in the Penis of Adult Rats and Humans,” *Biol. Reprod.* , vol. 60, no. 2, pp. 398–404, Feb. 1999.

[219] E. Tischer, R. Mitchell, T. Hartman, M. Silva, D. Gospodarowicz, J. C. Fiddes, and J. A. Abraham, “The human gene for vascular endothelial growth factor. Multiple protein forms are encoded through alternative exon splicing.,” *J. Biol. Chem.* , vol. 266, no. 18, pp. 11947–11954, Jun. 1991.

[220] Z. Poltorak, T. Cohen, R. Sivan, Y. Kandelis, G. Spira, I. Vlodavsky, E. Keshet, and G. Neufeld, “VEGF145, a Secreted Vascular Endothelial Growth Factor Isoform That Binds to Extracellular Matrix,” *J. Biol. Chem.* , vol. 272, no. 11, pp. 7151–7158, Mar. 1997.

[221] C. WHITTLE, K. GILLESPIE, R. HARRISON, P. W. MATHIESON, and S. J. HARPER, "Heterogeneous vascular endothelial growth factor (VEGF) isoform mRNA and receptor mRNA expression in human glomeruli, and the identification of VEGF148 mRNA, a novel truncated splice variant," *Clin. Sci.*, vol. 97, no. 3, p. 303 LP-312, Jul. 1999.

[222] J. Lei, A. Jiang, and D. Pei, "Identification and characterization of a new splicing variant of vascular endothelial growth factor: VEGF1831," *Biochim. Biophys. Acta - Gene Struct. Expr.*, vol. 1443, no. 3, pp. 400–406, Dec. 1998.

[223] K. A. Houck, N. Ferrara, J. Winer, G. Cachianes, B. Li, and D. W. Leung, "The Vascular Endothelial Growth Factor Family: Identification of a Fourth Molecular Species and Characterization of Alternative Splicing of RNA," *Mol. Endocrinol.*, vol. 5, no. 12, pp. 1806–1814, Dec. 1991.

[224] R. M. Perrin, O. Konopatskaya, Y. Qiu, S. Harper, D. O. Bates, and A. J. Churchill, "Diabetic retinopathy is associated with a switch in splicing from anti- to pro-angiogenic isoforms of vascular endothelial growth factor," *Diabetologia*, vol. 48, no. 11, pp. 2422–2427, 2005.

[225] D. O. Bates, T.-G. Cui, J. M. Doughty, M. Winkler, M. Sugiono, J. D. Shields, D. Peat, D. Gillatt, and S. J. Harper, "VEGF165b, an Inhibitory Splice Variant of Vascular Endothelial Growth Factor, Is Down-Regulated in Renal Cell Carcinoma," *Cancer Res.*, vol. 62, no. 14, p. 4123 LP-4131, Jul. 2002.

[226] V. Joukov, K. Pajusola, A. Kaipainen, D. Chilov, I. Lahtinen, E. Kukk, O. Saksela, N. Kalkkinen, and K. Alitalo, "A novel vascular endothelial growth factor, VEGF-C, is a ligand for the Flt4 (VEGFR-3) and KDR (VEGFR-2) receptor tyrosine kinases.," *EMBO J.*, vol. 15, no. 2, pp. 290–298, Jan. 1996.

[227] D. Maglione, V. Guerriero, G. Viglietto, P. Delli-Bovi, and M. G. Persico, “Isolation of a human placenta cDNA coding for a protein related to the vascular permeability factor.,” *Proc. Natl. Acad. Sci. U. S. A.*, vol. 88, no. 20, pp. 9267–9271, Oct. 1991.

[228] M. Shibuya, S. Yamaguchi, A. Yamane, T. Ikeda, A. Tojo, H. Matsushime, and M. Sato, “Nucleotide sequence and expression of a novel human receptor-type tyrosine kinase gene (flt) closely related to the fms family,” *Oncogene*, vol. 5, pp. 519–24, 1990.

[229] W. Matthews, C. T. Jordan, M. Gavin, N. A. Jenkins, N. G. Copeland, and I. R. Lemischka, “A receptor tyrosine kinase cDNA isolated from a population of enriched primitive hematopoietic cells and exhibiting close genetic linkage to c-kit.,” *Proc. Natl. Acad. Sci. U. S. A.*, vol. 88, no. 20, pp. 9026–9030, Oct. 1991.

[230] B. Terman, M. E. Carrion, E. Kovacs, B. A. Rasmussen, R. L. Eddy, and T. B. Shows, “Identification of a new endothelial cell growth factor receptor tyrosine kinase,” *Oncogene*, vol. 6, pp. 1677–83, 1991.

[231] J. M. L. Ebos, G. Bocci, S. Man, P. E. Thorpe, D. J. Hicklin, D. Zhou, X. Jia, and R. S. Kerbel, “A Naturally Occurring Soluble Form of Vascular Endothelial Growth Factor Receptor 2 Detected in Mouse and Human Plasma,” *Mol. Cancer Res.*, vol. 2, no. 6, p. 315 LP-326, Jul. 2004.

[232] O. Aprelikova, K. Pajusola, J. Partanen, E. Armstrong, R. Alitalo, S. K. Bailey, J. McMahon, J. Wasmuth, K. Huebner, and K. Alitalo, “FLT4, a Novel Class III Receptor Tyrosine Kinase in Chromosome 5q33-qter,” *Cancer Res.*, vol. 52, no. 3, p. 746 LP-748, Feb. 1992.

[233] H. Resat, L. Petzold, and M. F. Pettigrew, “Kinetic Modeling of Biological Systems,”

Methods Mol. Biol., vol. 541, pp. 311–335, 2009.

[234] G. M. Kirwan, E. Johansson, R. Kleemann, E. R. Verheij, Å. M. Wheelock, S. Goto, J. Trygg, and C. E. Wheelock, "Building Multivariate Systems Biology Models," *Anal. Chem.*, vol. 84, no. 16, pp. 7064–7071, Aug. 2012.

[235] C. R. A. F. Tonnesen MG Feng X and F. X. Tonnesen MG Clark RAF, "Angiogenesis in wound healing," *J Invest Derm Symp P*, vol. 5, pp. 40–46, 2000.

[236] G. C. Hughes and B. H. Annex, "Angiogenic therapy for coronary artery and peripheral arterial disease," *Expert Rev Cardio Ther*, vol. 3, pp. 521–535, 2005.

[237] NHLBI, "Peripheral artery disease," *Dis. Cond. Index*, p. NIH, 2010.

[238] A. Go, D. Mozaffarian, V. Roger, E. Benjamin, J. Berry, M. Blaha, S. Dai, E. Ford, C. Fox, S. Franco, H. Fullerton, C. Gillespie, S. Hailpern, J. Heit, V. Howard, and E. Al, "Heart disease and stroke statistics - 2014 update: A report from the American Heart Association," *Circulation*, vol. 129, pp. e28–e292, 2014.

[239] N. Nishida, H. Yano, T. Nishida, T. Kamura, and M. Kojiro, "Angiogenesis in Cancer," *Vasc. Health Risk Manag.*, vol. 2, no. 3, pp. 213–219, Sep. 2006.

[240] X. Ma, L. Wang, H. Li, Y. Zhang, Y. Gao, G. Guo, K. Liu, Q. Meng, C. Zhao, D. Wang, Z. Song, and X. Zhang, "Predictive Immunohistochemical Markers Related to Drug Selection for Patients Treated with Sunitinib or Sorafenib for Metastatic Renal Cell Cancer," *Sci. Rep.*, vol. 6, p. 30886, Aug. 2016.

[241] B. Beuselinck, J. Jean-Baptiste, P. Schöffski, G. Couchy, C. Meiller, F. Rolland, Y. Allory, S. Joniau, V. Verkarre, R. Elaidi, E. Lerut, T. Roskams, J.-J. Patard, S. Oudard, A. Méjean, D. Lambrechts, and J. Zucman-Rossi, "Validation of VEGFR1 rs9582036 as

predictive biomarker in metastatic clear-cell renal cell carcinoma patients treated with sunitinib," *BJU Int.*, p. n/a-n/a, 2016.

[242] M. Shibuya, "Vascular endothelial growth factor receptor-1 (VEGFR-1/Flt-1): a dual regulator for angiogenesis," *Angiogenesis*, vol. 9, pp. 225–230, 2006.

[243] L. A. Sullivan and R. A. Brekken, "The VEGF family in cancer and antibody-based strategies for their inhibition," *MAbs*, vol. 2, no. 2, pp. 165–175, Nov. 2010.

[244] K. Sato, "Cellular Functions Regulated by Phosphorylation of EGFR on Tyr845," *Int. J. Mol. Sci.*, vol. 14, no. 6, pp. 10761–10790, Jun. 2013.

[245] J. Tong, P. Taylor, S. M. Peterman, A. Prakash, and M. F. Moran, "Epidermal Growth Factor Receptor Phosphorylation Sites Ser(991) and Tyr(998) Are Implicated in the Regulation of Receptor Endocytosis and Phosphorylations at Ser(1039) and Thr(1041)," *Mol. Cell. Proteomics*, vol. 8, no. 9, pp. 2131–2144, Sep. 2009.

[246] V. Tchaikovski, G. Fellbrich, and J. Waltenberger, "The molecular basis of VEGFR-1 signal transduction pathways in primary human monocytes.," *Arterioscler. Thromb. Vasc. Biol.*, vol. 28, no. 2, pp. 322–8, Feb. 2008.

[247] D. C. Flynn, "Adaptor proteins.," *Oncogene*, vol. 20, no. 44, pp. 6270–2, Oct. 2001.

[248] T. Hunter, "Tyrosine phosphorylation: thirty years and counting," *Curr. Opin. Cell Biol.*, vol. 21, no. 2, pp. 140–146, Apr. 2009.

[249] N. Dephoure, K. L. Gould, S. P. Gygi, and D. R. Kellogg, "Mapping and analysis of phosphorylation sites: a quick guide for cell biologists," *Mol. Biol. Cell* , vol. 24, no. 5, pp. 535–542, Mar. 2013.

[250] H. Duan, L. Qu, and C. Shou, "Activation of EGFR-PI3K-AKT signaling is required for

Mycoplasma hyorhinis-promoted gastric cancer cell migration," *Cancer Cell Int.*, vol. 14, p. 135, Dec. 2014.

[251] R. N. Germain, M. Meier-Schellersheim, A. Nita-Lazar, and I. D. C. Fraser, "Systems Biology in Immunology – A Computational Modeling Perspective," *Annu. Rev. Immunol.*, vol. 29, pp. 527–585, Apr. 2011.

[252] A. R. Williams, J. Timmis, and E. E. Qwarnstrom, "Computational Models of the NF-KB Signalling Pathway," *Computation* , vol. 2, no. 4. 2014.

[253] R. V Hogg and E. A. Tanis, *Probability and statistical inference*. 2015.

[254] G. Manning, D. B. Whyte, R. Martinez, T. Hunter, and S. Sudarsanam, "The protein kinase complement of the human genome," *Science (80-.).*, vol. 298, pp. 1912–1934, Dec. 2002.

[255] B. N. Kholodenko, O. V. Demin, G. Moehren, and J. B. Hoek, "Quantification of short term signaling by the epidermal growth factor receptor.," *J. Biol. Chem.*, vol. 274, no. 42, pp. 30169–30181, Oct. 1999.

[256] S. Mathew and I. Banerjee, "Quantitative analysis of robustness of dynamic response and signal transfer in insulin mediated PI3K/Akt pathway," *Comput Chem Eng*, vol. 71, pp. 715–727, 2014.

[257] M. Hsieh, S. Yang, M. Raymond-Stinz, J. S. Edwards, and B. S. Wilson, "Spatio-temporal modeling of signaling protein recruitment to EGFR," *BMC Syst. Biol.*, vol. 4, no. 1, pp. 1–19, 2010.

[258] S. M. Peirce, E. J. Van Gieson, and E. C. Skalak, "Multicellular simulation predicts microvascular patterning and in silico tissue assembly," *FASEB J*, vol. 18, pp. 731–3,

2004.

[259] J. Vivas, D. Garzón-Alvarado, and M. Cerrolaza, “Modeling cell adhesion and proliferation: a cellular-automata based approach,” *Adv. Model. Simul. Eng. Sci.*, vol. 2, no. 1, pp. 1–12, 2015.

[260] D. Tian and P. K. Kreeger, “Analysis of the quantitative balance between insulin-like growth factor (IGF)-1 ligand, receptor, and binding protein levels to predict cell sensitivity and therapeutic efficacy,” *BMC Syst. Biol.*, vol. 8, p. 98, Aug. 2014.

[261] S. D. Finley, L. Chu, and A. S. Popel, “Computational systems biology approaches to anti-angiogenic cancer therapeutics,” *Drug Discov. Today*, vol. 20, pp. 187–97, 2014.

[262] J. S. Yu and N. Bagheri, “Multi-class and multi-scale models of complex biological phenomena,” *Curr. Opin. Biotechnol.*, vol. 39, pp. 167–173, Jun. 2016.

[263] N. Le Novere, “Quantitative and logic modelling of molecular and gene networks,” *Nat Rev Genet*, vol. 16, no. 3, pp. 146–158, Mar. 2015.

[264] G. W. Brodland, “How computational models can help unlock biological systems,” *Semin. Cell Dev. Biol.*, vol. 47–48, pp. 62–73, Dec. 2015.

[265] K. K. Pannu, E. T. Joe, S. B. Iyer, P. KK, J. ET, I. SB, K. K. Pannu, E. T. Joe, and S. B. Iyer, “Performance evaluation of quantiBRITE phycoerythrin beads,” *Cytometry*, vol. 45, no. 4, pp. 250–258, Dec. 2001.

[266] L. Wang, F. Abbasi, A. K. Gaigalas, R. F. Vogt, and G. E. Marti, “Comparison of fluorescein and phycoerythrin conjugates for quantifying CD20 expression on normal and leukemic B-cells.,” *Cytometry B. Clin. Cytom.*, vol. 70, no. 6, pp. 410–5, Nov. 2006.

[267] K. K. Pannu, E. T. Joe, and S. B. Iyer, “Performance evaluation of QuantiBRITE

phycoerythrin beads.," *Cytometry*, vol. 45, no. 4, pp. 250–8, Dec. 2001.

[268] C.-L. Ko, E. Voit, and F.-S. Wang, "Estimating parameters for generalized mass action models with connectivity information," *BMC Bioinformatics*, vol. 10, no. 1, p. 140, 2009.

[269] A. K. Bose and K. A. Janes, "A High-throughput Assay for Phosphoprotein-specific Phosphatase Activity in Cellular Extracts," *Mol. Cell. Proteomics*, vol. 12, no. 3, pp. 797–806, Mar. 2013.

[270] A. P. McLaughlin and G. W. De Vries, "Role of PLCγ and Ca2+ in VEGF- and FGF-induced choroidal endothelial cell proliferation," *Am J Physiol Cell Physiol*, vol. 281, pp. C1448-56, 2001.

[271] J. W. Putney, "PLC-gamma: an old player has a new role," *Nat Cell Biol*, vol. 4, no. 12, pp. E280–E281, Dec. 2002.

[272] J. E. Purvis, M. S. Chatterjee, L. F. Brass, and S. L. Diamond, "A molecular signaling model of platelet phosphoinositide and calcium regulation during homeostasis and P2Y1 activation," *Blood*, vol. 112, pp. 4069–4079, 2008.

[273] A. Jovic, B. Howell, M. Cote, S. M. Wade, K. Mehta, A. Miyawaki, R. R. Neubig, J. J. Linderman, and S. Takayama, "Phase-locked signals elucidate circuit architecture of an oscillatory pathway," *PLoS Comput Biol*, vol. 6, p. e1001040, 2010.

[274] A. Jovic, S. M. Wade, R. R. Neubig, J. J. Linderman, and S. Takayama, "Microfluidic interrogation and mathematical modeling of multi-regime calcium signaling dynamics," *Integr Biol*, vol. 5, pp. 932–939, 2013.

[275] A. T. Dolan and S. L. Diamond, "Systems Modeling of Ca2+ Homeostasis and Mobilization in Platelets Mediated by IP3 and Store-Operated Ca2+ Entry," *Biophys. J.*,

vol. 106, no. 9, pp. 2049–2060, May 2015.

[276] P. W. Marks and F. R. Maxfield, “Transient increases in cytosolic free calcium appear to be required for the migration of adherent human neutrophils,” *J. Cell Biol.*, vol. 110, no. 1, pp. 43–52, 1990.

[277] C. Wei, X. Wang, M. Chen, K. Ouyang, L. S. Song, and H. Cheng, “Calcium flickers steer cell migration,” *Nature*, vol. 457, no. 7231, pp. 901–905, Feb. 2009.

[278] K. Minton, “Cell migration: coordinating calcium signalling,” *Nat Rev Mol Cell Biol*, vol. 15, no. 3, p. 152, Mar. 2014.

[279] D. G. Cronshaw, A. Kouroumalis, R. Parry, A. Webb, Z. Brown, and S. G. Ward, “Evidence that phospholipase C-dependent, calcium-independent mechanisms are required for directional migration of T lymphocytes in response to the CCR4 ligands CCL17 and CCL22,” *J. Leukoc. Biol.* , vol. 79, no. 6, pp. 1369–1380, Jun. 2006.

[280] D. P. Noren, W. H. Chou, S. H. Lee, A. A. Qutub, A. Warmflash, D. S. Wagner, A. S. Popel, and A. Levchenko, “Endothelial cells decode VEGF-mediated Ca2+ signaling patterns to produce distinct functional responses,” *Sci. Signal.*, vol. 9, no. 416, p. ra20-ra20, Feb. 2016.

[281] F. Tsai, G. Kuo, S. Chang, and P. Tsai, “Ca2+ Signaling in Cytoskeletal Reorganization, Cell Migration, and Cancer Metastasis,” *Biomed Res. Int.*, vol. 2015, p. 13, 2015.

[282] K. Mikoshiba, “IP3 receptor/Ca2+ channel: from discovery to new signaling concepts,” *J. Neurochem.*, vol. 102, no. 5, pp. 1426–1446, 2007.

[283] T. J. Stefonek-Puccinelli and K. S. Masters, “Co-immobilization of gradient-patterned growth factors for directed cell migration,” *Ann. Biomed. Eng.*, vol. 36, no. 12, pp. 2121–

2133, Dec. 2008.

[284] B. Vanhaesebroeck, L. Stephens, and P. Hawkins, “PI3K signalling: the path to discovery and understanding,” *Nat Rev Mol Cell Biol*, vol. 13, no. 3, pp. 195–203, Mar. 2012.

[285] B. A. Hemmings and D. F. Restuccia, “PI3K-PKB/Akt pathway,” *Cold Spring Harb Perspect Biol*, vol. 4, p. a011189, 2012.

[286] P. Viard, A. J. Butcher, G. Halet, A. Davies, B. Nürnberg, F. Heblich, and A. C. Dolphin, “PI3K promotes voltage-dependent calcium channel trafficking to the plasma membrane.,” *Nat. Neurosci.*, vol. 7, no. 9, pp. 939–946, 2004.

[287] N. S. Dawson, D. C. Zawieja, M. H. Wu, and H. J. Granger, “Signaling pathways mediating VEGF165-induced calcium transients and membrane depolarization in human endothelial cells,” *FASEB J.* , vol. 20, no. 7, pp. 991–993, May 2006.

[288] S. Tauzin, B. Chaigne-Delalande, E. Selva, N. Khadra, S. Daburon, C. Contin-Bordes, P. Blanco, J. Le Seyec, T. Ducret, L. Counillon, J.-F. Moreau, P. Hofman, P. Vacher, and P. Legembre, “The Naturally Processed CD95L Elicits a c-Yes/Calcium/PI3K-Driven Cell Migration Pathway,” *PLoS Biol.*, vol. 9, no. 6, p. e1001090, Jun. 2011.

[289] L. E. Rameh, S. G. Rhee, K. Spokes, A. Kazlauskas, L. C. Cantley, and L. G. Cantley, “Phosphoinositide 3-kinase regulates phospholipase Cgamma-mediated calcium signaling.,” *J. Biol. Chem.*, vol. 273, no. 37, pp. 23750–23757, 1998.

[290] M. G. Cattaneo, G. Lucci, and L. M. Vicentini, “Oxytocin stimulates in vitro angiogenesis via a Pyk-2/Src-dependent mechanism,” *Exp. Cell Res.*, vol. 315, no. 18, pp. 3210–3219, Nov. 2009.

[291] H. He, V. J. Venema, X. Gu, R. C. Venema, M. B. Marrero, and R. B. Caldwell,

"Vascular Endothelial Growth Factor Signals Endothelial Cell Production of Nitric Oxide and Prostacyclin through Flk-1/KDR Activation of c-Src," *J. Biol. Chem.* , vol. 274, no. 35, pp. 25130–25135, Aug. 1999.

[292] M. Sun, L. Yang, R. I. Feldman, X. Sun, K. N. Bhalla, R. Jove, S. V Nicosia, and J. Q. Cheng, "Activation of Phosphatidylinositol 3-Kinase/Akt Pathway by Androgen through Interaction of p85α, Androgen Receptor, and Src," *J. Biol. Chem.* , vol. 278, no. 44, pp. 42992–43000, Oct. 2003.

[293] G. Liu, A. T. Place, Z. Chen, V. M. Brovkovych, S. M. Vogel, W. A. Muller, R. A. Skidgel, A. B. Malik, and R. D. Minshall, "ICAM-1–activated Src and eNOS signaling increase endothelial cell surface PECAM-1 adhesivity and neutrophil transmigration," *Blood*, vol. 120, no. 9, pp. 1942–1952, Aug. 2012.

[294] N. A. Maniatis, V. Brovkovych, S. E. Allen, T. A. John, A. N. Shajahan, C. Tiruppathi, S. M. Vogel, R. A. Skidgel, A. B. Malik, and R. D. Minshall, "Novel Mechanism of Endothelial Nitric Oxide Synthase Activation Mediated by Caveolae Internalization in Endothelial Cells," *Circ. Res.* , vol. 99, no. 8, pp. 870–877, Oct. 2006.

[295] A. Irmisch and J. Huelsken, "Metastasis: New insights into organ-specific extravasation and metastatic niches," *Exp. Cell Res.*, vol. 319, no. 11, pp. 1604–1610, Jul. 2013.

[296] D. F. Quail and J. A. Joyce, "Microenvironmental regulation of tumor progression and metastasis," *Nat Med*, vol. 19, no. 11, pp. 1423–1437, Nov. 2013.

[297] R. N. Kaplan, R. D. Riba, S. Zacharoulis, A. H. Bramley, L. Vincent, C. Costa, D. D. MacDonald, D. K. Jin, K. Shido, S. A. Kerns, Z. Zhu, D. Hicklin, Y. Wu, J. L. Port, N. Altorki, E. R. Port, D. Ruggero, S. V Shmelkov, K. K. Jensen, S. Rafii, and D. Lyden,

"VEGFR1-positive haematopoietic bone marrow progenitors initiate the pre-metastatic niche," *Nature*, vol. 438, no. 7069, pp. 820–827, Dec. 2005.

[298] K.-Y. Park, G. Li, and M. O. Platt, "Monocyte-derived macrophage assisted breast cancer cell invasion as a personalized, predictive metric to score metastatic risk," *Sci. Rep.*, vol. 5, p. 13855, Sep. 2015.

[299] B. Mayer, "SH3 domains : complexity in moderation," *J Cell Sci*, vol. 114, pp. 1253–63, 2001.

[300] Q. Hu, D. Milfay, and L. T. Williams, "Binding of NCK to SOS and activation of ras-dependent gene expression.," *Mol. Cell. Biol.*, vol. 15, no. 3, pp. 1169–1174, Mar. 1995.

[301] M. A. Lemmon and J. Schlessinger, "Cell signaling by receptor tyrosine kinases.," *Cell*, vol. 141, no. 7, pp. 1117–34, Jun. 2010.

[302] K. M. Naegle, F. M. White, D. A. Lauffenburger, and M. B. Yaffe, "Robust co-regulation of tyrosine phosphorylation sites on proteins reveals novel protein interactions," *Mol. Biosyst.*, vol. 8, no. 10, pp. 2771–2782, Oct. 2012.

[303] F. Böhmer, S. Szedlacsek, L. Tabernero, A. Östman, and J. den Hertog, "Protein tyrosine phosphatase structure–function relationships in regulation and pathogenesis," *FEBS J.*, vol. 280, no. 2, pp. 413–431, 2013.

[304] N. E. Hynes and H. A. Lane, "ERBB receptors and cancer: the complexity of targeted inhibitors," *Nat Rev Cancer*, vol. 5, no. 5, pp. 341–354, May 2005.

[305] M. Niepel, M. Hafner, E. A. Pace, M. Chung, D. H. Chai, L. Zhou, B. Schoeberl, and P. K. Sorger, "Profiles of Basal and Stimulated Receptor Signaling Networks Predict Drug Response in Breast Cancer Lines," *Sci. Signal.*, vol. 6, no. 294, p. ra84-ra84, Sep. 2013.

[306] E. Murphy, “Estrogen Signaling and Cardiovascular Disease,” *Circ. Res.*, vol. 109, no. 6, pp. 687–696, 2011.

[307] S. Wassmann and G. Nickenig, “Pathophysiological regulation of the AT1-receptor and implications for vascular disease,” *J Hypertens Suppl*, vol. 24, pp. S15-21, 2006.

[308] I. J. Uings and S. N. Farrow, “Cell receptors and cell signalling,” *Mol. Pathol.*, vol. 53, no. 6, pp. 295–299, Dec. 2000.

[309] I. N. Maruyama, “Mechanisms of Activation of Receptor Tyrosine Kinases: Monomers or Dimers,” *Cells*, vol. 3, no. 2, p. 304, 2014.

[310] P. Seshacharyulu, M. P. Ponnusamy, D. Haridas, M. Jain, A. Ganti, and S. K. Batra, “Targeting the EGFR signaling pathway in cancer therapy,” *Expert Opin. Ther. Targets*, vol. 16, no. 1, pp. 15–31, Jan. 2012.

[311] N. Kabbani, “Proteomics of membrane receptors and signaling,” *Proteomics*, vol. 8, no. 19, pp. 4146–4155, 2008.

[312] M. Arish, A. Husein, M. Kashif, P. Sandhu, S. E. Hasnain, Y. Akhter, and A. Rub, “Orchestration of membrane receptor signaling by membrane lipids,” *Biochimie*, vol. 113, pp. 111–124, Jun. 2015.

[313] S. Mukherjee, “Vesicular Trafficking of Tyrosine Kinase Receptors and Associated Proteins in the Regulation of Signaling and Vascular Function,” *Circ. Res.*, vol. 98, no. 6, pp. 743–756, 2006.

[314] M. Pálfy, A. Reményi, and T. Korcsmáros, “Endosomal crosstalk: meeting points for signaling pathways,” *Trends Cell Biol.*, vol. 22, no. 9, pp. 447–456, Sep. 2015.

[315] M. Miaczynska, L. Pelkmans, and M. Zerial, “Not just a sink: endosomes in control of

signal transduction," *Curr. Opin. Cell Biol.*, vol. 16, no. 4, pp. 400–406, Aug. 2004.

[316] D. A. Lauffenburger, J. Linderman, and L. Berkowitz, "Analysis of Mammalian Cell Growth Factor Receptor Dynamicsa," *Ann. N. Y. Acad. Sci.*, vol. 506, no. 1, pp. 147–162, 1987.

[317] J. J. Linderman and D. A. Lauffenburger, *Receptor/Ligand Sorting Along the Endocytic Pathway*. 1989.

[318] G. M. Di Guglielmo, P. C. Baass, W. J. Ou, B. I. Posner, and J. J. Bergeron, "Compartmentalization of SHC, GRB2 and mSOS, and hyperphosphorylation of Raf-1 by EGF but not insulin in liver parenchyma.," *EMBO J.*, vol. 13, no. 18, pp. 4269–4277, Sep. 1994.

[319] H. S. Wiley, J. J. Herbst, B. J. Walsh, D. A. Lauffenburger, M. G. Rosenfeld, and G. N. Gill, "The role of tyrosine kinase activity in endocytosis, compartmentation, and down-regulation of the epidermal growth factor receptor.," *J. Biol. Chem.* , vol. 266, no. 17, pp. 11083–11094, Jun. 1991.

[320] a Ciechanover, a L. Schwartz, a Dautry-Varsat, and H. F. Lodish, "Kinetics of internalization and recycling of transferrin and the transferrin receptor in a human hepatoma cell line," *J. Biol. Chem.*, vol. 258, no. 8, pp. 16–9681, 1983.

[321] C. M. Waters, K. C. Oberg, G. Carpenter, and K. A. Overholser, "Rate constants for binding, dissociation, and internalization of EGF: effect of receptor occupancy and ligand concentration," *Biochemistry*, vol. 29, no. 14, pp. 3563–3569, Apr. 1990.

[322] H. W. Platta and H. Stenmark, "Endocytosis and signaling," *Curr. Opin. Cell Biol.*, vol. 23, no. 4, pp. 393–403, Aug. 2011.

[323] E. Zwick, J. Bange, and A. Ullrich, “Receptor tyrosine kinase signalling as a target for cancer intervention strategies,” *Endocr Relat Cancer*, vol. 8, pp. 161–174, 2001.

[324] K. Takeuchi and F. Ito, “Receptor Tyrosine Kinases and Targeted Cancer Therapeutics,” *Biol. Pharm. Bull.*, vol. 34, no. 12, pp. 1774–1780, 2011.

[325] T. Kitazono, S. Ibayashi, T. Nagao, T. Kagiyama, J. Kitayama, and M. Fujishima, “Role of Tyrosine Kinase in Serotonin-Induced Constriction of the Basilar Artery In Vivo,” *Stroke* , vol. 29, no. 2, pp. 494–498, Feb. 1998.

[326] I. Gagalo, I. Rusiecka, and I. Kocic, “Tyrosine Kinase Inhibitor as a new Therapy for Ischemic Stroke and other Neurologic Diseases: is there any Hope for a Better Outcome?,” *Curr Neuropharm*, vol. 13, pp. 836–844, 2016.

[327] B. Schoeberl, C. Eichler-Jonsson, E. D. Gilles, and G. Muller, “Computational modeling of the dynamics of the MAP kinase cascade activated by surface and internalized EGF receptors,” *Nat. Biotech*, vol. 20, pp. 370–375, 2002.

[328] S. Chen, X. Guo, O. Imarenezor, and P. Imoukhuede, “Quantification of VEGFRs, NRP1, and PDGFRs on Endothelial Cells and Fibroblasts Reveals Serum, Intra-Family Ligand, and Cross-Family Ligand Regulation,” *Cell. Mol. Bioeng.*, vol. 8, no. 3, pp. 383–403, 2015.

[329] S. B. Mamer and P. I. Imoukhuede, “Identification and Quantification of Novel VEGF-PDGF Cross-family Binding,” in *Biomedical Engineering Society*, 2015.

[330] A. O’Neill, N. Shah, N. Zitomersky, M. Ladanyi, N. Shukla, A. Uren, D. Loeb, and J. Toretsky, “Insulin-like growth factor 1 receptor as a therapeutic target in ewing sarcoma: lack of consistent upregulation or recurrent mutation and a review of the clinical trial

literature.," *Sarcoma*, vol. 2013, p. 450478, 2013.

[331] B. E. Forbes, P. J. Hartfield, K. A. McNeil, K. H. Surinya, S. J. Milner, L. J. Cosgrove, and J. C. Wallace, "Characteristics of binding of insulin-like growth factor (IGF)-I and IGF-II analogues to the type 1 IGF receptor determined by BIAcore analysis," *Eur. J. Biochem.*, vol. 269, no. 3, pp. 961–968, 2002.

[332] W. Hu, J. Kumar, C. Huang, and W. Chen, "Computational Selection of RNA Aptamer against Angiopoietin-2 and Experimental Evaluation," *Biomed Res. Int.*, vol. 2015, p. 8, 2015.

[333] L. Comps-Agrar, D. R. Dunshee, D. L. Eaton, and J. Sonoda, "Unliganded Fibroblast Growth Factor Receptor 1 Forms Density-independent Dimers," *J. Biol. Chem.*, vol. 290, no. 40, pp. 24166–24177, 2015.

[334] O. A. Ibrahimi, F. Zhang, S. C. Lang Hrstka, M. Mohammadi, and R. J. Linhardt, "Kinetic Model for FGF, FGFR, and Proteoglycan Signal Transduction Complex Assembly," *Biochemistry*, vol. 43, no. 16, pp. 4724–4730, Apr. 2004.

[335] A. V Vieira, C. Lamaze, and S. L. Schmid, "Control of EGF Receptor Signaling by Clathrin-Mediated Endocytosis," *Sci.* , vol. 274, no. 5295, pp. 2086–2089, Dec. 1996.

[336] G. Auciello, D. L. Cunningham, T. Tatar, J. K. Heath, and J. Z. Rappoport, "Regulation of fibroblast growth factor receptor signalling and trafficking by Src and Eps8," *J. Cell Sci.*, vol. 126, no. 2, pp. 613–624, Jan. 2013.

[337] A. S. Martins, J. L. Ordonez, A. T. Amaral, F. Prins, G. Floris, M. Debiec-Rychter, P. C. W. Hogendoorn, and E. de Alava, "IGF1R Signaling in Ewing Sarcoma Is Shaped by Clathrin-/Caveolin-Dependent Endocytosis," *PLoS One*, vol. 6, no. 5, p. e19846, May

2011.

[338] M. Huang, J. B. DuHadaway, G. C. Prendergast, and L. D. Laury-Kleintop, “RhoB Regulates PDGFR-β Trafficking and Signaling in Vascular Smooth Muscle Cells,” *Arterioscler. Thromb. Vasc. Biol.*, vol. 27, no. 12, pp. 2597–2605, Dec. 2007.

[339] A. A. Lanahan, K. Hermans, F. Claes, J. S. Kerley-Hamilton, Z. W. Zhuang, F. J. Giordano, P. Carmeliet, and M. Simons, “VEGF receptor 2 endocytic trafficking regulates arterial morphogenesis,” *Dev. Cell*, vol. 18, no. 5, pp. 713–724, May 2010.

[340] D. Chen, D. Zuo, C. Luan, M. Liu, M. Na, L. Ran, Y. Sun, A. Persson, E. Englund, L. G. Salford, E. Renström, X. Fan, and E. Zhang, “Glioma Cell Proliferation Controlled by ERK Activity-Dependent Surface Expression of PDGFRA,” *PLoS One*, vol. 9, no. 1, p. e87281, Jan. 2014.

[341] R. L. Juliano, X. Ming, K. Carver, and B. Laing, “Cellular Uptake and Intracellular Trafficking of Oligonucleotides: Implications for Oligonucleotide Pharmacology,” *Nucleic Acid Ther.*, vol. 24, no. 2, pp. 101–113, Apr. 2014.

[342] P. D. Dobson and D. B. Kell, “Carrier-mediated cellular uptake of pharmaceutical drugs: an exception or the rule?,” *Nat Rev Drug Discov*, vol. 7, no. 3, pp. 205–220, Mar. 2008.

[343] Y. Nishimura, B. Bereczky, and M. Ono, “The EGFR inhibitor gefitinib suppresses ligand-stimulated endocytosis of EGFR via the early/late endocytic pathway in non-small cell lung cancer cell lines,” *Histochem. Cell Biol.*, vol. 127, no. 5, pp. 541–553, 2007.

[344] Y. Nishimura, K. Yoshioka, B. Bereczky, and K. Itoh, “Evidence for efficient phosphorylation of EGFR and rapid endocytosis of phosphorylated EGFR via the early/late endocytic pathway in a gefitinib-sensitive non-small cell lung cancer cell line.,”

Mol. Cancer, vol. 7, p. 42, 2008.

[345] P. C. Baass, G. M. Di Guglielmo, F. Authier, B. I. Posner, and J. J. M. Bergeron, "Compartmentalized signal transduction by receptor tyrosine kinases," *Trends Cell Biol.*, vol. 5, no. 12, pp. 465–470, 1995.

[346] P. Burke, K. Schooler, and H. S. Wiley, "Regulation of Epidermal Growth Factor Receptor Signaling by Endocytosis and Intracellular Trafficking," *Mol. Biol. Cell*, vol. 12, no. 6, pp. 1897–1910, Jun. 2001.

[347] Y. Wang, S. D. Pennock, X. Chen, A. Kazlauskas, and Z. Wang, "Platelet-derived growth factor receptor-mediated signal transduction from endosomes," *J. Biol. Chem.*, vol. 279, no. 9, pp. 8038–8046, 2004.

[348] H. M. Jopling, A. F. Odell, N. M. Hooper, I. C. Zachary, J. H. Walker, and S. Ponnambalam, "Rab GTPase regulation of VEGFR2 trafficking and signaling in endothelial cells," *Arter. Thromb Vasc Biol*, vol. 29, no. 7, pp. 1119–1124, Jul. 2009.

[349] P. Sharma, A. Chawla, and P. Pawar, "Design, Development, and Optimization of Polymeric Based-Colonic Drug Delivery System of Naproxen," *Sci. World J.*, vol. 654829, p. 12, 2013.

[350] R. Siegel and M. Rathbone, "Overview of Controlled Release Mechanisms," in *Fundamentals and Applications of Controlled Release Drug Delivery SE - 2*, J. Siepmann, R. A. Siegel, and M. J. Rathbone, Eds. Springer US, 2012, pp. 19–43.

[351] Y. Fu and W. J. Kao, "Drug Release Kinetics and Transport Mechanisms of Non-degradable and Degradable Polymeric Delivery Systems," *Expert Opin. Drug Deliv.*, vol. 7, no. 4, pp. 429–444, Apr. 2010.

[352] T. Kirchhausen, E. Macia, and H. E. Pelish, “Use of dynasore, the small molecule inhibitor of dynamin, the regulation of endocytosis,” *Methods Enzymol.*, vol. 438, pp. 77–93, 2008.

[353] E. Macia, M. Ehrlich, R. Massol, E. Boucrot, C. Brunner, and T. Kirchhausen, “Dynasore, a Cell-Permeable Inhibitor of Dynamin,” *Dev. Cell*, vol. 10, no. 6, pp. 839–850, Jun. 2006.

[354] N. Signoret, J. Oldridge, A. Pelchen-Matthews, P. J. Klasse, T. Tran, L. F. Brass, M. M. Rosenkilde, T. W. Schwartz, W. Holmes, W. Dallas, M. A. Luther, T. N. C. Wells, J. A. Hoxie, and M. Marsh, “Phorbol Esters and SDF-1 Induce Rapid Endocytosis and Down Modulation of the Chemokine Receptor CXCR4 ,” *J. Cell Biol.*, vol. 139, no. 3, pp. 651–664, Nov. 1997.

[355] N. García-Tardón, I. M. González-González, J. Martínez-Villarreal, E. Fernández-Sánchez, C. Giménez, and F. Zafra, “Protein Kinase C (PKC)-promoted Endocytosis of Glutamate Transporter GLT-1 Requires Ubiquitin Ligase Nedd4-2-dependent Ubiquitination but Not Phosphorylation,” *J. Biol. Chem.* , vol. 287, no. 23, pp. 19177–19187, Jun. 2012.

[356] A. Aballay, P. D. Stahl, and L. S. Mayorga, “Phorbol ester promotes endocytosis by activating a factor involved in endosome fusion.,” *J. Cell Sci.*, vol. 112 (Pt 1, pp. 2549–2557, 1999.

[357] L. Rodriguez, C. J. Stirling, and P. G. Woodman, “Multiple N-ethylmaleimide-sensitive components are required for endosomal vesicle fusion.,” *Mol. Biol. Cell*, vol. 5, no. 7, pp. 773–783, 1994.

[358] a T. Jones and M. Wessling-Resnick, “Inhibition of in vitro endosomal vesicle fusion activity by aminoglycoside antibiotics.,” *J. Biol. Chem.*, vol. 273, no. 39, pp. 25301–9, 1998.

[359] H. M. Jopling, A. F. Odell, N. M. Hooper, I. C. Zachary, J. H. Walker, and S. Ponnambalam, “Rab GTPase Regulation of VEGFR2 Trafficking and Signaling in Endothelial Cells,” *Arter. Thromb Vasc Biol*, vol. 29, pp. 1119–1124, 2009.

[360] B. a. Mainou and T. S. Dermody, “Transport to Late Endosomes Is Required for Efficient Reovirus Infection,” *J. Virol.*, vol. 86, no. 16, pp. 8346–8358, 2012.

[361] A. H. Hutagalung and P. J. Novick, “Role of Rab GTPases in Membrane Traffic and Cell Physiology,” *Physiol. Rev.*, vol. 91, no. 1, pp. 119–149, Jan. 2011.

[362] B. P. Ceresa, “Regulation of EGFR endocytic trafficking by rab proteins,” *Histol. Histopathol.*, vol. 21, no. 7–9, pp. 987–993, 2006.

[363] C. C. Williams, J. G. Allison, G. A. Vidal, M. E. Burrow, B. S. Beckman, L. Marrero, and F. E. Jones, “The ERBB4/HER4 receptor tyrosine kinase regulates gene expression by functioning as a STAT5A nuclear chaperone,” *J Cell Biol*, vol. 167, pp. 469–478, 2004.

[364] S. C. Wang, H.-C. Lien, W. Xia, I.-F. Chen, H.-W. Lo, Z. Wang, M. Ali-Seyed, D.-F. Lee, G. Bartholomeusz, F. Ou-Yang, D. K. Giri, and M.-C. Hung, “Binding at and transactivation of the COX-2 promoter by nuclear tyrosine kinase receptor ErbB-2,” *Cancer Cell*, vol. 6, no. 3, pp. 251–261, Sep. 2004.

[365] M. K. Chen and M. C. Hung, “Proteolytic cleavage, trafficking, and functions of nuclear receptor tyrosine kinases,” *FEBS J.*, p. n/a-n/a, 2015.

[366] Y. N. Wang, H. Yamaguchi, J. M. Hsu, and M. C. Hung, “Nuclear trafficking of the

epidermal growth factor receptor family membrane proteins," *Oncogene*, vol. 29, no. 28, pp. 3997–4006, Jul. 2010.

[367] E. Rovida and P. Dello Sbarba, "Possible mechanisms and function of nuclear trafficking of the colony-stimulating factor-1 receptor," *Cell. Mol. Life Sci.*, vol. 71, no. 19, pp. 3627–3631, 2014.

[368] G. Carpenter and H.-J. Liao, "Receptor tyrosine kinases in the nucleus.," *Cold Spring Harb. Perspect. Biol.*, vol. 5, no. 10, p. a008979, 2013.

[369] S. Moens, J. Goveia, P. C. Stapor, A. R. Cantelmo, and P. Carmeliet, "The multifaceted activity of VEGF in angiogenesis – Implications for therapy responses," *Cytokine Growth Factor Rev.*, vol. 25, no. 4, pp. 473–482, Aug. 2014.

[370] G. McMahon, "VEGF Receptor Signaling in Tumor Angiogenesis," *Oncol.* , vol. 5, no. suppl 1, pp. 3–10, Apr. 2000.

[371] H. M. Jopling, G. J. Howell, N. Gamper, and S. Ponnambalam, "The VEGFR2 receptor tyrosine kinase undergoes constitutive endosome-to-plasma membrane recycling," *Biochem. Biophys. Res. Commun.*, vol. 410, no. 2, pp. 170–176, Jul. 2011.

[372] P. I. Imoukhuede and A. S. Popel, "Expression of VEGF receptors on endothelial cells in mouse skeletal muscle," *PLoS One*, vol. 7, no. 305, p. e44791, 2012.

[373] a. Wicki, C. Rochlitz, a. Orleth, R. Ritschard, I. Albrecht, R. Herrmann, G. Christofori, and C. Mamot, "Targeting Tumor-Associated Endothelial Cells: Anti-VEGFR2 Immunoliposomes Mediate Tumor Vessel Disruption and Inhibit Tumor Growth," *Clin. Cancer Res.*, vol. 18, no. 2, pp. 454–464, 2012.

[374] S. Chen, J. C. Weddell, P. Gupta, G. Conard, J. Parkin, and P. I. Imoukhuede,

"Nanosensor-based flow cytometry for quantifying membrane VEGFR1, NRP1, Tie2 and PDGFRs," *Methods Mol Biol*, vol. In submiss, 2015.

[375] D. Kumar, R. Srikanth, H. Ahlfors, R. Lahesmaa, and K. V. S. Rao, "Capturing cell-fate decisions from the molecular signatures of a receptor-dependent signaling response," *Mol. Syst. Biol.*, vol. 3, p. 150, Dec. 2007.

[376] M. Schilling, T. Maiwald, S. Hengl, D. Winter, C. Kreutz, W. Kolch, W. D. Lehmann, J. Timmer, and U. Klingmüller, "Theoretical and experimental analysis links isoform-specific ERK signalling to cell fate decisions," *Mol. Syst. Biol.*, vol. 5, no. 1, p. 334, Dec. 2009.

[377] Y. Mosesson, G. B. Mills, and Y. Yarden, "Derailed endocytosis: an emerging feature of cancer," *Nat Rev Cancer*, vol. 8, no. 11, pp. 835–850, Nov. 2008.

[378] A. Sorkin and M. von Zastrow, "Signal transduction and endocytosis: close encounters of many kinds," *Nat Rev Mol Cell Biol*, vol. 3, no. 8, pp. 600–614, Aug. 2002.

[379] H. Lodish, A. Berk, S. L. Zipursky, P. Matsudaira, D. Baltimore, and J. Darnell, "Receptor-mediated endocytosis and the sorting of internalized proteins.," in *Molecular Cell Biology 4th ed*, 2000, p. Section 17.9.

[380] J. P. Luzio, P. R. Pryor, and N. A. Bright, "Lysosomes: fusion and function," *Nat Rev Mol Cell Biol*, vol. 8, no. 8, pp. 622–632, Aug. 2007.

[381] Corning, "Surface Areas and Recommend Volumes for Corning® Cell Culture Vessels," 2008.

[382] S. C. D. van IJzendoorn, "Recycling endosomes," *J Cell Sci*, vol. 119, pp. 1679–1681, 2006.

[383] G. R. Bright, G. W. Fisher, J. Rogowska, and D. L. Taylor, “Fluorescence ratio imaging microscopy: temporal and spatial measurements of cytoplasmic pH,” *J. Cell Biol.*, vol. 104, no. 4, pp. 1019–1033, Apr. 1987.

[384] J. Llopis, J. M. McCaffery, A. Miyawaki, M. G. Farquhar, and R. Y. Tsien, “Measurement of cytosolic, mitochondrial, and Golgi pH in single living cells with green fluorescent proteins,” *Proc. Natl. Acad. Sci. U. S. A.*, vol. 95, no. 12, pp. 6803–6808, Jun. 1998.

[385] K. Maeda, Y. Kato, and Y. Sugiyama, “pH-dependent receptor/ligand dissociation as a determining factor for intracellular sorting of ligands for epidermal growth factor receptors in rat hepatocytes,” *J. Control. Release*, vol. 82, no. 1, pp. 71–82, Jul. 2002.

[386] K. Ek and P. G. Righetti, “Original papers Determination of protein-ligand dissociation constants and of their pH dependence by combined isoelectric Binding of phosphorylases a and b to glycogen,” *Electrophoresis*, vol. 1, pp. 137–140, 1980.

[387] B. S. Hendriks, J. Cook, J. M. Burke, D. A. Beusmans, J M Lauffenburger, and D. de Graaf, “Computational modelling of ErbB family phosphorylation dynamics in response to transforming growth factor alpha and heregulin indicates spatial compartmentation of phosphatase activity,” *Syst Biol*, vol. 153, pp. 22–33, 2006.

[388] Z. L. Zhang, J. F. Zhang, Y. F. Yuan, Y. M. He, Q. Y. Liu, X. W. Mao, Y. B. Ai, and Z. S. Liu, “Suppression of angiogenesis and tumor growth in vitro and in vivo using an anti-angiopoietin-2 single-chain antibody,” *Exp. Ther. Med.*, vol. 7, no. 3, pp. 543–552, Mar. 2014.

[389] J. M. Taylor, S. Cohen, and W. M. Mitchell, “Epidermal growth factor: high and low molecular weight forms.,” *Proc. Natl. Acad. Sci. U. S. A.*, vol. 67, no. 1, pp. 164–71, 1970.

[390] K. Chlebova, V. Bryja, P. Dvorak, A. Kozubik, W. R. Wilcox, and P. Krejci, “High molecular weight FGF2: the biology of a nuclear growth factor,” *Cell. Mol. Life Sci.*, vol. 66, no. 2, pp. 225–235, Jan. 2009.

[391] E. Rinderknecht and R. E. Humbel, “The amino acid sequence of human insulin-like growth factor I and its structural homology with proinsulin,” *J Biol Chem*, vol. 253, pp. 2769–76, 1978.

[392] A. Ostman, J. Thyberg, B. Westermark, and C. H. Heldin, “PDGF-AA and PDGF-BB biosynthesis: proprotein processing in the golgi complex and lysosomal degradation of PDGF-BB retained intracelluarly,” *J Cell Biol*, vol. 118, pp. 509–519, 1992.

[393] M. O. Stefanini, F. T. H. Wu, F. Mac Gabhann, A. S. Popel, W. F. T. Stefanini MO Mac Gabhann F, Popel AS, M. O. Stefanini, F. T. H. Wu, F. Mac Gabhann, A. S. Popel, and M. G. F. P. A. S. Stefanini MO Wu FT, “A compartment model of VEGF distribution in blood, healthy and diseased tissues.,” *BMC Syst Biol*, vol. 2, no. 77, p. 77, Jan. 2008.

[394] D. Wang and M. W. Quick, “Trafficking of the plasma membrane γ-aminobutyric acid transporter GAT1: Size and rates of an acutely recycling pool,” *J. Biol. Chem.*, vol. 280, no. 19, pp. 18703–18709, 2005.

[395] R. Villaseñor, H. Nonaka, P. Del Conte-Zerial, Y. Kalaidzidis, and M. Zerial, “Regulation of EGFR signal transduction by analogue-to-digital conversion in endosomes,” *Elife*, vol. 4, p. e06156, Dec. 2015.

[396] H. J. Geuze, J. W. Slot, and A. L. Schwartz, “Membranes of sorting organelles display lateral heterogeneity in receptor distribution,” *J. Cell Biol.*, vol. 104, no. 6, pp. 1715–1723, Jun. 1987.

[397] T. Annussek, T. Szuwart, J. Kleinheinz, C. Koiky, and K. Wermker, “In vitro inhibition of HUVECs by low dose methotrexate – insights into oral adverse events,” *Head Face Med.*, vol. 10, no. 1, p. 19, 2014.

[398] T. Umezu, K. Ohyashiki, M. Kuroda, and J. H. Ohyashiki, “Leukemia cell to endothelial cell communication via exosomal miRNAs,” *Oncogene*, vol. 32, no. 22, pp. 2747–2755, May 2013.

[399] H. Klingberg, L. B. Oddershede, K. Loeschner, E. H. Larsen, S. Loft, and P. Møller, “Uptake of gold nanoparticles in primary human endothelial cells,” *Toxicol Res*, vol. 4, pp. 655–666, 2015.

[400] D. Poteryaev, S. Datta, K. Ackema, M. Zerial, and A. Spang, “Identification of the Switch in Early-to-Late Endosome Transition,” *Cell*, vol. 141, no. 3, pp. 497–508, Apr. 2010.

[401] F. Shi, Y.-C. Wang, T.-Z. Zhao, S. Zhang, T.-Y. Du, C.-B. Yang, Y.-H. Li, and X.-Q. Sun, “Effects of Simulated Microgravity on Human Umbilical Vein Endothelial Cell Angiogenesis and Role of the PI3K-Akt-eNOS Signal Pathway,” *PLoS One*, vol. 7, no. 7, p. e40365, Jul. 2012.

[402] M. Hantera, H. Abd El-Hafiz, and A. Y. Abdelnaby, “Serum levels of angiopoietin-2 and vascular endothelial growth factor in severe refractory asthma,” *Egypt. J. Chest Dis. Tuberc.*, vol. 63, no. 4, pp. 751–754, Oct. 2014.

[403] Y. Lemos-Gonzalez, F. J. Rodriguez-Berrocal, O. J. Cordero, C. Gomez, and M. Paez de la Cadena, “Alteration of the serum levels of the epidermal growth factor receptor and its ligands in patients with non-small cell lung cancer and head and neck carcinoma,” *Br J Cancer*, vol. 96, no. 10, pp. 1569–1578, Apr. 2007.

[404] G. Ascherl, C. Sgadari, R. Bugarini, J. Bogner, O. Schatz, B. Ensoli, and M. Sturzl, "Serum Concentrations of Fibroblast Growth Factor 2 Are Increased in HIV Type 1-Infected Patients and Inversely Related to Survival Probability," *AIDS Res Hum Retroviruses*, vol. 17, pp. 1035–9, 2001.

[405] P. W. Rosario, "Normal values of serum IGF-1 in adults: results from a Brazilian population," *Arq Bras Endocrinol Metab.*, vol. 54, no. 5, pp. 477–481, 2010.

[406] M. Nowak, B. Marek, J. Karpe, B. Kos-Kudla, L. Sieminska, D. Kajdaniuk, and M. Treszer, "Serum concentration of VEGF and PDGF-AA in patients with active thyroid orbitopathy before and after immunosuppressive therapy," *Exp Clin Endocrinol Diabetes*, vol. 122, pp. 582–6, 2014.

[407] H. Takayama, Y. Miyake, K. Nouso, F. Ikeda, H. Shiraha, A. Takaki, H. Kobashi, and K. Yamamoto, "Serum levels of platelet-derived growth factor-BB and vascular endothelial growth factor as prognostic factors for patients with fulminant hepatic failure," *J. Gastroenterol. Hepatol.*, vol. 26, no. 1, pp. 116–121, Jan. 2011.

[408] C. W. Tan, B. S. Gardiner, Y. Hirokawa, D. W. Smith, and A. W. Burgess, "Analysis of Wnt signaling β-catenin spatial dynamics in HEK293T cells.," *BMC Syst. Biol.*, vol. 8, no. 1, p. 44, 2014.

[409] D. Nicklas and L. Saiz, "Computational modelling of Smad-mediated negative feedback and crosstalk in the TGF-β superfamily network," *J. R. Soc. Interface*, vol. 10, no. 86, p. 20130363, Jun. 2013.

[410] Y. Wu, X. Zhuo, Z. Dai, X. Guo, Y. Wang, C. Zhang, and L. Lai, "Modeling the mitotic regulatory network identifies highly efficient anti-cancer drug combinations," *Mol.*

BioSyst., vol. 11, pp. 497–505, 2015.

[411] C. Wu, M. H. Ma, K. R. Brown, M. Geisler, L. Li, E. Tzeng, C. Y. H. Jia, I. Jurisica, and S. S.-C. Li, "Systematic identification of SH3 domain-mediated human protein-protein interactions by peptide array target screening.," *Proteomics*, vol. 7, no. 11, pp. 1775–85, Jun. 2007.

[412] F. Anselmi, M. Orlandini, M. Rocchigiani, C. De Clemente, A. Salameh, C. Lentucci, S. Oliviero, and F. Galvagni, "c-ABL modulates MAP kinases activation downstream of VEGFR-2 signaling by direct phosphorylation of the adaptor proteins GRB2 and NCK1," *Angiogenesis*, vol. 15, no. 2, pp. 187–197, Jun. 2012.

[413] J. H. Qi and L. Claesson-Welsh, "VEGF-Induced Activation of Phosphoinositide 3-Kinase Is Dependent on Focal Adhesion Kinase," *Exp. Cell Res.*, vol. 263, no. 1, pp. 173–182, Feb. 2001.

[414] R. Bhattacharya, J. Kwon, X. Li, E. Wang, S. Patra, J. P. Bida, Z. Bajzer, L. Claesson-Welsh, and D. Mukhopadhyay, "Distinct role of PLCbeta3 in VEGF-mediated directional migration and vascular sprouting.," *J. Cell Sci.*, vol. 122, no. Pt 7, pp. 1025–34, Apr. 2009.

[415] C. H. Ha, A. M. Bennett, and Z. G. Jin, "A novel role of vascular endothelial cadherin in modulating c-Src activation and downstream signaling of vascular endothelial growth factor.," *J. Biol. Chem.*, vol. 283, no. 11, pp. 7261–70, Mar. 2008.

[416] T. Matsumoto, S. Bohman, J. Dixelius, T. Berge, A. Dimberg, P. Magnusson, L. Wang, C. Wikner, J. H. Qi, C. Wernstedt, J. Wu, S. Bruheim, H. Mugishima, D. Mukhopadhyay, A. Spurkland, and L. Claesson-Welsh, "VEGF receptor-2 Y951 signaling and a role for the

adapter molecule TSAd in tumor angiogenesis," *EMBO J.*, vol. 24, no. 13, pp. 2342–2353, Jul. 2005.

[417] D. A. Oyarzún, J. L. Bramhall, F. López-Caamal, F. M. Richards, D. I. Jodrell, and B. F. Krippendorff, "The EGFR demonstrates linear signal transmission.," *Integr. Biol.*, vol. 6, pp. 736–42, 2014.

[418] M. R. Birtwistle, M. Hatakeyama, N. Yumoto, B. A. Ogunnaike, J. B. Hoek, and B. N. Kholodenko, "Ligand-dependent responses of the ErbB signaling network: experimental and modeling analyses.," *Mol. Syst. Biol.*, vol. 3, no. 144, p. 144, Jan. 2007.

[419] P. I. Imoukhuede and A. S. A. Popel, "Quantification and cell-to-cell variation of vascular endothelial growth factor receptors," *Exp. Cell Res.*, vol. 317, no. 7, pp. 955–965, 2011.

[420] B. J. Roxworthy, M. T. Johnston, F. T. Lee-Montiel, R. H. Ewoldt, P. I. Imoukhuede, and K. C. Toussaint, "Plasmonic optical trapping in biologically relevant media.," *PLoS One*, vol. 9, no. 4, p. e93929, Jan. 2014.

[421] B. He, R. Baird, R. Butera, A. Datta, S. George, B. Hecht, A. Hero, G. Lazzi, R. C. Lee, J. Liang, M. Neuman, G. C. Y. Peng, E. J. Perreault, M. Ramasubramanian, M. D. Wang, J. Wikswo, G.-Z. Yang, and Y.-T. Zhang, "Grand challenges in interfacing engineering with life sciences and medicine.," *IEEE Trans. Biomed. Eng.*, vol. 60, pp. 589–98, 2013.

[422] R. a Burrell, N. McGranahan, J. Bartek, and C. Swanton, "The causes and consequences of genetic heterogeneity in cancer evolution.," *Nature*, vol. 501, pp. 338–45, 2013.

[423] C. G. Willett, Y. Boucher, E. di Tomaso, D. G. Duda, L. L. Munn, R. T. Tong, D. C. Chung, D. V Sahani, S. P. Kalva, S. V Kozin, M. Mino, K. S. Cohen, D. T. Scadden, A. C. Hartford, A. J. Fischman, J. W. Clark, D. P. Ryan, A. X. Zhu, L. S. Blaszkowsky, H. X.

Chen, P. C. Shellito, G. Y. Lauwers, and R. K. Jain, “Direct evidence that the VEGF-specific antibody bevacizumab has antivascular effects in human rectal cancer.,” 2004.

[424] G. Bergers, S. Song, N. Meyer-Morse, E. Bergsland, and D. Hanahan, “Benefits of targeting both pericytes and endothelial cells in the tumor vasculature with kinase inhibitors.,” *J. Clin. Invest.*, vol. 111, pp. 1287–1295, 2003.

[425] R. Erber, A. Thurnher, A. D. Katsen, G. Groth, H. Kerger, H.-P. Hammes, M. D. Menger, A. Ullrich, and P. Vajkoczy, “Combined inhibition of VEGF and PDGF signaling enforces tumor vessel regression by interfering with pericyte-mediated endothelial cell survival mechanisms.,” *FASEB J.*, vol. 18, no. 2, pp. 338–340, Feb. 2004.

[426] O. Casanovas, D. J. Hicklin, G. Bergers, and D. Hanahan, “Drug resistance by evasion of antiangiogenic targeting of VEGF signaling in late-stage pancreatic islet tumors.,” *Cancer Cell*, vol. 8, no. 4, pp. 299–309, Oct. 2005.

[427] E. M. Chislock, C. Ring, and A. M. Pendergast, “Abl kinases are required for vascular function, Tie2 expression, and angiopoietin-1–mediated survival,” *Proc. Natl. Acad. Sci. U. S. A.*, vol. 110, no. 30, pp. 12432–12437, Jul. 2013.

[428] K. Takeuchi, Y. Morizane, C. Kamami-Levy, J. Suzuki, M. Kayama, W. Cai, J. W. Miller, and D. G. Vavvas, “AMP-dependent Kinase Inhibits Oxidative Stress-induced Caveolin-1 Phosphorylation and Endocytosis by Suppressing the Dissociation between c-Abl and Prdx1 Proteins in Endothelial Cells,” *J. Biol. Chem.*, vol. 288, no. 28, pp. 20581–20591, Jul. 2013.

[429] S. Ikeda, M. Ushio-Fukai, L. Zuo, T. Tojo, S. Dikalov, N. A. Patrushev, and R. W. Alexander, “Novel Role of ARF6 in Vascular Endothelial Growth Factor–Induced

Signaling and Angiogenesis," *Circ. Res.* , vol. 96, no. 4, pp. 467–475, Mar. 2005.

[430] L. Fang, S.-H. Choi, J. S. Baek, C. Liu, F. Almazan, F. Ulrich, P. Wiesner, A. Taleb, E. Deer, J. Pattison, J. Torres-Vazquez, A. C. Li, and Y. I. Miller, "Control of angiogenesis by AIBP-mediated cholesterol efflux," *Nature*, vol. 498, no. 7452, pp. 118–122, Jun. 2013.

[431] H. Song, S. Pasula, M. Brophy, H. Wu, Y. Dong, and H. Chen, "Novel epsin-VEGFR2 interactions facilitated by c-Cbl ubiquitination of epsin and VEGFR2 regulate VEGFR2 signaling and physiological and pathological angiogenesis," in *Vasculata*, 2014, p. Poster Presentation.

[432] T. Ohmori, Y. Yatomi, H. Okamoto, Y. Miura, G. Rile, K. Satoh, and Y. Ozaki, "Gi-mediated Cas Tyrosine Phosphorylation in Vascular Endothelial Cells Stimulated with Sphingosine 1-Phosphate: POSSIBLE INVOLVEMENT IN CELL MOTILITY ENHANCEMENT IN COOPERATION WITH Rho-MEDIATED PATHWAYS ," *J. Biol. Chem.* , vol. 276, no. 7, pp. 5274–5280, Feb. 2001.

[433] C. Jean, X. L. Chen, J. O. Nam, I. Tancioni, S. Uryu, C. Lawson, K. K. Ward, C. T. Walsh, N. L. G. Miller, M. Ghassemian, P. Turowski, E. Dejana, S. Weis, D. a Cheresh, and D. D. Schlaepfer, "Inhibition of endothelial FAK activity prevents tumor metastasis by enhancing barrier function.," *J. Cell Biol.*, vol. 204, no. 2, pp. 247–63, Jan. 2014.

[434] X. L. Chen, J.-O. Nam, C. Jean, C. Lawson, C. T. Walsh, E. Goka, S.-T. Lim, A. Tomar, I. Tanjoni, S. Uryu, J.-L. Guan, L. M. Acevedo, S. M. Weis, D. A. Cheresh, and D. D. Schlaepfer, "VEGF-induced vascular permeability is mediated by FAK," *Dev. Cell*, vol. 22, no. 1, pp. 146–157, Jan. 2012.

[435] B. Herzog, C. Pellet-Many, G. Britton, B. Hartzoulakis, and I. C. Zachary, “VEGF binding to NRP1 is essential for VEGF stimulation of endothelial cell migration, complex formation between NRP1 and VEGFR2, and signaling via FAK Tyr407 phosphorylation,” *Mol. Biol. Cell*, vol. 22, no. 15, pp. 2766–2776, Aug. 2011.

[436] S. Sinha, P. K. Vohra, R. Bhattacharya, S. Dutta, S. Sinha, and D. Mukhopadhyay, “Dopamine regulates phosphorylation of VEGF receptor 2 by engaging Src-homology-2-domain-containing protein tyrosine phosphatase 2.,” *J. Cell Sci.*, vol. 122, no. Pt 18, pp. 3385–92, Sep. 2009.

[437] L. H. Hoeppner, S. Sinha, Y. Wang, R. Bhattacharya, S. Dutta, X. Gong, V. M. Bedell, S. Suresh, C. Chun, R. Ramchandran, S. C. Ekker, and D. Mukhopadhyay, “RhoC maintains vascular homeostasis by regulating VEGF-induced signaling in endothelial cells,” *J. Cell Sci.*, vol. 128, no. 19, pp. 3556–3568, Oct. 2015.

[438] L. Lai, J. Liu, D. Zhai, Q. Lin, L. He, Y. Dong, J. Zhang, B. Lu, Y. Chen, Z. Yi, and M. Liu, “Plumbagin inhibits tumour angiogenesis and tumour growth through the Ras signalling pathway following activation of the VEGF receptor-2,” *Br. J. Pharmacol.*, vol. 165, no. 4b, pp. 1084–1096, Feb. 2012.

[439] K. Yoshioka, K. Yoshida, H. Cui, T. Wakayama, N. Takuwa, Y. Okamoto, W. Du, X. Qi, K. Asanuma, K. Sugihara, S. Aki, H. Miyazawa, K. Biswas, C. Nagakura, M. Ueno, S. Iseki, R. J. Schwartz, H. Okamoto, T. Sasaki, O. Matsui, M. Asano, R. H. Adams, N. Takakura, and Y. Takuwa, “Endothelial PI3K-C2[alpha], a class II PI3K, has an essential role in angiogenesis and vascular barrier function,” *Nat Med*, vol. 18, no. 10, pp. 1560–1569, Oct. 2012.

[440] T. Tabata, H. Kawakatsu, E. Maidji, T. Sakai, K. Sakai, J. Fang-Hoover, M. Aiba, D.

Sheppard, and L. Pereira, “Induction of an Epithelial Integrin αvβ6 in Human Cytomegalovirus-Infected Endothelial Cells Leads to Activation of Transforming Growth Factor-β1 and Increased Collagen Production,” *Am. J. Pathol.*, vol. 172, no. 4, pp. 1127–1140, Jul. 2016.

[441] J. Arroyo, R. J. Torry, and D. S. Torry, “Deferential regulation of placenta growth factor (PlGF)-mediated signal transduction in human primary term trophoblast and endothelial cells.,” *Placenta*, vol. 25, no. 5, pp. 379–86, May 2004.

[442] A. Dubrac, G. Genet, R. Ola, F. Zhang, L. Pibouin-Fragner, J. Han, J. Zhang, J.-L. Thomas, A. Chedotal, M. A. Schwartz, and A. Eichmann, “Targeting NCK-Mediated Endothelial Cell Front-Rear Polarity Inhibits NeovascularizationCLINICAL PERSPECTIVE,” *Circulation*, vol. 133, no. 4, pp. 409–421, Jan. 2016.

[443] S. Li, Y. Y. Dang, G. O. L. Che, Y. W. Kwan, S. W. Chan, G. P. H. Leung, S. M.-Y. Lee, and M. P. M. Hoi, “VEGFR tyrosine kinase inhibitor II (VRI) induced vascular insufficiency in zebrafish as a model for studying vascular toxicity and vascular preservation.,” *Toxicol. Appl. Pharmacol.*, vol. 280, pp. 408–20, Sep. 2014.

[444] G. G.-L. Yue, J. K.-M. Lee, H.-F. Kwok, L. Cheng, E. C.-W. Wong, L. Jiang, H. Yu, H.-W. Leung, Y.-L. Wong, P.-C. Leung, K.-P. Fung, and C. B.-S. Lau, “Novel PI3K/AKT targeting anti-angiogenic activities of 4-vinylphenol, a new therapeutic potential of a well-known styrene metabolite,” *Sci. Rep.*, vol. 5, p. 11149, Jun. 2015.

[445] B. G. Coon, N. Baeyens, J. Han, M. Budatha, T. D. Ross, J. S. Fang, S. Yun, J.-L. Thomas, and M. A. Schwartz, “Intramembrane binding of VE-cadherin to VEGFR2 and VEGFR3 assembles the endothelial mechanosensory complex,” *J. Cell Biol.* , vol. 208, no. 7, pp. 975–986, Mar. 2015.

[446] Y. Xiong, Z. Hu, X. Han, B. Jiang, R. Zhang, X. Zhang, Y. Lu, C. Geng, W. Li, Y. He, Y. Huo, M. Shibuya, and J. Luo, "Hypertensive stretch regulates endothelial exocytosis of Weibel-Palade bodies through VEGF receptor 2 signaling pathways.," *Cell Res.*, vol. 23, no. 6, pp. 820–34, Jun. 2013.

[447] S.-W. Han, Y.-K. Jung, E.-J. Lee, H.-R. Park, G.-W. Kim, J.-H. Jeong, M.-S. Han, and J.-Y. Choi, "DICAM inhibits angiogenesis via suppression of AKT and p38 MAP kinase signalling," *Cardiovasc. Res.*, vol. 98, no. 1, pp. 73–82, Mar. 2013.

[448] K. E. Ratcliffe, Q. Tao, B. Yavuz, K. V Stoletov, S. C. Spring, and B. I. Terman, "Sck is expressed in endothelial cells and participates in vascular endothelial growth factor-induced signaling.," *Oncogene*, vol. 21, no. 41, pp. 6307–6316, 2002.

[449] C. K. Lindholm, M. L. Henriksson, B. Hallberg, and M. Welsh, "Shb links SLP-76 and Vav with the CD3 complex in Jurkat T cells," *Eur. J. Biochem.*, vol. 269, no. 13, pp. 3279–3288, 2002.

[450] Aviva_Systems_Biology, "SHB Antibody," 2014.

[451] Z. Ma, Z. Liu, R.-F. Wu, and L. S. Terada, "p66Shc restrains Ras hyperactivation and suppresses metastatic behavior," *Oncogene*, vol. 29, no. 41, pp. 5559–5567, Oct. 2010.

[452] J. Oshikawa, S.-J. Kim, E. Furuta, C. Caliceti, G.-F. Chen, R. D. McKinney, F. Kuhr, I. Levitan, T. Fukai, and M. Ushio-Fukai, "Novel role of p66Shc in ROS-dependent VEGF signaling and angiogenesis in endothelial cells," *Am. J. Physiol. - Hear. Circ. Physiol.*, vol. 302, no. 3, pp. H724–H732, Jan. 2012.

[453] L. W. Wu, L. D. Mayo, J. D. Dunbar, K. M. Kessler, O. N. Ozes, R. S. Warren, and D. B. Donner, "VRAP is an adaptor protein that binds KDR, a receptor for vascular endothelial

cell growth factor.," *J. Biol. Chem.*, vol. 275, no. 9, pp. 6059–6062, 2000.

[454] X. Xiong, P. Cui, S. Hossain, R. Xu, B. Warner, X. Guo, X. An, A. K. Debnath, D. Cowburn, and L. Kotula, "Allosteric inhibition of the nonMyristoylated c-Abl tyrosine kinase by phosphopeptides derived from Abi1/Hssh3bp1.," *Biochim. Biophys. Acta*, vol. 1783, no. 5, pp. 737–47, May 2008.

[455] J. H. Huang, L. Lu, H. Lu, X. Chen, S. Jiang, and Y. H. Chen, "Identification of the HIV-1 gp41 core-binding motif in the scaffolding domain of caveolin-1.," *J. Biol. Chem.*, vol. 282, no. 9, pp. 6143–52, Mar. 2007.

[456] L. Huang, C. Q. Pan, B. Li, L. Tucker-Kellogg, B. Tidor, Y. Chen, and B. C. Low, "Simulating EGFR-ERK signaling control by scaffold proteins KSR and MP1 reveals differential ligand-sensitivity co-regulated by Cbl-CIN85 and endophilin.," *PLoS One*, vol. 6, no. 8, p. e22933, Jan. 2011.

[457] M. Matsuda, S. Ota, R. Tanimura, H. Nakamura, K. Matuoka, T. Takenawa, K. Nagashima, and T. Kurata, "Interaction between the amino-terminal SH3 domain of CRK and its natural target proteins," *J. Biol. Chem.*, vol. 271, no. 24, pp. 14468–14472, Jun. 1996.

[458] S. T. Arold, T. S. Ulmer, T. D. Mulhern, J. M. Werner, J. E. Ladbury, I. D. Campbell, and M. E. Noble, "The role of the Src homology 3-Src homology 2 interface in the regulation of Src kinases.," *J. Biol. Chem.*, vol. 276, no. 20, pp. 17199–205, May 2001.

[459] S. A. Solheim, E. Petsalaki, A. J. Stokka, R. B. Russell, K. Taskén, and T. Berge, "Interactions between the Fyn SH3-domain and adaptor protein Cbp/PAG derived ligands, effects on kinase activity and affinity.," *FEBS J.*, vol. 275, no. 19, pp. 4863–74, Oct. 2008.

[460] S. Frese, W. Schubert, A. C. Findeis, T. Marquardt, Y. S. Roske, T. E. B. Stradal, and D. W. Heinz, “The phosphotyrosine peptide binding specificity of Nck1 and Nck2 Src homology 2 domains,” *J. Biol. Chem.*, vol. 281, no. 26, pp. 18236–18245, Jun. 2006.

[461] G. Payne, S. E. Shoelson, G. D. Gish, T. Pawson, and C. T. Walsh, “Kinetics of p56lck and p60src Src homology 2 domain binding to tyrosine-phosphorylated peptides determined by a competition assay or surface plasmon resonance.,” *Proc. Natl. Acad. Sci. U. S. A.*, vol. 90, no. 11, pp. 4902–6, Jun. 1993.

[462] M.-M. Zhou, J. E. Harlan, W. S. Wade, S. Crosby, K. S. Ravichandran, S. J. Burakoff, and S. W. Fesik, “Binding Affinities of Tyrosine-phosphorylated Peptides to the COOH-terminal SH2 and NH-terminal Phosphotyrosine Binding Domains of Shc ,” *J. Biol. Chem.* , vol. 270, no. 52, pp. 31119–31123, Dec. 1996.

[463] W. Yan, B. Bentley, and R. Shao, “Distinct angiogenic mediators are required for basic fibroblast growth factor- and vascular endothelial growth factor-induced angiogenesis: the role of cytoplasmic tyrosine kinase c-Abl in tumor angiogenesis,” *Mol. Biol. Cell*, vol. 19, no. 5, pp. 2278–2288, May 2008.

[464] S. Roumiantsev, N. P. Shah, M. E. Gorre, J. Nicoll, B. B. Brasher, C. L. Sawyers, and R. A. Van Etten, “Clinical resistance to the kinase inhibitor STI-571 in chronic myeloid leukemia by mutation of Tyr-253 in the Abl kinase domain P-loop.,” *Proc. Natl. Acad. Sci. U. S. A.*, vol. 99, no. Track II, pp. 10700–10705, 2002.

[465] K. Fang, W. Fu, A. R. Beardsley, X. Sun, M. P. Lisanti, and J. Liu, “Overexpression of caveolin-1 inhibits endothelial cell proliferation by arresting the cell cycle at G0/G1 phase,” *Cell Cycle*, vol. 6, no. February 2015, pp. 199–204, 2007.

[466] S. A. Tahir, S. Park, and T. C. Thompson, “Caveolin-1 regulates VEGF-stimulated angiogenic activities in prostate cancer and endothelial cells,” *Cancer Biol. Ther.*, vol. 8, no. 23, pp. 2284–2294, Oct. 2014.

[467] K. V Stoletov, C. Gong, and B. I. Terman, “Nck and Crk mediate distinct VEGF-induced signaling pathways that serve overlapping functions in focal adhesion turnover and integrin activation,” *Exp. Cell Res.*, vol. 295, pp. 258–268, 2004.

[468] P. W. Bryant, Q. Zheng, and K. M. Pumiglia, “Focal adhesion kinase is a phospho-regulated repressor of Rac and proliferation in human endothelial cells,” *Biol. Open*, vol. 1, pp. 723–730, 2012.

[469] F. Le Boeuf, F. Houle, M. Sussman, and J. Huot, “Phosphorylation of focal adhesion kinase (FAK) on Ser732 is induced by rho-dependent kinase and is essential for proline-rich tyrosine kinase-2–mediated phosphorylation of FAK on Tyr407 in response to vascular endothelial growth factor,” *Mol. Biol. Cell*, vol. 17, no. 8, pp. 3508–3520, Aug. 2006.

[470] X. Q. Werdich and J. S. Penn, “Src, Fyn and Yes play differential roles in VEGF-mediated endothelial cell events.,” *Angiogenesis*, vol. 8, no. 4, pp. 315–26, Jan. 2005.

[471] L. Yin, K. I. Morishige, T. Takahashi, K. Hashimoto, S. Ogata, S. Tsutsumi, K. Takata, T. Ohta, J. Kawagoe, K. Takahashi, and H. Kurachi, “Fasudil inhibits vascular endothelial growth factor-induced angiogenesis in vitro and in vivo.,” *Mol. Cancer Ther.*, vol. 6, no. May, pp. 1517–1525, 2007.

[472] Y. Rikitake, H. H. Kim, Z. Huang, M. Seto, K. Yano, T. Asano, M. A. Moskowitz, and J. K. Liao, “Inhibition of Rho kinase (ROCK) leads to increased cerebral blood flow and

stroke protection," *Stroke*, vol. 36, pp. 2251–2257, 2005.

[473] J. V Soriano, N. Liu, Y. Gao, Z. Yao, T. Ishibashi, C. Underhill, T. R. Burke, and D. P. Bottaro, "Inhibition of angiogenesis by growth factor receptor bound protein 2-Src homology 2 domain binding antagonists," *Mol. Cancer Ther.*, vol. 3, pp. 1289–1300, 2004.

[474] A. Giubellino, Y. Gao, S. Lee, M. J. Lee, J. R. Vasselli, S. Medepalli, J. B. Trepel, T. R. Burke, and D. P. Bottaro, "Inhibition of tumor metastasis by a growth factor receptor bound protein 2 Src homology 2 domain-binding antagonist," *Cancer Res.*, vol. 67, no. 13, pp. 6012–6016, 2007.

[475] S. P. Chaki, R. Barhoumi, M. E. Berginski, H. Sreenivasappa, A. Trache, S. M. Gomez, and G. M. Rivera, "Nck enables directional cell migration through the coordination of polarized membrane protrusion with adhesion dynamics.," *J. Cell Sci.*, vol. 126, no. Pt 7, pp. 1637–49, Apr. 2013.

[476] H. Kim, H. Ko, S. Choi, and D. Seo, "Anti-angiogenic effects of Siegesbeckia glabrescens are mediated by suppression of the Akt and p70S6K-dependent signaling pathways," *Oncol. Rep.*, vol. 33, pp. 699–704, 2015.

[477] S. M. Short, A. Derrien, R. P. Narsimhan, J. Lawler, D. E. Ingber, and B. R. Zetter, "Inhibition of endothelial cell migration by thrombospondin-1 type-1 repeats is mediated by β1 integrins," *J. Cell Biol.*, vol. 168, no. 4, pp. 643–653, 2005.

[478] A. Arcaro and M. P. Wymann, "Wortmannin is a potent phosphatidylinositol 3-kinase inhibitor: the role of phosphatidylinositol 3,4,5-trisphosphate in neutrophil responses.," *Biochem. J.*, vol. 296 (Pt 2), pp. 297–301, 1993.

[479] H. Zeng, H. F. Dvorak, and D. Mukhopadhyay, “Vascular permeability factor (VPF)/vascular endothelial growth factor (VEGF) receptor-1 down-modulates VPF/VEGF receptor-2-mediated endothelial cell proliferation, but not migration, through phosphatidylinositol 3-kinase-dependent pathways,” *J. Biol. Chem.*, vol. 276, no. 29, pp. 26969–26979, 2001.

[480] A. Tatrai, S. K. Lee, and P. H. Stern, “U-73122, a phospholipase C antagonist, inhibits effects of endothelin-1 and parathyroid hormone on signal transduction in UMR-106 osteoblastic cells,” *Biochim Biophys Acta*, vol. 1224, no. 3, pp. 575–82, 1994.

[481] D. T. Sweet, Z. Chen, D. M. Wiley, V. L. Bautch, and E. Tzima, “The adaptor protein Shc integrates growth factor and ECM signaling during postnatal angiogenesis,” *Blood*, vol. 119, no. 8, pp. 1946–1955, Feb. 2012.

[482] N. Ali, M. Yoshizumi, S. Yano, S. Sone, H. Ohnishi, K. Ishizawa, Y. Kanematsu, K. Tsuchiya, and T. Tamaki, “The novel Src kinase inhibitor M475271 inhibits VEGF-induced vascular endothelial-cadherin and beta-catenin phosphorylation but increases their association,” *J. Pharmacol. Sci.*, vol. 102, no. 1, pp. 112–120, 2006.

[483] C. Rivat, N. Le Floch, M. Sabbah, I. Teyrol, G. Redeuilh, E. Bruyneel, M. Mareel, L. M. Matrisian, H. C. Crawford, C. Gespach, and S. Attoub, “Synergistic cooperation between the AP-1 and LEF-1 transcription factors in activation of the matrilysin promoter by the src oncogene: implications in cellular invasion,” *FASEB J*, vol. 17, no. 12, pp. 1721–3, 2003.

[484] S. A. Cunningham, M. P. Arrate, T. A. Brock, and M. N. Waxham, “Interactions of FLT-1 and KDR with phospholipase C gamma: identification of the phosphotyrosine binding sites.,” *Biochem. Biophys. Res. Commun.*, vol. 240, no. 3, pp. 635–9, Nov. 1997.

[485] K. Podar, R. Shringarpure, Y. T. Tai, M. Simoncini, M. Sattler, K. Ishitsuka, P. G. Richardson, T. Hideshima, D. Chauhan, and K. C. Anderson, “Caveolin-1 is required for vascular endothelial growth factor-triggered multiple myeloma cell migration and is targeted by bortezomib,” *Cancer Res*, vol. 64, no. 20, pp. 7500–7506, 2004.

[486] L. Lamalice, F. Houle, and J. Huot, “Phosphorylation of Tyr1214 within VEGFR-2 triggers the recruitment of Nck and activation of Fyn leading to SAPK2/p38 activation and endothelial cell migration in response to VEGF.,” *J. Biol. Chem.*, vol. 281, no. 45, pp. 34009–20, Nov. 2006.

[487] E. M. Chislock and A. M. Pendergast, “Abl Family Kinases Regulate Endothelial Barrier Function <italic>In Vitro</italic> and in Mice,” *PLoS One*, vol. 8, no. 12, p. e85231, Dec. 2013.

[488] S. Ahmad, P. W. Hewett, P. Wang, B. Al-Ani, M. Cudmore, T. Fujisawa, J. J. Haigh, F. le Noble, L. Wang, D. Mukhopadhyay, and A. Ahmed, “Direct evidence for endothelial vascular endothelial growth factor receptor-1 function in nitric oxide-mediated angiogenesis.,” *Circ. Res.*, vol. 99, no. 7, pp. 715–22, Sep. 2006.

[489] Y. Matsumoto, K. Tanaka, G. Hirata, M. Hanada, S. Matsuda, T. Shuto, and Y. Iwamoto, “Possible Involvement of the Vascular Endothelial Growth Factor-Flt-1-Focal Adhesion Kinase Pathway in Chemotaxis and the Cell Proliferation of Osteoclast Precursor Cells in Arthritic Joints,” *J. Immunol.*, vol. 168, no. 11, pp. 5824–5831, Jun. 2002.

[490] V. Dayanir, M. RD, K. Lashkari, N. Rahimi, D. V, M. RD, L. K, and R. N, “Identification of Tyrosine Residues in Vascular Endothelial Growth Factor Receptor-2/FLK-1 Involved in Activation of Phosphatidylinositol 3-Kinase and Cell Proliferation,” *J Biol Chem*, vol. 276, pp. 17686–17692, 2001.

[491] A. Zanetti, M. G. Lampugnani, G. Balconi, F. Breviario, M. Corada, L. Lanfrancone, and E. Dejana, “Vascular endothelial growth factor induces Shc association with vascular endothelial cadherin: A potential feedback mechanism to control vascular endothelial growth factor receptor-2 signaling,” *Arterioscler. Thromb. Vasc. Biol.*, vol. 22, no. 4, pp. 617–622, 2002.

[492] Q. Xu, J. Lee, E. Jankowska-Gan, J. Schultz, D. a Roenneburg, L. D. Haynes, S. Kusaka, H. W. Sollinger, S. J. Knechtle, A. M. VanBuskirk, J. R. Torrealba, and W. J. Burlingham, “Human CD4+CD25low adaptive T regulatory cells suppress delayed-type hypersensitivity during transplant tolerance.,” *J. Immunol.*, vol. 178, no. 6, pp. 3983–3995, 2007.

[493] A. Sawano, T. Takahashi, S. Yamaguchi, and M. Shibuya, “The phosphorylated 1169-tyrosine containing region of flt-1 kinase (VEGFR-1) is a major binding site for PLCgamma.,” *Biochem. Biophys. Res. Commun.*, vol. 238, no. 2, pp. 487–91, Sep. 1997.

[494] L. W. Wu, L. D. Mayo, J. D. Dunbar, K. M. Kessler, M. R. Baerwald, E. a Jaffe, D. Wang, R. S. Warren, and D. B. Donner, “Utilization of distinct signaling pathways by receptors for vascular endothelial cell growth factor and other mitogens in the induction of endothelial cell proliferation.,” *J. Biol. Chem.*, vol. 275, no. 7, pp. 5096–5103, 2000.

[495] M. Shibuya, “Vascular Endothelial Growth Factor Receptor Family Genes: When Did the Three Genes Phylogenetically Segregate?,” *Biol. Chem.*, vol. 383, no. 10, pp. 1573–1579, 2002.

[496] J. M. Vieira, C. Ruhrberg, and Q. Schwarz, “VEGF receptor signaling in vertebrate development,” *Organogenesis*, vol. 6, no. 2, pp. 97–106, Apr. 2010.

[497] N. Ito, C. Wernstedt, U. Engstrom, and L. Claesson-Welsh, “Identification of vascular endothelial growth factor receptor-1 tyrosine phosphorylation sites and binding of SH2 domain-containing molecules,” *J. Biol. Chem.*, vol. 273, no. 36, pp. 23410–23418, Sep. 1998.

[498] A. J. Warner, J. Lopez-Dee, E. L. Knight, J. R. Feramisco, and S. A. Prigent, “The Shc-related adaptor protein, Sck, forms a complex with the vascular-endothelial-growth-factor receptor KDR in transfected cells.,” *Biochem. J.*, vol. 347, no. Pt 2, pp. 501–509, Apr. 2000.

[499] K. Igarashi, T. Isohara, T. Kato, K. Shigeta, T. Yamano, and I. Uno, “Tyrosine 1213 of Flt-1 Is a Major Binding Site of Nck and SHP-2,” *Biochem. Biophys. Res. Commun.*, vol. 246, no. 1, pp. 95–99, May 1998.

[500] R. D. Meyer, C. Latz, and N. Rahimi, “Recruitment and Activation of Phospholipase Cγ1 by Vascular Endothelial Growth Factor Receptor-2 Are Required for Tubulogenesis and Differentiation of Endothelial Cells,” *J. Biol. Chem.*, vol. 278, no. 18, pp. 16347–16355, May 2003.

[501] C. Caron, K. Spring, M. Laramée, C. Chabot, M. Cloutier, H. Gu, and I. Royal, “Non-redundant roles of the Gab1 and Gab2 scaffolding adapters in VEGF-mediated signalling, migration, and survival of endothelial cells,” *Cell. Signal.*, vol. 21, no. 6, pp. 943–953, Jun. 2009.

[502] Y. Maru, H. Hirosawa, and M. Shibuya, “An oncogenic form of the Flt-1 kinase has a tubulogenic potential in a sinusoidal endothelial cell line.,” *Eur. J. Cell Biol.*, vol. 79, no. 2, pp. 130–43, Mar. 2000.

[503] H. Zeng, S. Sanyal, and D. Mukhopadhyay, “Tyrosine Residues 951 and 1059 of Vascular Endothelial Growth Factor Receptor-2 (KDR) Are Essential for Vascular Permeability Factor/Vascular Endothelial Growth Factor-induced Endothelium Migration and Proliferation, Respectively,” *J. Biol. Chem.*, vol. 276, no. 35, pp. 32714–32719, 2001.

[504] K. Igarashi, K. Shigeta, T. Isohara, T. Yamano, and I. Uno, “Sck interacts with KDR and Flt-1 via its SH2 domain.,” *Biochem. Biophys. Res. Commun.*, vol. 251, no. 1, pp. 77–82, 1998.

[505] S. Kobayashi, A. Sawano, Y. Nojima, M. Shibuya, Y. Maru, and S. A. Kobayashi S Nojima Y, Shibuya M, and Maru Y, “The c-Cbl/CD2AP complex regulates VEGF-induced endocytosis and degradation of Flt-1 (VEGFR-1).,” *FASEB J.*, vol. 18, no. 7, pp. 929–31, May 2004.

[506] N. S. Raikwar, K. Z. Liu, and C. P. Thomas, “N-Terminal Cleavage and Release of the Ectodomain of Flt1 Is Mediated via ADAM10 and ADAM 17 and Regulated by VEGFR2 and the Flt1 Intracellular Domain,” *PLoS One*, vol. 9, no. 11, p. e112794, Nov. 2014.

[507] R. D. Meyer, D. B. Sacks, and N. Rahimi, “IQGAP1-Dependent Signaling Pathway Regulates Endothelial Cell Proliferation and Angiogenesis,” *PLoS One*, vol. 3, no. 12, p. e3848, Dec. 2008.

[508] J. H. Qi and L. Claesson-Welsh, “VEGF-induced activation of phosphoinositide 3-kinase is dependent on focal adhesion kinase.,” *Exp. Cell Res.*, vol. 263, no. 1, pp. 173–182, 2001.

[509] Y. Yu, J. D. Hulmes, M. T. Herley, R. G. Whitney, J. W. Crabb, and J. D. Sato, “Direct identification of a major authophosphorylation site on vascular endothelial growth factor

receptor Flt-1 that mediates phosphatidylinositol 3'-kinase binding," *Biochem J*, vol. 358, no. Pt 2, pp. 465–472, 2001.

[510] A. J. Singh, R. D. Meyer, G. Navruzbekov, R. Shelke, L. Duan, H. Band, S. E. Leeman, and N. Rahimi, "A critical role for the E3-ligase activity of c-Cbl in VEGFR-2-mediated PLCγ1 activation and angiogenesis," *Proc. Natl. Acad. Sci.*, vol. 104, no. 13, pp. 5413–5418, Mar. 2007.

[511] T. Takahashi, S. Yamaguchi, K. Chida, and M. Shibuya, "A single autophosphorylation site on KDR/Flk-1 is essential for VEGF-A-dependent activation of PLC-[gamma] and DNA synthesis in vascular endothelial cells," *EMBO J*, vol. 20, no. 11, pp. 2768–2778, 2001.

[512] L. Lamalice, F. F. Houle, G. Jourdan, and J. Huot, "Phosphorylation of tyrosine 1214 on VEGFR2 is required for VEGF-induced activation of Cdc42 upstream of SAPK2//p38," *Oncogene*, vol. 23, no. 2, pp. 434–445, 2004.

[513] M. T. Chou, J. Wang, and D. J. Fujita, "Src kinase becomes preferentially associated with the VEGFR, KDR/Flk-1, following VEGF stimulation of vascular endothelial cells," *BMC Biochem.*, vol. 3, p. 32, 2002.

[514] A. Tiwari, J.-J. Jung, S. M. Inamdar, D. Nihalani, and A. Choudhury, "The myosin motor Myo1c is required for VEGFR2 delivery to the cell surface and for angiogenic signaling.," *Am. J. Physiol. Heart Circ. Physiol.*, vol. 304, no. 5, pp. H687-96, 2013.

[515] M. C. Jones, P. T. Caswell, K. Moran-Jones, M. Roberts, S. T. Barry, A. Gampel, H. Mellor, and J. C. Norman, "VEGFR1 (Flt1) Regulates Rab4 Recycling to Control Fibronectin Polymerization and Endothelial Vessel Branching," *Traffic*, vol. 10, pp. 754–

766, 2009.

[516] S. Koch and L. Claesson-Welsh, “Signal Transduction by Vascular Endothelial Growth Factor Receptors,” *Cold Spring Harb. Perspect. Med.*, vol. 2, no. 7, p. a006502, Jul. 2012.

[517] N. Bahary, K. Goishi, C. Stuckenholz, G. Weber, J. LeBlanc, C. A. Schafer, S. S. Berman, M. Klagsbrun, and L. I. Zon, “Duplicate VegfA genes and orthologues of the KDR receptor tyrosine kinase family mediate vascular development in the zebrafish,” *Blood*, vol. 110, no. 10, pp. 3627–3636, Nov. 2007.

[518] S. Y. Park, X. Shi, J. Pang, C. Yan, and B. C. Berk, “Thioredoxin-interacting protein mediates sustained VEGFR2 signaling in endothelial cells required for angiogenesis,” *Arterioscler. Thromb. Vasc. Biol.*, vol. 33, no. 4, pp. 737–743, 2013.

[519] F. Grebien, O. Hantschel, J. Wojcik, I. Kaupe, B. Kovacic, A. M. Wyrzucki, G. D. Gish, S. Cerny-Reiterer, A. Koide, H. Beug, T. Pawson, P. Valent, S. Koide, and G. Superti-Furga, “Targeting the SH2-kinase interface in Bcr-Abl inhibits leukemogenesis,” *Cell*, vol. 147, no. 2, pp. 306–319, Oct. 2011.

[520] K. Takeshita, T. Tezuka, Y. Isozaki, E. Yamashita, M. Suzuki, M. Kim, Y. Yamanashi, T. Yamamoto, and A. Nakagawa, “Structural flexibility regulates phosphopeptide-binding activity of the tyrosine kinase binding domain of Cbl-c,” *J. Biochem.*, vol. 152, no. 5, pp. 487–495, Nov. 2012.

[521] Y. Kobashigawa, M. Sakai, M. Naito, M. Yokochi, H. Kumeta, Y. Makino, K. Ogura, S. Tanaka, and F. Inagaki, “Structural basis for the transforming activity of human cancer-related signaling adaptor protein CRK,” *Nat Struct Mol Biol*, vol. 14, no. 6, pp. 503–510, Jun. 2007.

[522] K. Brami-Cherrier, N. Gervasi, D. Arsenieva, K. Walkiewicz, M. C. Boutterin, A. Ortega, P. G. Leonard, B. Seantier, L. Gasmi, T. Bouceba, G. Kadaré, J. A. Girault, and S. T. Arold, "FAK dimerization controls its kinase-dependent functions at focal adhesions," *EMBO J.*, vol. 33, no. 4, pp. 356–370, Jan. 2014.

[523] T. D. Mulhern, G. L. Shaw, C. J. Morton, A. J. Day, and I. D. Campbell, "The SH2 domain from the tyrosine kinase Fyn in complex with a phosphotyrosyl peptide reveals insights into domain stability and binding specificity.," *Structure*, vol. 5, no. 10, pp. 1313–23, 1997.

[524] J. M. Myslinski, J. H. Clements, and S. F. Martin, "Protein–ligand interactions: Probing the energetics of a putative cation–π interaction," *Bioorg. Med. Chem. Lett.*, vol. 24, no. 14, pp. 3164–3167, Jul. 2014.

[525] R. A. Pauptit, C. A. Dennis, D. J. Derbyshire, A. L. Breeze, S. A. Weston, S. Rowsell, and G. N. Murshudov, "NMR trial models: experiences with the colicin immunity protein Im7 and the p85alpha C-terminal SH2-peptide complex.," *Acta Crystallogr D Biol Crystallogr*, vol. 57, no. Pt 10, pp. 1397–404, 2001.

[526] T. D. Bunney, D. Esposito, C. Mas-Droux, E. Lamber, R. W. Baxendale, M. Martins, A. Cole, D. Svergun, P. C. Driscoll, and M. Katan, "Structural and functional integration of the PLCγ interaction domains critical for regulatory mechanisms and signaling deregulation," *Struct. England1993)*, vol. 20, no. 12, pp. 2062–2075, Dec. 2012.

[527] T. Kaneko, H. Huang, X. Cao, X. Li, C. Li, C. Voss, S. S. Sidhu, and S. S. C. Li, "Superbinder SH2 domains act as antagonists of cell signaling," *Sci. Signal.*, vol. 5, no. 243, p. ra68-ra68, Sep. 2012.

[528] M. M. Zhou, K. S. Ravichandran, E. F. Olejniczak, A. M. Petros, R. P. Meadows, M. Sattler, J. E. Harlan, W. S. Wade, S. J. Burakoff, and S. W. Fesik, "Structure and ligand recognition of the phosphotyrosine binding domain of Shc," *Nature*, vol. 378, no. 6557, pp. 584–592, 1995.

[529] E. K. Greuber and A. M. Pendergast, "Abl Family Kinases Regulate FcgR-Mediated Phagocytosis in Murine Macrophages," *J Immunol*, vol. 189, pp. 5382–92, 2012.

[530] C.-C. Wu, S.-H. Wang, I.-I. Kuan, W.-K. Tseng, M.-F. Chen, J.-C. Wu, and Y.-L. Chen, "OxLDL upregulates caveolin-1 expression in macrophages: Role for caveolin-1 in the adhesion of oxLDL-treated macrophages to endothelium," *J. Cell. Biochem.*, vol. 107, no. 3, pp. 460–472, 2009.

[531] M. Kundu, S. K. Pathak, K. Kumawat, S. Basu, G. Chatterjee, S. Pathak, T. Noguchi, K. Takeda, H. Ichijo, C. B. F. Thien, W. Y. Langdon, and J. Basu, "A TNF- and c-Cbl-dependent FLIPS-degradation pathway and its function in Mycobacterium tuberculosis-induced macrophage apoptosis," *Nat Immunol*, vol. 10, no. 8, pp. 918–926, Aug. 2009.

[532] M.-Y. Hsieh, M. Y. Chang, Y.-J. Chen, Y. K. Li, T.-H. Chuang, G.-Y. Yu, C. H. A. Cheung, H.-C. Chen, M.-C. Maa, and T.-H. Leu, "The Inducible Nitric-oxide Synthase (iNOS)/Src Axis Mediates Toll-like Receptor 3 Tyrosine 759 Phosphorylation and Enhances Its Signal Transduction, Leading to Interferon-β Synthesis in Macrophages," *J. Biol. Chem.*, vol. 289, no. 13, pp. 9208–9220, Mar. 2014.

[533] M. Wolfson, C.-P. H. Yang, and S. B. Horwitz, "Taxol induces tyrosine phosphorylation of SHC and its association with GRB2 in murine raw 264.7 cells," *Int. J. Cancer*, vol. 70, no. 2, pp. 248–252, 1997.

[534] M. G. Coppolino, M. Krause, P. Hagendorff, D. A. Monner, W. Trimble, S. Grinstein, J. Wehland, and A. S. Sechi, “Evidence for a molecular complex consisting of Fyb/SLAP, SLP-76, Nck, VASP and WASP that links the actin cytoskeleton to Fcγ receptor signalling during phagocytosis,” *J. Cell Sci.*, vol. 114, no. 23, pp. 4307–4318, Dec. 2001.

[535] Y. Zhang, Z. W. Zhou, H. Jin, C. Hu, Z. X. He, Z. L. Yu, K. M. Ko, T. Yang, X. Zhang, S. Y. Pan, and S. F. Zhou, “Schisandrin B inhibits cell growth and induces cellular apoptosis and autophagy in mouse hepatocytes and macrophages: implications for its hepatotoxicity,” *Drug Des Devel Ther*, vol. 9, pp. 2001–2027, 2015.

[536] C.-Y. Chiang, V. Veckman, K. Limmer, and M. David, “Phospholipase Cγ-2 and Intracellular Calcium Are Required for Lipopolysaccharide-induced Toll-like Receptor 4 (TLR4) Endocytosis and Interferon Regulatory Factor 3 (IRF3) Activation,” *J. Biol. Chem.*, vol. 287, no. 6, pp. 3704–3709, Feb. 2012.

[537] T. Heckel, C. Czupalla, A. I. Expirto Santo, M. Anitei, M. Arantzazu Sanchez-Fernandez, K. Mosch, E. Krause, and B. Hoflack, “Src-dependent repression of ARF6 is required to maintain podosome-rich sealing zones in bone-digesting osteoclasts,” *Proc. Natl. Acad. Sci. U. S. A.*, vol. 106, no. 5, pp. 1451–1456, Feb. 2009.

[538] V. A. McGuire, A. Gray, C. E. Monk, S. G. Santos, K. Lee, A. Aubareda, J. Crowe, N. Ronkina, J. Schwermann, I. H. Batty, N. R. Leslie, J. L. E. Dean, S. J. O’Keefe, M. Boothby, M. Gaestel, and J. S. C. Arthur, “Cross Talk between the Akt and p38α Pathways in Macrophages Downstream of Toll-Like Receptor Signaling,” *Mol. Cell. Biol.* , vol. 33, no. 21, pp. 4152–4165, Nov. 2013.

[539] Y. Liu, W. Su, S. Wang, and P. Li, “Naringin inhibits chemokine production in an LPS‐induced RAW 264.7 macrophage cell line,” *Mol Med Rep*, vol. 6, pp. 1343–50,

2012.

[540] S. Tateya, N. O. Rizzo, P. Handa, A. M. Cheng, V. Morgan-Stevenson, G. Daum, A. W. Clowes, G. J. Morton, M. W. Schwartz, and F. Kim, "Endothelial NO/cGMP/VASP Signaling Attenuates Kupffer Cell Activation and Hepatic Insulin Resistance Induced by High-Fat Feeding," *Diabetes*, vol. 60, no. 11, pp. 2792–2801, Nov. 2011.

[541] S. Muro, X. Cui, C. Gajewski, J.-C. Murciano, V. R. Muzykantov, and M. Koval, "Slow intracellular trafficking of catalase nanoparticles targeted to ICAM-1 protects endothelial cells from oxidative stress," *Am. J. Physiol. - Cell Physiol.*, vol. 285, no. 5, pp. C1339–C1347, Oct. 2003.

[542] S. Muro, C. Gajewski, M. Koval, and V. R. Muzykantov, "ICAM-1 recycling in endothelial cells: a novel pathway for sustained intracellular delivery and prolonged effects of drugs," *Blood*, vol. 105, no. 2, pp. 650–658, Sep. 2004.

[543] W. Greene, W. Zhang, M. He, C. Witt, F. Ye, and S.-J. Gao, "The Ubiquitin/Proteasome System Mediates Entry and Endosomal Trafficking of Kaposi's Sarcoma-Associated Herpesvirus in Endothelial Cells," *PLoS Pathog*, vol. 8, no. 5, p. e1002703, May 2012.

[544] M. G. Lampugnani, F. Orsenigo, M. C. Gagliani, C. Tacchetti, and E. Dejana, "Vascular endothelial cadherin controls VEGFR-2 internalization and signaling from intracellular compartments," *J. Cell Biol.*, vol. 174, no. 4, pp. 593–604, Aug. 2006.

[545] L. Danglot, M. Chaineau, M. Dahan, M.-C. Gendron, N. Boggetto, F. Perez, and T. Galli, "Role of TI-VAMP and CD82 in EGFR cell-surface dynamics and signaling," *J. Cell Sci.*, vol. 123, no. 5, pp. 723–735, Feb. 2010.

[546] C. S. Monast, C. M. Furcht, and M. J. Lazzara, "Computational Analysis of the

Regulation of EGFR by Protein Tyrosine Phosphatases," *Biophys. J.*, vol. 102, no. 9, pp. 2012–2021, May 2012.

[547] B. S. Hendriks, L. K. Opresko, H. S. Wiley, H. E. R. O. Effects, and D. Lauffenburger, "Coregulation of Epidermal Growth Factor Receptor / Human Epidermal Growth Factor Receptor 2 (HER2) Levels and Locations : Quantitative Analysis of HER2 Overexpression Effects Coregulation of Epidermal Growth Factor Receptor / Human Epidermal Growth Fact," *Cancer R*, vol. 2, no. 63, pp. 1130–1137, 2003.

APPENDIX A: SUPPLEMENTARY ADAPTER MODELING METHODS

A.1 Computational methods

A.1.1 Obtaining adapter protein initial concentrations.

Adapter initial concentrations in human umbilical vein endothelial cells (HUVECs) were obtained from Western blot data (Appendix A, Table A.1). I quantified the adapter intensity, and the intensity of a separate protein that had a known concentration, with ImageJ. The background intensities were measured and subtracted from the adapter known protein intensities. I normalized the adapter and known protein intensities to their respective control loading proteins. I calculated the initial adapter concentration as follows:

$$\frac{[\text{adapter}]_0}{[\text{protein}]_0} = \frac{I_{\text{adapter-background}}/I_{\text{control-background}}}{I_{\text{protein-background}}/I_{\text{control-background}}} \tag{A.1}$$

where $[\text{adapter}]_0$ is the initial adapter concentration, $[\text{protein}]_0$ is the known protein concentration, and I is the intensity. This is a standard technique for initializing and validating computational models [159], [408]–[410].

A.1.2 Obtaining receptor-adapter interaction rates.

Rates for VEGFR-adapter interactions are obtained from isothermal titration calorimetry or surface plasmon resonance experiments (Appendix A, Table A.2). If VEGFR-adapter specific interaction kinetics are unavailable, I use the kinetics between the adapter SH2 domain and a phosphorylated tyrosine kinase fragment. I assume adapters bind all VEGFR tyrosine sites with the same rate. Forward rates are implemented in $\text{cell}/(\text{molecule}\cdot\text{s})$, using a conversion factor of $1(\text{M}\cdot\text{s})^{-1} = 1.66\cdot10^{-12}\,\text{cell}/(\text{molecule}\cdot\text{s})$, based on an assumed 1 pL cell volume.

A.1.3 Modeling adapter phosphorylation and dephosphorylation.

I assume all adapter phosphorylation rates (kp) are 0.01 s^{-1}, so adapter phosphorylation is only dependent on VEGFR interaction kinetics. To account for adapter dephosphorylation, I model phosphatase binding to phosphorylated adapters and subsequent adapter dephosphorylation. I assume all adapters are dephosphorylated by a generalized protein tyrosine phosphatase non-receptor type (PTPN) phosphatase [411]. Furthermore, I assume that the PTPN

has the same binding kinetics for every adapter, and that the PTPN concentration is sufficiently high to not limit adapter dephosphorylation (Appendix A, Table A.2).

A.1.4 Adapter contribution to overall cell response.

The contribution of each adapter to proliferation and migration were obtained from previous experimental studies (Appendix A, Table A.3). In these experiments, each adapter was inhibited individually, and the percent of endothelial cell proliferation or migration inhibited in response was quantified. I assume for all experiments that the VEGF and drug treatments saturated all cells present. To calculate overall predicted cell response in my simulations, I weigh and sum the response contribution of each adapter as follows:

$$\boldsymbol{R_{cell}} = \sum_{\boldsymbol{i}=1}^{12} \boldsymbol{w_{R,i} P_i} \tag{A.2}$$

where $\boldsymbol{R_{cell}}$ is the overall cell response (proliferation or migration), $\boldsymbol{w_{R,i}}$ is the amount of regulation adapter $\boldsymbol{i}$ gives to that response, and P_i is the phosphorylation of adapter $\boldsymbol{i}$. The adapter weights are determined through by solving the linear problem

$$\boldsymbol{S_p w_R} = \boldsymbol{e_R} \tag{A.3}$$

Here, $\boldsymbol{w_R}$ is a vector containing the weights each adapter contributes to the cell response $\boldsymbol{R_{cell}}$. $\boldsymbol{e_R}$ is a vector containing the experimental cell responses, relative to the no inhibition case (Appendix A, Table A.3). $\boldsymbol{S_p}$ is a matrix containing the model predicted phosphorylated adapter integrated responses, for each inhibition scheme. Lastly, the weights for proliferation and migration were normalized such that the migration weights summed to one. As these experimental drug treatments look at VEGF signaling in HUVECs as a whole, i.e. signaling contributions from VEGFR1 and VEGFR2, I use both receptors in the drug treatment simulations.

A.1.5 Goodness of fit tests.

Models were validated against published empirical data [412]–[416] by calculating the chi-squared value $\left(\chi^2\right)$ (Appendix A, Fig A.1). χ^2 is calculated as follows:

$$\chi^2 = \sum_{i=1}^{N} \frac{\left(y_i - f_i\right)^2}{f_i} \tag{A.4}$$

where y_i is the empirical measurement at index i, f_i is the simulated value, and N is the total number of empirical measurements. Goodness-of-fit was determined by testing the hypothesis that model predicted adapter phosphorylation differs from experimental adapter phosphorylation at the 0.05 significance level. The hypothesis is rejected, which is interpreted as the model accurately predicting experimental adapter phosphorylation, based on the degrees of freedom (df): $\chi^2 < 0.103$ for df = 2 (Appendix A, Fig A.1F), $\chi^2 < 0.352$ for df = 3 (Appendix A, Fig A.1E), $\chi^2 < 0.711$ for df = 4 (Fig 3.3B-C; Appendix A, Fig A.1A-B, Fig A.1D), $\chi^2 < 1.145$ for df = 5 (Fig 3.3A), and $\chi^2 < 2.167$ for df = 7 (Appendix A, Fig A.1C) [253].

A.1.6 Modeling adapters binding specific VEGFR tyrosine sites.

I assume that multiple adapters can bind a single receptor if the combined size of the adapters is smaller than the available space between tyrosine sites (i.e. the adapters have enough room to bind). To determine what adapter-tyrosine site distributions are possible, I use three pieces of information: (1) the specific tyrosine sites each adapter binds (Appendix A, Table A.4), (2) the size of each adapter (Appendix A, Table A.5), and (3) the space between each tyrosine site. These measurements were performed as follows:

A.1.7 Determining adapter sizes.

Adapter protein sizes were determined by measuring their crystal structures (Appendix A, Table A.5). To determine the length each adapter blocks on VEGFR1, the intracellular domain of VEGFR1 was assumed to be 1-dimensional (in the y-direction). Adapter protein crystal structures were then oriented such that they bound, via their SH2 domain, to the 1-dimensional VEGFR1. The largest y-direction size of the crystal structure was then measured. I further assume tyrosine sites are bound by the center of adapter proteins, such that half the adapter protein blocks VEGFR1 in the +y-direction and the other half blocks VEGFR1 in the –y-direction. For example, if an adapter protein is 30 Å, it blocks all tyrosine sites within 15 Å of the tyrosine site it is bound to (Fig 3.1).

A.1.8 Determining distance between VEGFR1 tyrosine sites.

To determine the distance between VEGFR tyrosine sites, I measured the average distance between amino acids in the VEGFRs tyrosine kinase domain crystal structure (Fig 3.1A-B). I oriented the tyrosine kinase domain crystal structure to match my 1-dimensional VEGFR assumption; if the crystal structure contained multiple kinase domains, the tyrosine binding sites fall on a vertical line. The tyrosine kinase domain was measured, and that length was divided by the number of amino acids within the crystal structure to give the distance between individual amino acids. The distance between individual amino acids is multiplied by the number of amino acids between VEGFR tyrosine sites to give the distance between VEGFR tyrosine sites. For example, the distance between individual amino acids in VEGFR1 was measured as 0.171 Å/amino acid, so the distance between tyrosine sites Tyr^{1242} and Tyr^{1333} is 15.6 Å.

A.1.9 Metrics for model analyses.

Cell response was predicted by quantifying two metrics obtained from model simulations: integrated response and amplitude. The integrated response is the area under the phosphorylation versus time curve, while phosphorylation amplitude is simply the peak phosphorylation an adapter reaches [375], [376]. These metrics are commonly used to quanitfy total signal propagation and signal propagation speed, respectively [375]. For example, Oyarzún *et. al.* showed that integrated EGFR responses scales linearly with applied ligand stimulus, suggesting that total signal propagation linearly increases with ligand concentration [417]. Likewise, Schilling *et. al.* found that CFU-E cell proliferation is directly correlated with integrated ERK response [376]. Conversely, Kumar *et. al.* found that quantifying these metrics predicts the cell response itself; the Akt phosphorylation amplitude directs apoptosis, whereas Akt integrated response directs proliferation [375]. Therefore, integrated response and phosphorylation amplitude of signaling molecules allow the cell response to be predicted.

To compare a single adapter binding VEGFR1 in a tyrosine site independent manner to multiple adapters binding specific VEGFR1 tyrosine sites, I use the fractional change metric [418], given by:

$$1+\frac{(x_2-x_1)}{x_1} \tag{A.5}$$

where x_1 is the value of interest (adapter activation or cell response) with a single adapter binding VEGFR1, and x_2 is the corresponding value with multiple adapters binding specific VEGFR1 tyrosine sites. A fractional change of 1 means the value is the same for both adapter binding motifs. A fractional change > 1 indicates the value is greater given site specific adapter binding, whereas a fractional change < 1 indicates the comparison value is smaller in the second model.

A.2 Experimental Methods

A.2.1 Quantifying protein phosphorylation.

RAW macrophages were seeded into a 96-well plate and grown to ~80% confluence. The cells were then serum starved overnight with DMEM supplemented with 0.5% FBS and 1% PS, and pretreated with any inhibitor overnight: 100 nM Wortmannin (Anti-PI3K, IC_{50} = 3 nM), 10 µM U73122 (Anti-PLC_γ, IC_{50} = 1 µM), or 6 µM Imatinib Mesylate (Anti-Abl, IC_{50} = 0.6 µM). Cells were then stimulated with VEGF-A_{164} (50 ng/mL) for various time periods, and stimulation was stopped by washing the cells with ice cold TBS. Cells were fixed, quenched, blocked, and incubated at 4^{o}C overnight with primary antibodies specific for phosphorylated $Tyr^{467/199}$ PI3K, total PI3K, phosphorylated Tyr^{783} PLC_γ, total PLC_γ, phosphorylated Tyr^{245} Abl, or total Abl. Corresponding HRP-conjugated secondary antibodies were added to the cells, treated with substrate, and absorbance in each well was read at 450 nm to measure protein concentration. Experiments were independently carried out in triplicate. Data is represented as the mean phosphorylated over mean total protein (p/t) ratio ± standard error of the mean (SEM) for each treatment type and treatment time; here SEM is the sum of the phosphorylated and total protein SEMs. The (p/t) ratio given inhibitor treatment specific to the protein of interest was subtracted as background for each treatment time. For example, the PI3K (p/t) ratio given 30 minutes of VEGF stimulation is subtracted by the PI3K (p/t) ratio given 30 minutes of VEGF + Wortmannin stimulation.

A.2.2 Cell migration assays.

RAWs were seeded into a 12-well plate and grown to ~90% confluence. The cells were then serum starved overnight. The monolayer was then scratched with a 100 µL pipette tip and

washed once with PBS to remove floating cells. After the scratch, wells were treated with 750 µL of the serum starved growth factor media containing VEGF-A_{164} (50 ng/mL), 10 µM Wortmannin, 10 µM U73122, 10 µM Imatinib Mesylate, or a combination of VEGF-A_{164} and an inhibitor. Images of the wounded cell monolayer were taken using a microscope at 0 h and 24 h after scratching. All experiments were independently carried out in triplicate. Cell migration was quantified as the number of cells contained within the total gap area relative to the number of cells immediately after the scratch. Cells were counted within the wound margin using ImageJ.

A.2.3 Cell proliferation assays.

RAWs were seeded into a 96-well plate and grown to ~50% confluence. The cells were then serum starved overnight. Culture medium was removed and cells were stimulated with fresh serum starved media containing VEGF-A_{164} (50 ng/mL), 10 µM Wortmannin, 10 µM U73122, 10 µM Imatinib Mesylate, or a combination of VEGF-A_{164} and an inhibitor for 24 h. MTT was added to each well and incubated at 37^{o}C for 4 hours. SDS-HCl solution was added to each well and incubated for another 4 hours at 37^{o}C. The solution in each well was mixed with a pipette, and absorbance was read at 570 nm. All experiments were independently carried out in triplicate.

A.2.4 Cell harvest for qFlow cytometry.

RAWs were harvested when they reach 80- 90% confluency. Cellstripper^{TM} (Millipore, Billerica, MA), a non-enzymatic cell dissociation solution was applied to RAWs and incubated for 4-7 minutes at 37°C/5% CO_2. Culture flasks were then tapped gently on the side to dislodge cell adherence. Dissociated RAWs were re-suspended in stain buffer (PBS, bovine serum albumin, sodium azide)[419], [420] and centrifuged at 500 ×g for 5 minutes. Supernatant was removed, and RAWs were re-suspended to a final concentration of 4 x 10^6 cells/mL in stain buffer.

A.2.5 Cell staining for flow cytometry.

Cells were aliquoted at 25 µL (~1 x 10^5 cells) to 5 ml polystyrene round-bottom tubes (BD Biosciences, New Jersey). Phycoerythrin (PE)-conjugated monoclonal antibodies were added to each tube at the optimal concentrations: 14 µg/mL for VEGFR1 and VEGFR2, determined by titration (Appendix A, Fig A.3B). A PE fluorophore is used as the basis of the

quantitative fluorescence measurements because its high extinction coefficient reduces error due to photobleaching, its fluorescence is not quenched by common biomolecules (e.g., antibodies), its fluorescence is independent of pH, and its size minimizes the possibility of multiple fluorophores conjugated to an antibody [421], [422]. Samples were incubated in dark for 40 minutes and kept on ice. Samples were then centrifuged at 500 ×g with 4 mL stain buffer for 4 minutes, and supernatant was removed. This washing step was repeated twice. Washed samples were resuspended in 200 – 300 µL stain buffer. For each culture flask, PE-conjugated antibodies were not added in 1 – 2 samples as controls, which undergo the same procedures as the labeled samples. Those unlabeled samples were used as control to eliminate cell auto-fluorescence and other background noises.

A.2.6 Quantitative flow cytometry**.**

The precision and accuracy of qFlow cytometry profiling has been rigorously tested [423]–[426]. Flow cytometry was performed on a LSR Fortessa (BD) Flow cytometer; BD FACSDIVA software was used for data acquisition, and FlowJo (TreeStar) software was used for data analysis. Sytox Blue (Invitrogen), a live/dead cell stain, was added to each sample at a final concentration of 5 µg/mL prior to placement in the flow cytometer. Sytox Blue was excited with a violet laser (407 nm) and its emission was collected using a 450/50 bandpass filter. Histograms of Sytox Blue fluorescence were plotted to identify the live cell population. PE was excited with a yellow-green laser (561 nm) and its emission was collected using a 582/15 bandpass filter. Cells exhibiting little to no Sytox Blue fluorescence were gated as live cells. These gated cells were examined in a plot of forward scatter area (FSC-A) versus side scatter area (SSC-A) to gate the single-cell population. Next, 8,000 - 10,000 live single cells were collected from each tube based on the gating. For each receptor, 2 – 4 biological replicates were collected from 3 independent RAW cultures.

A.2.7 Statistical analysis: ensemble-averaged data**.**

Quantibrite PE beads (BD) were collected and analyzed under the same compensation and voltage settings as cell fluorescence data. Quantibrite PE beads comprise a combination of polystyrene beads conjugated with different density of PE molecules: low (474 PE molecules/bead), medium-low (5,359 PE molecules/bead), medium-high (23,843 PE

molecules/bead), and high (62,336 PE molecules/bead). A calibration curve that translated PE geometric mean to the number of bound molecules was determined using linear regression: $y = mx+b$, where $x=\log_{10}{}^{\text{Number of PE molecules per bead}}$, y represented $\log_{10}{}^{\text{PE geometric mean per bead}}$, and m and b represented the slope and intercept of the linear regression, respectively. Receptor levels for VEGFR1 and VEGFR2 were calculated as described previously [217].

A.3 Figures and Tables

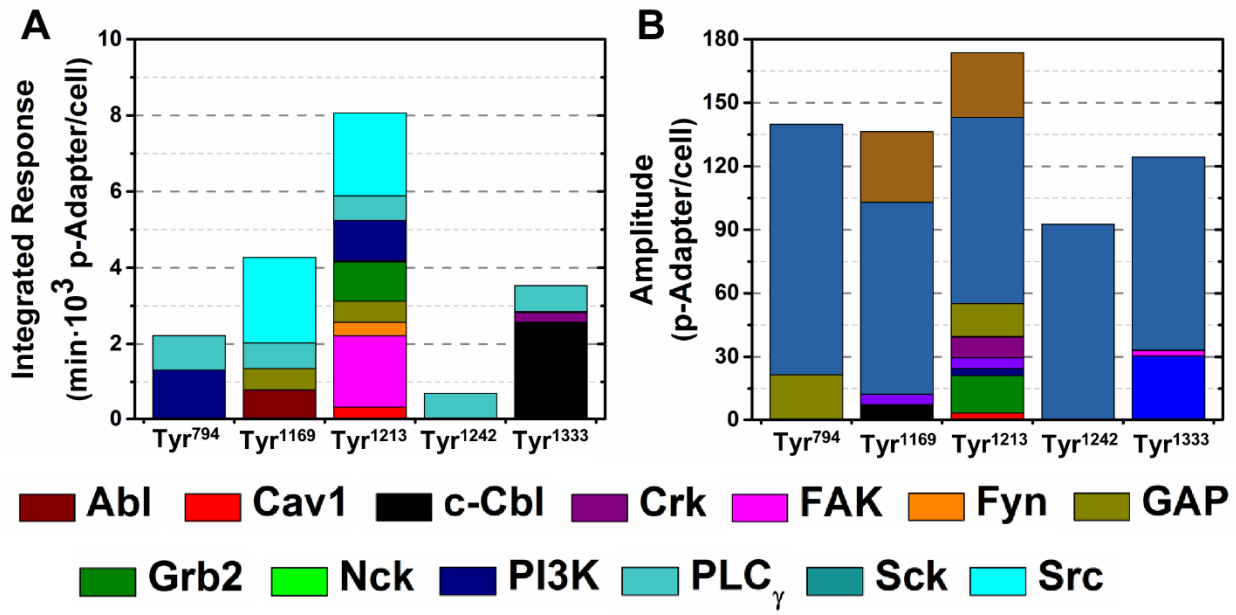

Fig A.1: PLC and PI3K are preferentially activated at Tyr^{794} on VEGFR1.

The (A) integrated responses and (B) phosphorylation amplitudes of all adapters were quantified at each specific VEGFR1 tyrosine site at 60 minutes following VEGF stimulus.

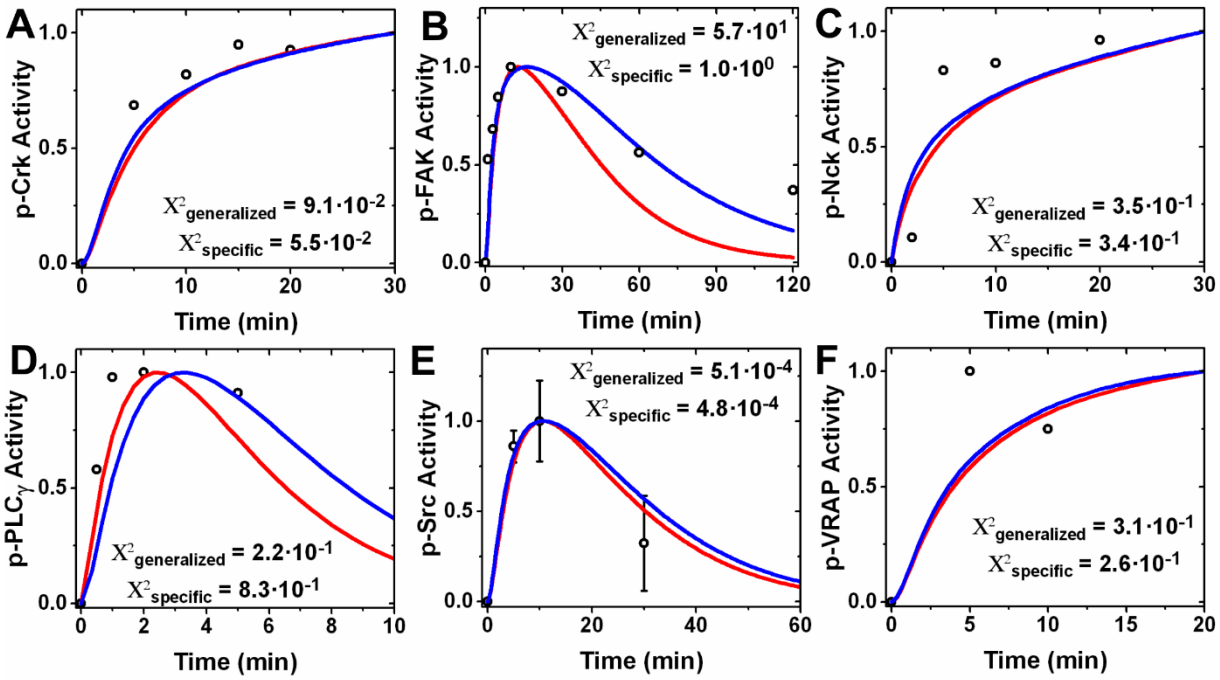

Fig A.2: Both nonspecific and specific VEGFR1 site models predict relative adapter phosphorylation.

Fitting model predicted adapter phosphorylation versus time to relative adapter phosphorylation through both VEGFR1 and VEGFR2. Experimental data was normalized so the maximum adapter phosphorylation is 1. Adapter phosphorylation was simulated for the same time length given by experimental measurements, and the maximum predicted adapter phosphorylation was normalized to 1. Model accuracy is tested with the X^2 goodness-of-fit test [253]. References for experimental data are: (A) Crk [412], (B) Nck [412], (C) FAK [413], (D) PLC_γ [414], (E) Src [415], and (F) VRAP [416].

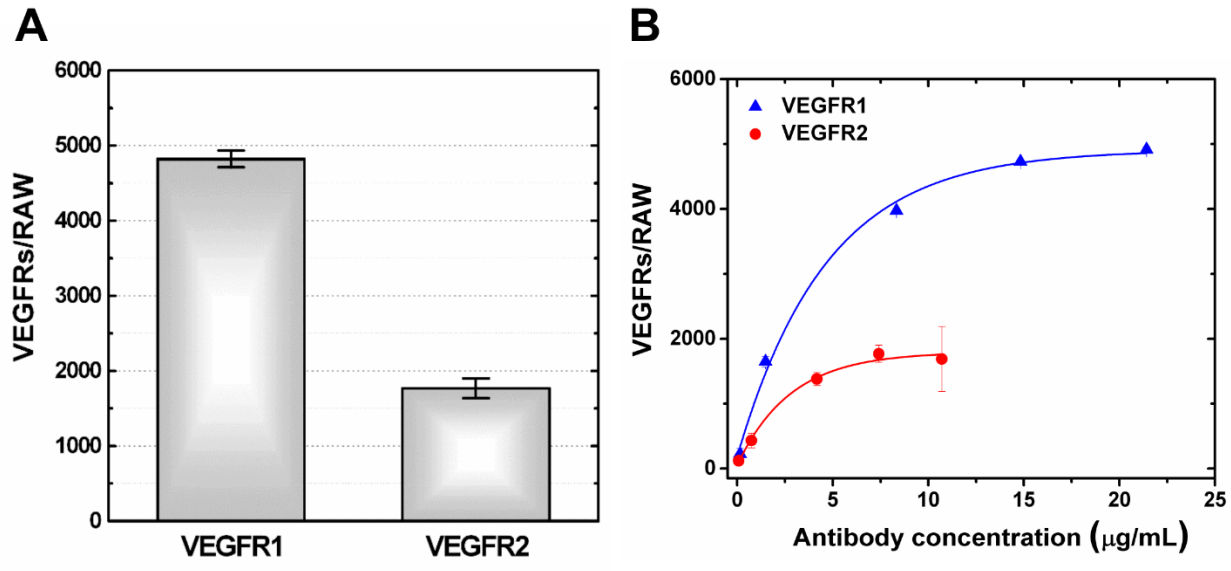

Fig A.3: VEGFR1 and VEGFR2 quantification on RAWs.

(A) Membrane VEGFR1 and VEGFR2 levels on RAWs were measured by quantitative flow cytometry. Data is represented as mean ± standard error of the mean. (B) Saturation curves of VEGFR1 and VEGFR2 antibodies on RAWs show that all receptors are labeled, ensuring accurate quantification.

Table A.1: Model protein concentrations.

	Protein	Model concentration (molecules/cell)	Experimental concentration (molecules/cell)	Reference Protein	Cell Line	Cell Conditions
	VEGFR1	$9.90 \cdot 10^2$	990 [328]	-	HUVEC	Growth media (EGM-2)
	VEGFR2	$1.89 \cdot 10^3$	1890 [328]	-		
	PTPN	$8.00 \cdot 10^4$	Estimated	-	-	-
Both VEGFRs	Abl	$1.50 \cdot 10^3$	$2.11 \cdot 10^3$ [412] $1.20 \cdot 10^3$ [427] $1.18 \cdot 10^3$ [428]	VEGFR2 VEGFR2 Cav1	HUVEC	Growth media (M199) 24 h serum starvation Growth media (EGM-2)
	Cav1	$2.41 \cdot 10^3$	$2.02 \cdot 10^3$ [429] $2.80 \cdot 10^3$ [430]	VEGFR2 VEGFR2		Growth media Growth media (EBM)
	c-Cbl	$1.19 \cdot 10^3$	$1.19 \cdot 10^3$ [431]	VEGFR2		Growth media
	Crk	$1.11 \cdot 10^3$	$1.48 \cdot 10^3$ [412] $7.42 \cdot 10^2$ [432]	VEGFR2 FAK		Growth media (M199) 2 h serum starvation
	FAK	$1.38 \cdot 10^3$	$1.76 \cdot 10^3$ [433] $1.53 \cdot 10^3$ [434] $8.43 \cdot 10^2$ [435]	VEGFR2 VEGFR2 VEGFR2		2 h serum starvation 6 h serum starvation 24 h serum starvation
	Fyn	$8.97 \cdot 10^2$	$9.96 \cdot 10^2$ [436] $7.98 \cdot 10^2$ [432]	VEGFR2 FAK		24 h serum starvation 2 h serum starvation
	GAP	$1.26 \cdot 10^3$	$1.32 \cdot 10^3$ [437] $1.09 \cdot 10^3$ [438] $1.38 \cdot 10^3$ [439]	VEGFR2 VEGFR2 VEGFR2		24 h serum starvation Overnight serum starvation Overnight serum starvation
	Grb2	$7.10 \cdot 10^2$	$9.53 \cdot 10^2$ [412] $4.66 \cdot 10^2$ [440]	VEGFR2 ALK1[a]		Growth media (M199) Growth media (EBM-2)
	Nck	$7.07 \cdot 10^3$	$3.23 \cdot 10^3$ [441] $1.09 \cdot 10^4$ [442]	PLCγ VEGFR2		6 h serum starvation 18 h serum starvation
	PI3K[a]	$8.34 \cdot 10^2$	$9.33 \cdot 10^2$ [443] $6.07 \cdot 10^2$ [444] $9.63 \cdot 10^2$ [445]	VEGFR2 Src VEGFR2		24 h serum starvation Growth media (DMEM) Growth media (M199)
	PLCγ	$1.10 \cdot 10^3$	$1.03 \cdot 10^3$ [446] $1.01 \cdot 10^3$ [437] $1.25 \cdot 10^3$ [414]	VEGFR2 VEGFR2 GAP		16 h serum starvation 24 h serum starvation Overnight serum starvation
	Src	$1.62 \cdot 10^3$	$1.99 \cdot 10^3$ [433] $1.48 \cdot 10^3$ [434] $1.38 \cdot 10^3$ [447]	VEGFR2 VEGFR2 VEGFR2		2 h serum starvation 6 h serum starvation Overnight serum starvation
	Sck	$1.35 \cdot 10^3$	$1.35 \cdot 10^3$ [448]	VEGFR2		1 h serum starvation
VEGFR2 Only	Shb	$2.14 \cdot 10^3$	$2.14 \cdot 10^3$ [449], [450][b]	GAP		20 min serum starvation
	Shc	$1.84 \cdot 10^3$	$1.40 \cdot 10^3$ [451] $2.28 \cdot 10^3$ [452]	GAP VEGFR2		Growth media Serum starvation
	VRAP	$9.01 \cdot 10^3$	$9.01 \cdot 10^2$ [453]	PLCγ		16 h serum starvation

Adapter, receptor, and phosphatase concentrations in HUVECs were obtained from the references provided. Adapter model concentrations are the mean of the experimental concentrations. Reference protein indicates the known protein concentration used to determine the adapter concentration. In cases where adapters are the reference protein, the model concentration was used as the known concentration. Cell line and conditions used for the experiment are given.

[a]PI3K is modeled as the p85α domain
[b]ALK1 concentration in HUVECs was quantified by flow cytometry in [440].
[c]To calculate the Shb concentration in HUVECs, the Shb/GAP ratio is assumed to be the same in HUVEC and Jurkat cells.

Table A.2: Computational model kinetics.

	Receptor	VEGF-receptor forward rate (cell/molecule·s)	VEGF-receptor reverse rate (1/s)	Receptor phosphorylation rate
	VEGFR1	$1.81 \cdot 10^{-5}$	$1.00 \cdot 10^{-3}$ [178]	Immediate[a]
	VEGFR2	$6.02 \cdot 10^{-6}$	$1.00 \cdot 10^{-3}$ [178]	Immediate[a]
	Protein	Adapter-receptor forward rate (cell/molecule·s)	Adapter-receptor reverse rate (1/s)	Adapter phosphorylation rate (1/s)
Both VEGFRs	Abl	$1.06 \cdot 10^{-7}$	$2.27 \cdot 10^{-3}$ [454]	0.01[c]
	Cav1	$2.47 \cdot 10^{-8}$	$1.76 \cdot 10^{-3}$ [455]	
	c-Cbl	$8.30 \cdot 10^{-7}$	$5.00 \cdot 10^{-3}$ [456]	
	Crk	$4.65 \cdot 10^{-8}$	$3.10 \cdot 10^{-3}$ [457]	
	FAK	$5.50 \cdot 10^{-7}$	$1.00 \cdot 10^{-2}$ [458]	
	Fyn	$1.28 \cdot 10^{-7}$	$1.00 \cdot 10^{-2}$ [459]	
	GAP	$1.66 \cdot 10^{-6}$	$2.00 \cdot 10^{-1}$ [327]	
	Grb2	$1.66 \cdot 10^{-5}$	$5.50 \cdot 10^{-1}$ [327]	
	Nck	$4.98 \cdot 10^{-8}$	$8.10 \cdot 10^{-1}$ [460]	
	PI3K	$1.50 \cdot 10^{-6}$	$2.00 \cdot 10^{-2}$ [158]	
	PLCɣ	$9.96 \cdot 10^{-5}$	$2.00 \cdot 10^{-2}$ [255]	
	Src	$5.48 \cdot 10^{-7}$	$1.20 \cdot 10^{-3}$ [461]	
	Sck	$3.32 \cdot 10^{-9}$	$1.00 \cdot 10^{-1}$ [b]	
VEGFR2	Shb	$3.32 \cdot 10^{-9}$	$1.00 \cdot 10^{-1}$ [b]	
	Shc	$3.32 \cdot 10^{-9}$	$1.00 \cdot 10^{-1}$ [462]	
	VRAP	$1.00 \cdot 10^{-7}$	$1.00 \cdot 10^{-2}$ [453]	
All Adapters	Protein	Adapter-PTPN forward rate (cell/molecule·s)	Adapter-PTPN reverse rate (1/s)	PTPN dephosphorylation rate
	PTPN	$8.10 \cdot 10^{-6}$	1.63 [159]	3.39 [159]

Adapter-receptor interaction rates were derived from the references provided. Forward and reverse rates for each adapter are from the same reference. Adapter-receptor interaction rates are assumed to be the same for VEGFR1 and VEGFR2.

[a]VEGFRs are assumed to phosphorylate immediately upon VEGF binding.
[b]Due to limited information, binding rates of Shb and Sck to VEGFRs are assumed to be the same as Shc, as these adapters are part of the same family.
[c]Phosphorylation rate is assumed the same for all adapters.

Table A.3: Adapter contribution to cell proliferation and migration with VEGF treatment.

Adapter	% Proliferation Inhibition	Inhibitor	% Migration Inhibition	Inhibitor	Inhibitor IC_{50}	Model Proliferation Weight	Model Migration Weight
Abl	59% [463] (HMVEC)	STI571 10 μM	10% [463] (HMVEC)	STI571 10 μM	0.8 μM [464]	$1.8 \cdot 10^{-1}$	$-8.0 \cdot 10^{-2}$
Cav1	-42% [465] (HUVEC)	Cav1 transfection	46% [466] (HUVEC)	siRNA	-	$-6.5 \cdot 10^{-2}$	$3.3 \cdot 10^{-1}$
c-Cbl	Negligible[a]	-	Negligible[a]	-	-	0	0
Crk	Negligible[a]	-	60% [467] (HUVEC)	Mutation	-	0	$3.1 \cdot 10^{-1}$
FAK	< 1% [468] (HUVEC)	siRNA	30% [469] (HUVEC)	siRNA	-	0	$1.5 \cdot 10^{-2}$
Fyn	15% [470] (HRMEC)	siRNA	-25% [470] (HRMEC)	siRNA	-	$1.4 \cdot 10^{-2}$	$-2.1 \cdot 10^{-1}$
GAP	63% [471] (HUVEC)	Fasudil 10 μM	50% [471] (HUVEC)	Fasudil 10 μM	1.2 μM [472]	$2.1 \cdot 10^{-2}$	$1.2 \cdot 10^{-2}$
Grb2	40% [473] (HUVEC)	C90 0.3 μM	47% [473] (HUVEC)	C90 0.3 μM	150 nM [474]	$1.3 \cdot 10^{-1}$	$1.1 \cdot 10^{-1}$
Nck	Negligible[a]	-	40% [475] (HUVEC)	shRNA	-	0	$5.1 \cdot 10^{-2}$
PI3K	28% [476] (HUVEC)	LY294002 10 μM	48% [477] (HUVEC)	LY294002 10 μM	0.5 μM [478]	$1.1 \cdot 10^{-1}$	$1.7 \cdot 10^{-1}$
PLC_{γ}	50% [479] (HUVEC)	U73122 10 μM	65% [477] (HUVEC)	U73122 6 μM	0.8 μM [480]	$1.9 \cdot 10^{-1}$	$2.5 \cdot 10^{-1}$
Sck	Negligible[a]	-	Negligible[a]	-	-	0	0
Shb	Negligible[a]	-	Negligible[a]	-	-	0	0
Shc	Negligible [481]	shRNA	Negligible [481]	shRNA	-	0	0
Src	29% [482] (HUVEC)	M475271 3 μM	68% [482] (HUVEC)	M475271 3 μM	25 nM [483]	$5.8 \cdot 10^{-2}$	$1.7 \cdot 10^{-1}$
VRAP	-9% [416] (HUVEC)	siRNA	44% [416] (HUVEC)	siRNA	-	$-1.4 \cdot 10^{-1}$	$1.6 \cdot 10^{-1}$

Percent decrease in EC proliferation and migration when each adapter is inhibited, given by the provided references. Negative percentages indicate an anti-proliferative or anti-migratory role. The cell type, inhibitor concentration, and inhibitor IC_{50} are given. Proliferation and migration weights used to correlate adapter phosphorylation to cell response are given for each adapter. I assume that only c-Cbl phosphorylation contributes to the activation of cell degradation.

HUVEC – Human umbilical vein endothelial cell; HMVEC – Human microvascular endothelial cell;
HRMEC – Human retinal microvascular endothelial cell;
[a]Not identified, I assume the adapter contribution is negligible to other adapters

Table A.4: Adapter-VEGFR tyrosine site interaction references.

VEGFR1 Interaction	Reference	VEGFR1 Interaction	Reference	VEGFR2 Interaction	Reference	VEGFR2 Interaction	Reference
Y794-PLC$_\gamma$	[484]	Y1213-Cav1	[485], [486][g]	Y801-PLC$_\gamma$	[484]	Y1175-Abl	[487]
Y794-PI3K	[488]	Y1213-FAK	[486], [489][h]	Y801-PI3K	[490]	Y1175-Shc	[158], [491], [492][i]
Y1169-PLC$_\gamma$	[493]	Y1242-PLC$_\gamma$	[484]	Y951-PLC$_\gamma$	[488], [494]	Y1175-Shb	[492]
Y1169-GAP	[495], [496][a]	Y1333-PLC$_\gamma$	[497]	Y951-VRAP	[416]	Y1175-Sck	[498]
Y1169-Src	[495], [496][b]	Y1333-Nck	[497], [499]	Y1008-PLC$_\gamma$	[500]	Y1214-PI3K	[499], [501][j]
Y1169-Abl	[495], [496], [502][c]	Y1333-Crk	[497]	Y1059-PLC$_\gamma$	[157], [503]	Y1214-Fyn	[486]
Y1169-Sck	[498], [504][d]	Y1333-c-Cbl	[505], [506]	Y1059-Src	[507]	Y1214-Nck	[486]
Y1213-PLC$_\gamma$	[497]	-	-	Y1059-GAP	[507]	Y1214-FAK	[508]
Y1213-PI3K	[509]	-	-	Y1059-c-Cbl	[507], [510]	Y1214-Crk	[467], [486][k]
Y1213-Fyn	[486]	-	-	Y1175-PLC$_\gamma$	[487], [511]	Y1214-Src	[486], [507]
Y1213-Nck	[499]	-	-	Y1175-Src	[507]	Y1214-GAP	[512]
Y1213-Src	[486], [513][e]	-	-	Y1175-PI3K	[490]	Y1214-Cav1	[512], [514]
Y1213-GAP	[486], [515][f]	-	-	Y1175-Grb2	[516]	Y1305-FAK	[508], [517]
Y1213-Grb2	[497]	-	-	Y1175-GAP	[359], [518]	-	-

References indicate were the adapter-VEGFR tyrosine site interaction was derived. These interactions are either empirically observed, or provide information leading to an assumed interaction. For example, showing an interaction between an adapter and an amino acid chain that correlates to a VEGFR tyrosine site. Several adapter-VEGFR interactions were also empirically observed without specifying the specific tyrosine site; assumptions for these tyrosine sites are given in the footnotes, with all references relating to the assumption in the table.

[a] Assumed based on GAP interaction at VEGFR2-Y1175, and VEGFR1-Y1169 homology with VEGFR2-Y1175.
[b] Assumed based on Src interaction at VEGFR2-Y1175, and VEGFR1-Y1169 homology with VEGFR2-Y1175.
[c] Assumed based on Abl interaction at VEGFR2-Y1175, and VEGFR1-Y1169 homology with VEGFR2-Y1175.
[d] Assumed based on Sck interaction at VEGFR2-Y1175, and VEGFR1-Y1169 homology with VEGFR2-Y1175.
[e] Assumed based on Src interaction at VEGFR2-Y1214, and VEGFR1-Y1213 homology with VEGFR2-Y1214.
[f] Assumed based on GAP interaction at VEGFR2-Y1214, and VEGFR1-Y1213 homology with VEGFR2-Y1214.
[g] Assumed based on Cav1 interaction at VEGFR2-Y1214, and VEGFR1-Y1213 homology with VEGFR2-Y1214.
[h] Assumed based on FAK interaction at VEGFR2-Y1214, and VEGFR1-Y1213 homology with VEGFR2-Y1214.
[i] Assumed based on Shb interaction at VEGFR2-Y1175, and Shc homology with Shb.
[j] Assumed based on PI3K interaction at VEGFR1-Y1213, and VEGFR2-Y1214 homology with VEGFR1-Y1213.
[k] Assumed based on Nck interaction at VEGFR2-Y1214, and Crk homology with Nck.

Table A.5: Adapter sizes.

Adapter[a]	Domain	Crystal AA	Total AA	Size (Å)	PDB Entry	Reference
Abl	SH2	38-512	1130	31.34	3T04	[519]
c-Cbl	SH2, N-term	1-323	474	53.57	3VRR	[520]
Crk	SH2	1-204	304	31.39	2EYY	[521]
FAK	FA	891-1052	1052	33.55	4NY0	[522]
Fyn	SH2	143-248	537	33.97	1AOT	[523]
GAP	SH2	341-446	1047	39.13	2GSB	-
Grb2	SH2	53-163	217	31.31	4P9V	[524]
Nck	SH2	281-377	377	30.41	2CI9	[460]
PI3K	SH2	617-724	724	32.57	1H9O	[525]
PLC_{γ}	SH2	545-790	1290	34.29	4FBN	[526]
Src	SH2	144-252	536	32.76	4F5B	[527]
Shc[b]	SH2	147-311	583	37.28	1SHC	[528]

Sizes of each adapter protein used in the VEGFR1-adapter protein models. Note that entire crystal structures are rarely available, and so the domain each crystal structure contains is given. The segment of amino acids (AA) contained in the crystal structure is given compared to the total AA in the protein sequence. The Protein Data Bank and reference for each crystal structure are given if available.

[a]No crystal structure for VRAP or Cav1 available. I assume they have a 30 Å lower size limit.
[b]No crystal structures for Shb and Sck available. I assume they are the same size as Shc as they are part of the same family.

Table A.6: RAW macrophage adapter concentrations.

Protein	Model concentration (molecules/cell)	Reference Protein	Cell Line	Cell Condition
VEGFR1	$4.82 \cdot 10^3 \pm 1.12 \cdot 10^2$	Measured	RAW	Growth media (DMEM)
VEGFR2	$1.77 \cdot 10^3 \pm 1.32 \cdot 10^2$	Measured		
PTPN	$8.00 \cdot 10^4$	Estimated	-	-
Abl	$3.20 \cdot 10^3 \pm 5.92 \cdot 10^2$ [529]	FAK	RAW	Growth media (DMEM)
Cav1	$4.29 \cdot 10^3 \pm 7.94 \cdot 10^2$ [530]	p38		Growth media (DMEM)
c-Cbl	$2.48 \cdot 10^3 \pm 4.58 \cdot 10^2$ [531]	p38		Growth media (DMEM)
Crk	$2.71 \cdot 10^3 \pm 5.00 \cdot 10^2$ [529]	FAK		Growth media (DMEM)
FAK	$3.30 \cdot 10^3 \pm 6.10 \cdot 10^2$ [489]	VEGFR1		Growth media (alpha-MEM)
Fyn[a]	$2.70 \cdot 10^3 \pm 5.00 \cdot 10^2$ [532]	FAK		Growth media (RPMI 1640)
GAP	$9.90 \cdot 10^3 \pm 1.84 \cdot 10^3$ [533]	ERK		Growth media
Grb2	$7.13 \cdot 10^3 \pm 1.32 \cdot 10^3$ [533]	ERK		Growth media
Nck	$3.80 \cdot 10^3 \pm 7.02 \cdot 10^2$ [534]	VASP		Growth media (alpha-MEM)
PI3K	$2.28 \cdot 10^3 \pm 4.22 \cdot 10^2$ [535]	Akt		Growth media (DMEM)
PLCγ	$2.28 \cdot 10^3 \pm 4.22 \cdot 10^2$ [536]	IKBα		Growth media (RPMI 1640)
Sck[b]	$2.00 \cdot 10^3$	-		-
Shb[b]	$2.00 \cdot 10^3$	-		-
Shc	$1.08 \cdot 10^4 \pm 2.00 \cdot 10^3$ [533]	ERK		Growth media
Src	$2.61 \cdot 10^3 \pm 4.82 \cdot 10^2$ [537]	FAK		Growth media (DMEM)
VRAP[b]	$2.00 \cdot 10^3$	-		-
Akt	$2.28 \cdot 10^3 \pm 4.22 \cdot 10^2$ [538]	p38		Growth media (DMEM)
ERK	$5.21 \cdot 10^3 \pm 9.68 \cdot 10^2$ [538]	p38		Growth media (DMEM)
IKBα	$2.19 \cdot 10^3 \pm 4.04 \cdot 10^2$ [539]	p38		Growth media (DMEM)
p38	$2.24 \cdot 10^3 \pm 4.15 \cdot 10^2$ [529]	FAK		Growth media (DMEM)
VASP	$2.38 \cdot 10^3 \pm 4.40 \cdot 10^2$ [540]	IKBα		Growth media (DMEM)

Adapter, receptor, and phosphatase concentrations in RAW 264.7 macrophages were derived from the references provided. reference protein indicates the known protein concentration that was used to determine the adapter concentration. Concentrations for all reference proteins are provided. The cell line and conditions used for the experimental measurements are also given. For cell condition, starvation time and growth media is given, if available. Adapter concentrations are given as mean ± standard error of the mean, from the experimental measurement.

[a]The Fyn concentration was unavailable. Instead, I assume the Fyn concentration is equal to the Lyn concentration, as they are a part of the same family.

[b]The adapter concentration is unavailable. Since VRAP and Shb do not bind to VEGFR1, and I found Sck to not significantly direct VEGFR1 signaling, their concentrations are not essential for determining VEGFR1 signaling. Thus, I assume these concentrations are $2.00 \cdot 10^3$ molecules/cell, within the range of the other adapter concentrations.

APPENDIX B: SUPPLEMENTARY ENDOCYTOSIS INFORMATION

B.1 Figures and Tables

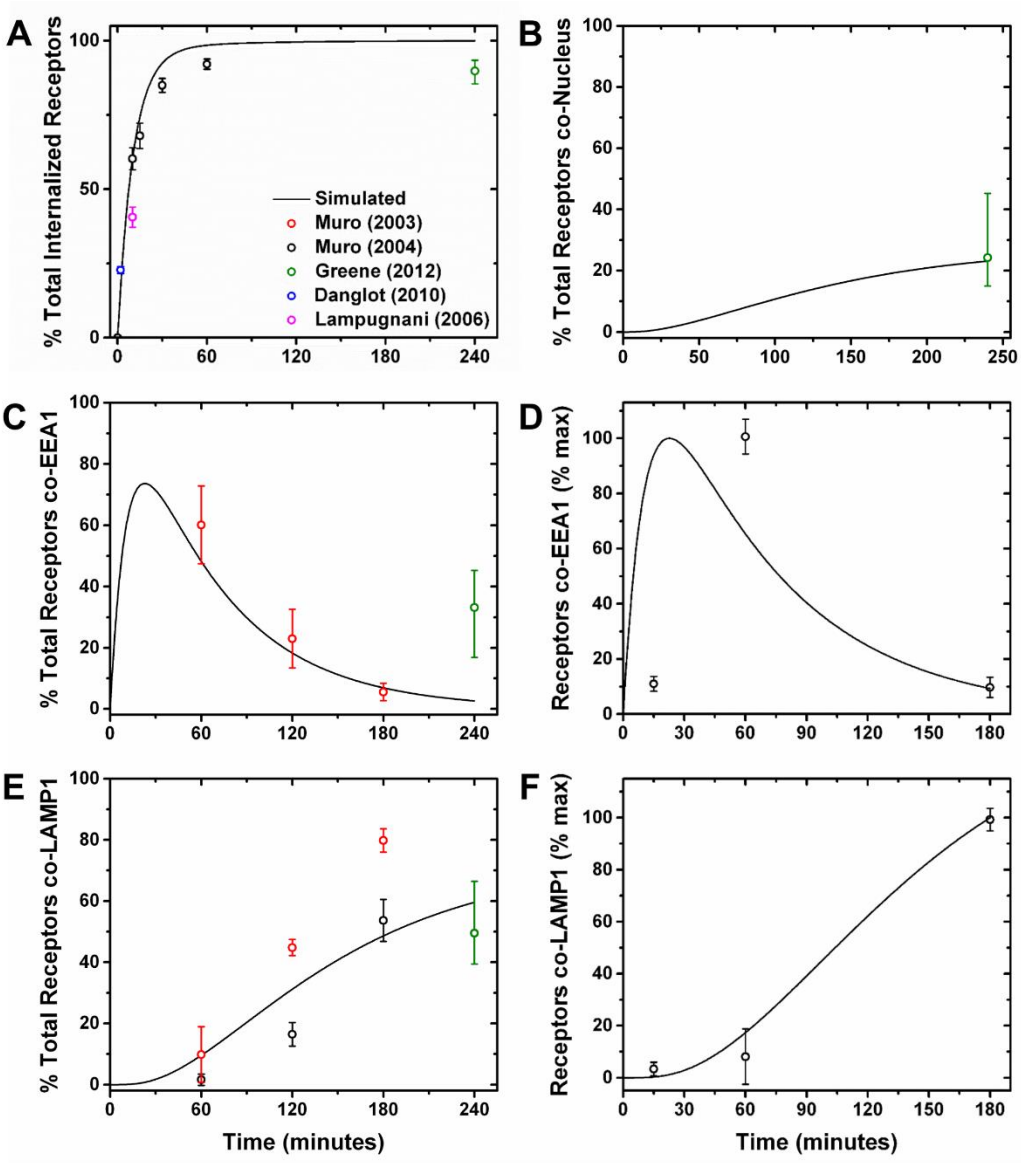

Figure B.1: Model trafficking parameters determined by fitting experimental data.

Trafficking parameters were fit by comparing generalized receptor model results to experimental data [541]–[545]. Experimental data includes (A) percent total receptor internalized, (B) percent total receptor localized to the nucleus, (C) percent total receptor co-localization with early endosomes, (D) receptor co-localization with early endosomes over time, (E) percent total receptor co-localization with late endosomes, and (F) receptor co-localization with late endosomes over time.

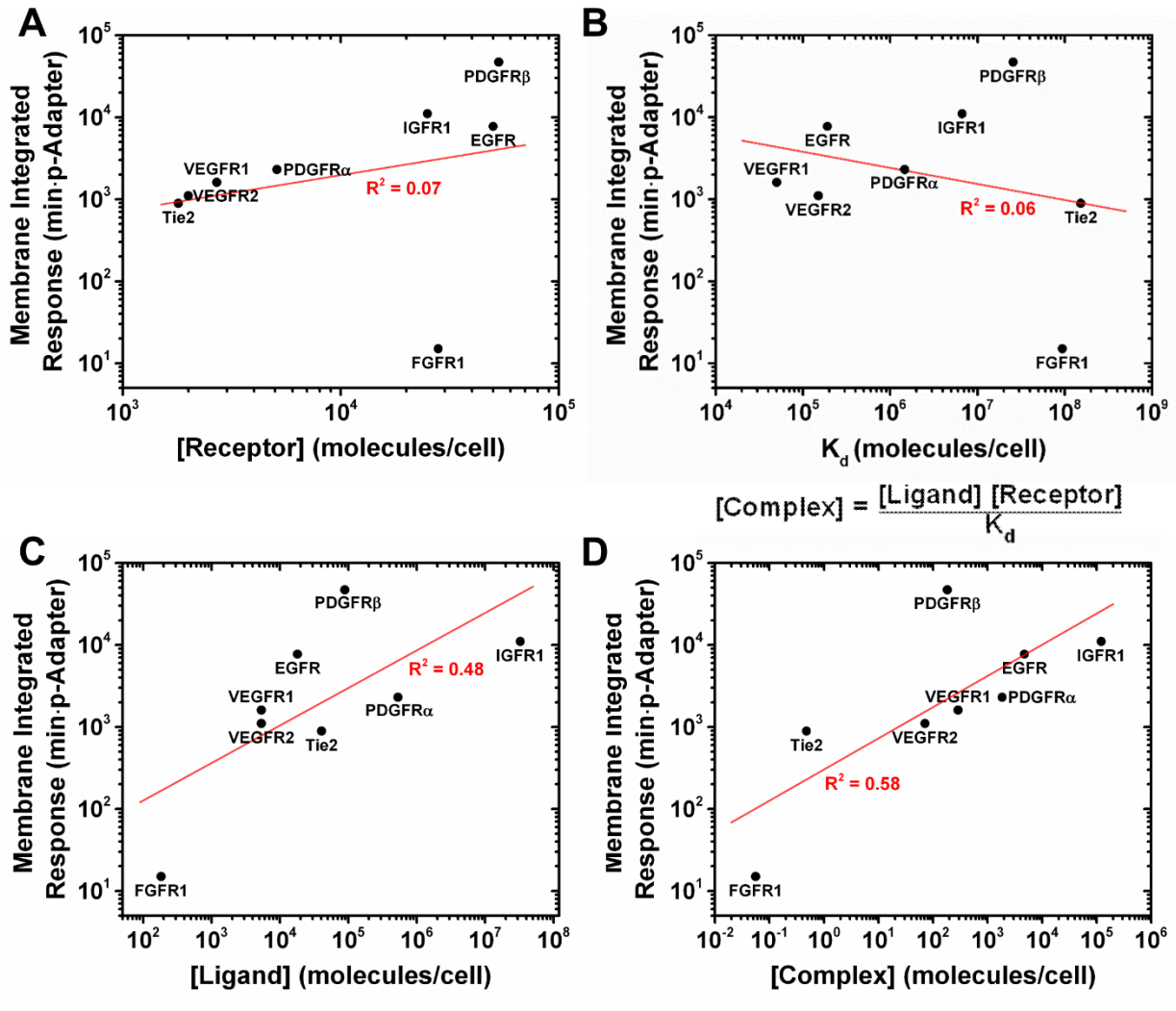

Figure B.2: Correlation analysis between RTK parameters and membrane signaling.

Membrane signaling amongst the 8 RTKs was fit to the following RTK parameters: (A) receptor level, (B) extracellular ligand concentration, (C) ligand-receptor dissociation constant, and (D) complex level, defined as the product of extracellular ligand concentration and membrane receptor level divided by the ligand-receptor dissociation constant. The R^2 goodness of fit, using a lognormal fit assumption, is given for each RTK parameter.

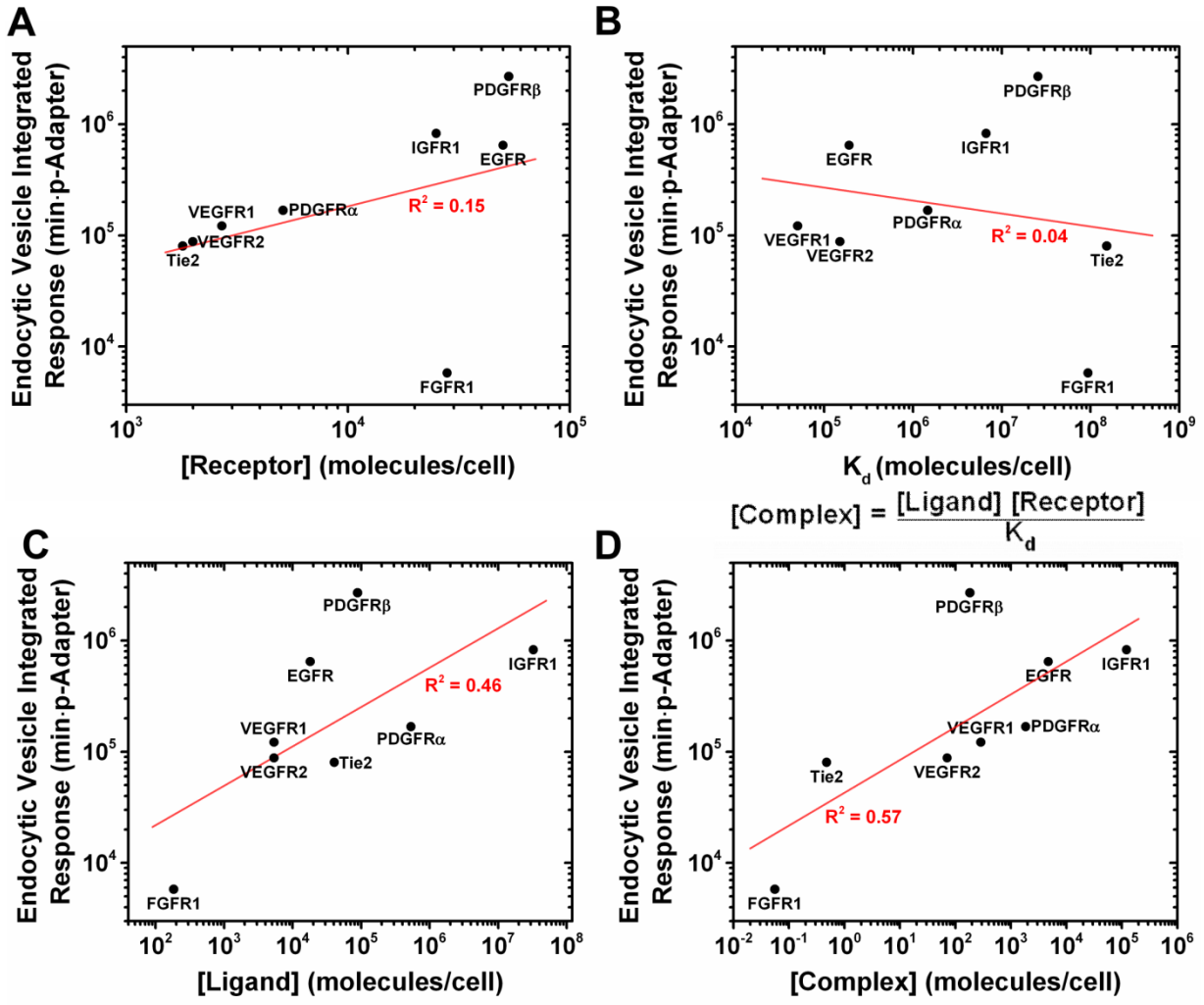

Figure B.3: Correlation analysis between RTK parameters and endocytic vesicle signaling.

Endocytic vesicle signaling amongst the 8 RTKs was fit to the following RTK parameters: (A) receptor level, (B) extracellular ligand concentration, (C) ligand-receptor dissociation constant, and (D) complex level, defined as the product of extracellular ligand concentration and membrane receptor level divided by the ligand-receptor dissociation constant. The R^2 goodness of fit, using a lognormal fit assumption, is given for each RTK parameter.

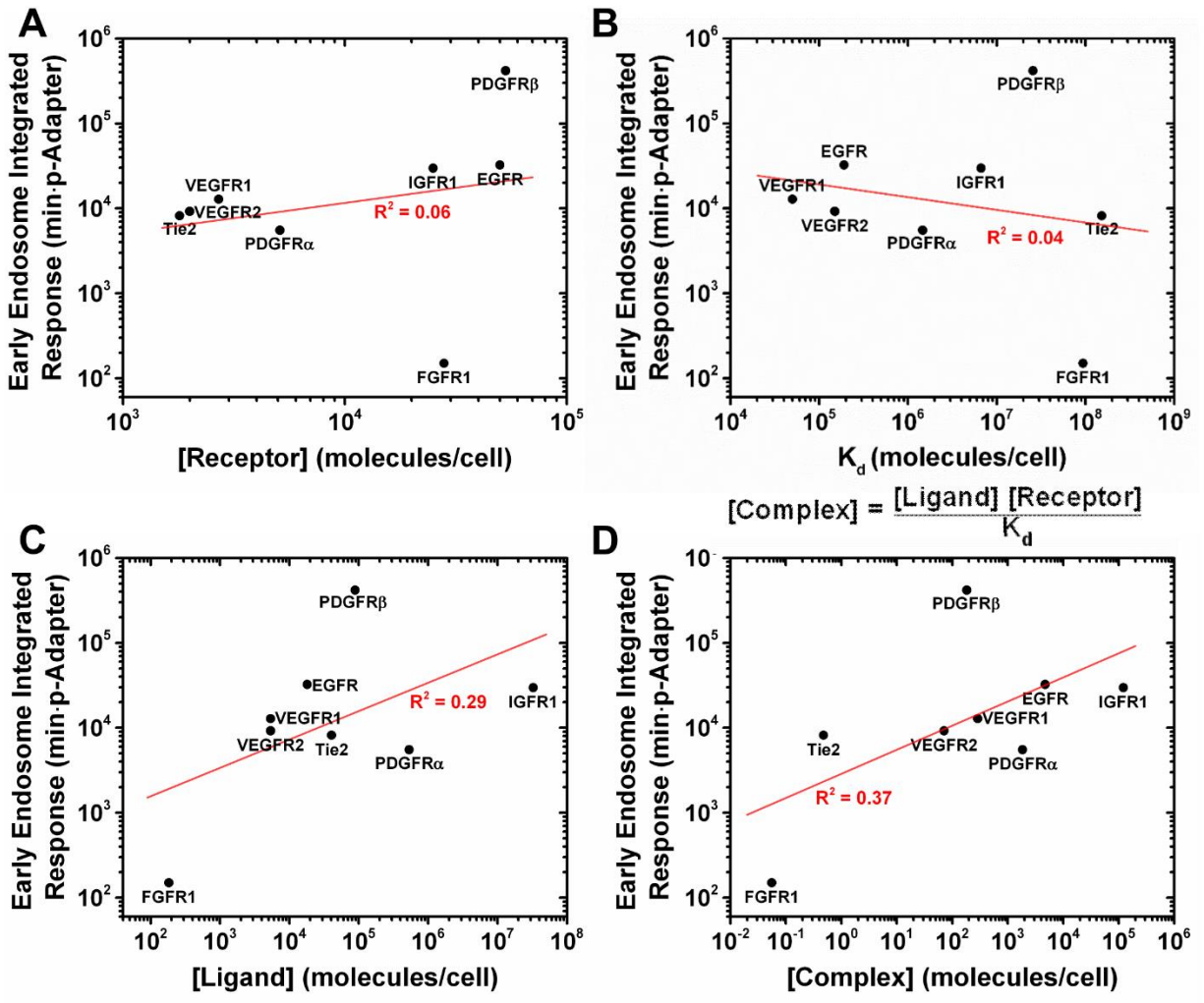

Figure B.4: Correlation analysis between RTK parameters and early endosome signaling.

Early endosome signaling amongst the 8 RTKs was fit to the following RTK parameters: (A) receptor level, (B) extracellular ligand concentration, (C) ligand-receptor dissociation constant, and (D) complex level, defined as the product of extracellular ligand concentration and membrane receptor level divided by the ligand-receptor dissociation constant. The R^2 goodness of fit, using a lognormal fit assumption, is given for each RTK parameter.

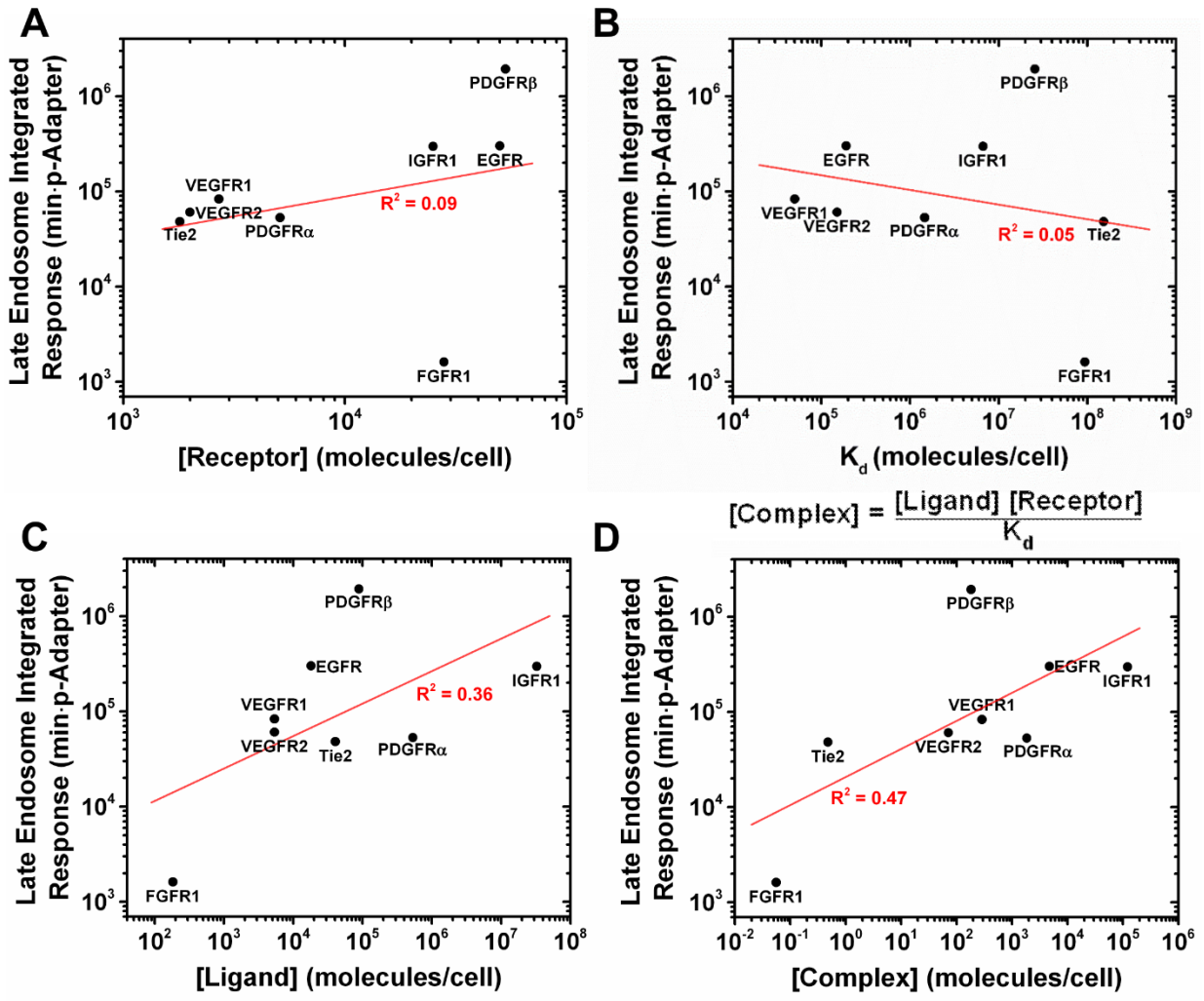

Figure B.5: Correlation analysis between RTK parameters and late endosome signaling.

Late endosome signaling amongst the 8 RTKs was fit to the RTK parameters: (A) receptor level, (B) extracellular ligand concentration, (C) ligand-receptor dissociation constant, and (D) complex level, defined as the product of extracellular ligand concentration and membrane receptor level divided by the ligand-receptor dissociation constant. The R^2 goodness of fit, using a lognormal fit assumption, is given for each RTK parameter.

Table B.1: Model implemented trafficking kinetics compared to previous endocytosis models.

Parameter	Implemented Rate	VEGFR2[a]	EGFR[b]	EGFR[c]	HER2[d]
k_{int} (R)	$1.5 \cdot 10^{-3}$	$1.6 \cdot 10^{-3}$	$5.0 \cdot 10^{-5}$	0	$1.7 \cdot 10^{-4}$
k_{int} (pR)	$1.0 \cdot 10^{-2}$	$1.7 \cdot 10^{-2}$	$5.0 \cdot 10^{-5}$	$3.5 \cdot 10^{-3}$	$7.2 \cdot 10^{-4}$
k_{deg} (R)	$1.0 \cdot 10^{-4}$	$3.8 \cdot 10^{-4}$	$6.7 \cdot 10^{-4}$	$1.3 \cdot 10^{-4}$	$7.0 \cdot 10^{-5}$
k_{deg} (pR)	$1.0 \cdot 10^{-4}$	$9.6 \cdot 10^{-2}$	$6.7 \cdot 10^{-4}$	$3.3 \cdot 10^{-4}$	$7.0 \cdot 10^{-5}$
k_{recEE} (R)	$1.0 \cdot 10^{-3}$	$7.8 \cdot 10^{-2}$	$5.0 \cdot 10^{-3}$	$5.3 \cdot 10^{-4}$	$1.1 \cdot 10^{-3}$
k_{recEE} (pR)	$1.0 \cdot 10^{-3}$	$9.4 \cdot 10^{-2}$	0	$3.3 \cdot 10^{-4}$	$1.1 \cdot 10^{-3}$
k_{recRE} (R)	$1.0 \cdot 10^{-2}$	-	-	-	-
k_{recRE} (pR)	$1.0 \cdot 10^{-2}$	-	-	-	-
k_{VCtoEE} (R)	$5.0 \cdot 10^{-5}$	-	-	-	-
k_{VCtoEE} (pR)	$5.0 \cdot 10^{-4}$	-	-	-	-
k_{EEtoRE} (R)	$1.0 \cdot 10^{-4}$	-	-	-	-
k_{EEtoRE} (pR)	$1.0 \cdot 10^{-4}$	-	-	-	-
k_{EEtoLE} (R)	$1.0 \cdot 10^{-2}$	-	-	-	-
k_{EEtoLE} (pR)	$1.0 \cdot 10^{-3}$	-	-	-	-
k_{EEtoN} (R)	$1.0 \cdot 10^{-4}$	-	-	-	-
k_{EEtoN} (pR)	$1.0 \cdot 10^{-4}$	-	-	-	-
k_{LEtoLS} (R)	$3.0 \cdot 10^{-5}$	-	-	-	-
k_{LEtoLS} (pR)	$3.0 \cdot 10^{-4}$	-	-	-	-
k_{LEtoN} (R)	$5.0 \cdot 10^{-5}$	-	-	-	-
k_{LEtoN} (pR)	$5.0 \cdot 10^{-5}$	-	-	-	-

Trafficking parameters for movement between each endocytic compartment. Different rates were fit for phosphorylated (pR) and unphosphorylated (R) receptors. Kinetic parameters used in several previous endocytosis models are given as a comparison. Dashes indicate rates that were not used in previous models. All rates are given in units of s^{-1}.

[a][159]; [b][327]; [c][546]; [d][547]